Status and Perspectives of Solid State Photo-Detectors

G.Collazuol
Department of Physics and Astronomy - University of Padova and INFN

Overview

- Focus on single photon detectors
- Recent advances by illustration of key features
- 3 examples of Cherenkov imaging detectors with SSPD

Photo-Detectors family tree

Gas
External photoemission

gas photoionization
(TMAE, TEA, …)

and/or

multiplication in gas
by avalanche
(MWPC, GEM, …)

Vacuum devices
External photoemission

secondary electron multiplication

Dynodes:
- discrete (PMT)
- continuous dynode (channeltron, MCP)

Anode:
- multi-anode
- strip lines RF

hybrid
photocathode +

- multiplication by **ionization in Si** (HPD, HAPD, VSiPMT)

or

- multiplication by **luminescent anodes** (light amplifiers: SMART/Quasar, X-HPD, …)

Solid state
Internal photoemission

- Photo-Diode (PD)
- Avalanche PD (APD)
- GM-APD (SPAD, SiPM)

- Imaging CCD, CMOS, EMCCD, CMOS-APS, …

- Quantum well detectors
- Supercond. Tunnel Junc.

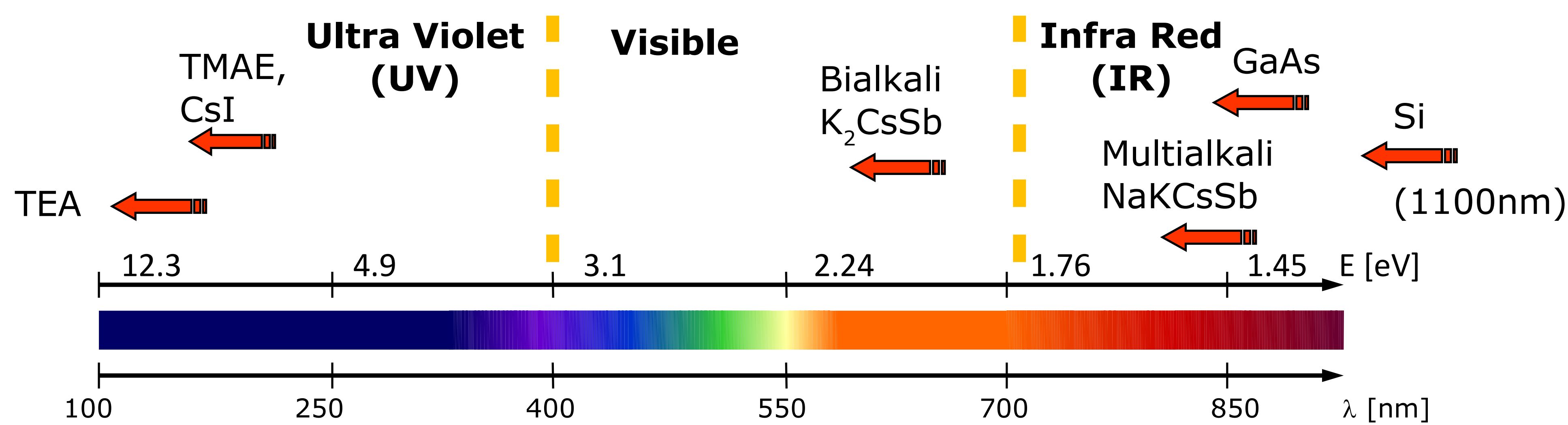

G.Collazuol - RICH 2013

GM-APD → Single Photon Avalanche Diodes

- **Arrays** for
  - wide area
  - multi-photon detection

Two types of cell implementation

planar

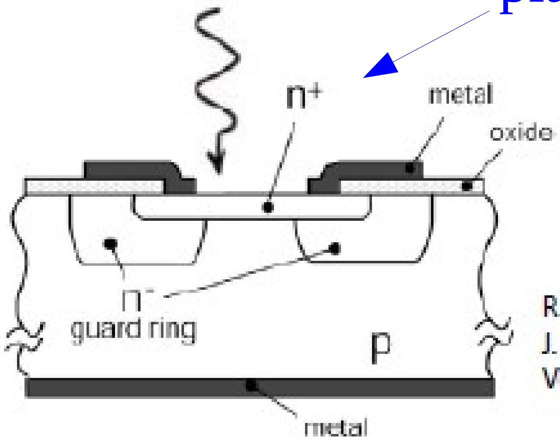

R.H. Haitz
J. Appl. Phys.,
Vol. 36, No. 10 (1965) 3123

reach through

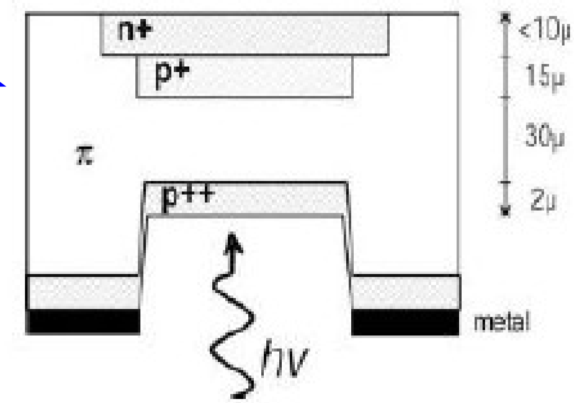

J.R. McIntire
IEEE Trans. Elec. Dev.
ED-13 (1966) 164

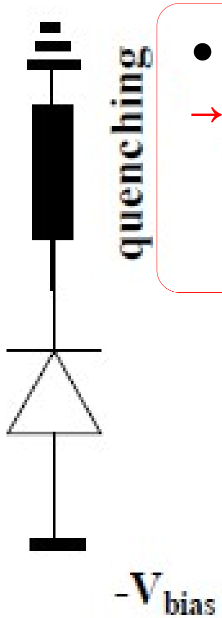

- Need **Quenching** and **Reset**

→ various ways for implementation
  - Passive quenching: large resistance
  - Active quenching: analog circuits

S. Cova & al., App. Opt. 35 (1996) 1956-1976

Standard output signal
$Q = 10^5\text{-}10^6 e$

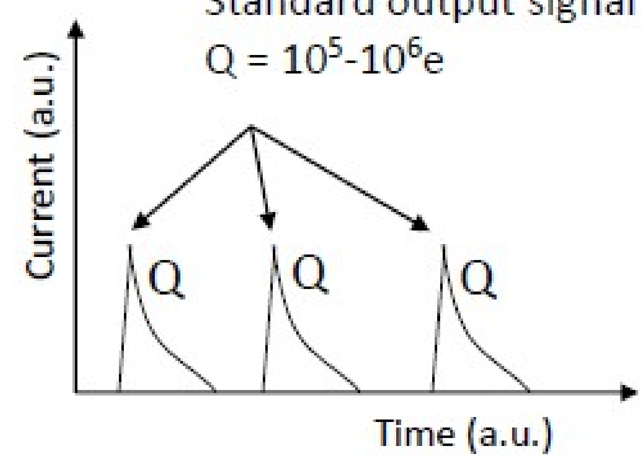

Binary device

- If one or more simultaneous photons fire the GM-APD, the output is anytime a standard signal: $Q \sim C(V_{bias} - V_{BD})$
- GM-APD does not give information on the light intensity

Arranging SPADs into packed matrices

Transition single SPAD → hundreds of GM-APD cells packed in arrays is not just design... need addressing new issues:

• an additional factor enters in the photo-detection efficiency (PDE): the **fill factor** that for small cell size can be quite low

• how to control the **dark rate** because of
- limited space for gettering techniques
- high probability to include noisy cells in a device

• optical **cross-talk** among cells

• production **yield** and **uniformity** affect performances

• **electronics** (integrated, external, hybrid)

"Analog" SiPM: array of passively decoupled GM-APD

Single GM-APD gives **no information** on light intensity → use array of GM-APDs'
first proposed in the late '80-ies by Golovin and Sadygov

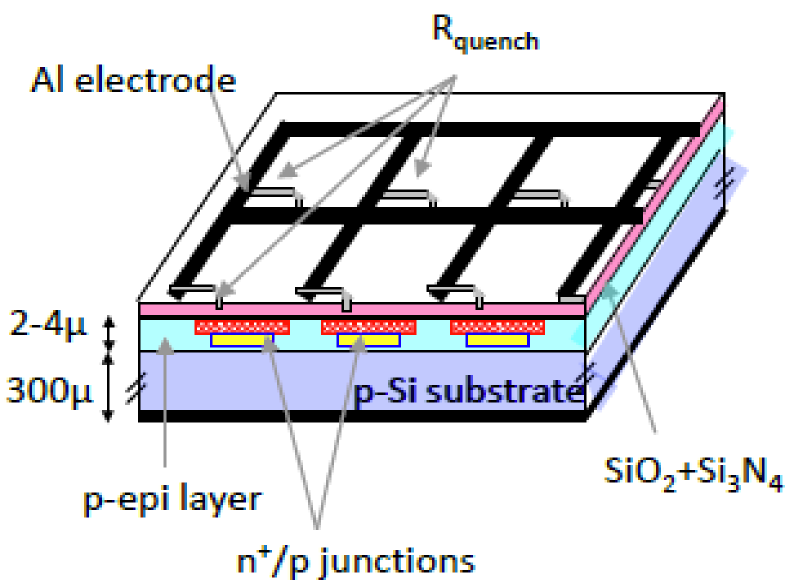

A SiPM is segmented in tiny GM-APD cells and connected in parallel trough a decoupling resistor, which is also used for quenching avalanches in the cells

Each element is independent and gives the same signal when fired by a photon

Σ of binary signals → analog signal

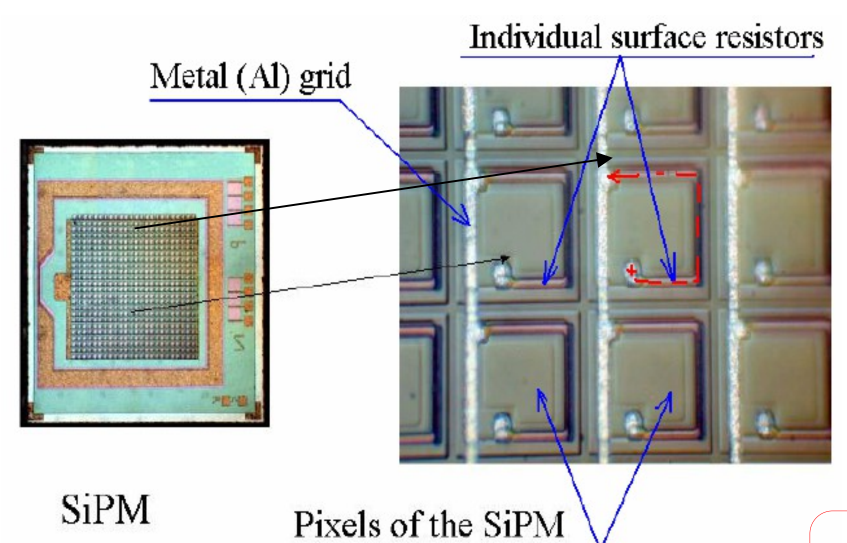

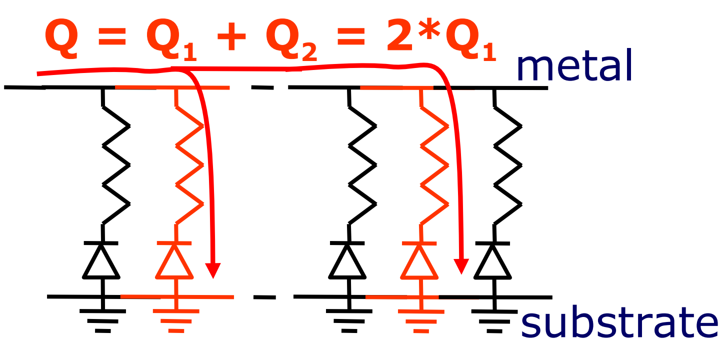

Output ∝ number incident photons

→ Linear response to multi-photon pulse

SiPM development and production

Many institutes (R&D) and companies involved
→ competition... but prices still far (~ x20)
from asympt. production cost O(10€/cm²)

- **CPTA**, Moscow, Russia
- **MePhi/Pulsar** Enterprise, Moscow, Russia
- **Zecotek,** Vancouver, Canada
- **Hamamatsu HPK**, Hamamatsu, Japan
- **FBK-AdvanSiD**, Trento, Italy
- **ST Microelectronics**, Catania, Italy
- **Amplification Technologies** Orlando, USA
- **SensL**, Cork, Ireland
- **MPI-HLL**, Munich, Germany
- **RMD**, Boston, USA
- **Philips**, Aachen, Germany
- **Excelitas** tech. (formerly Perkin-Elmer)
- **KETEK**, Munich, Germany
- **National Nano Fab Center**, Korea
- **Novel Device Laboratory** (**NDL**), Bejing, China
- **E2V**
- **CSEM**

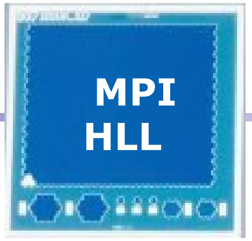

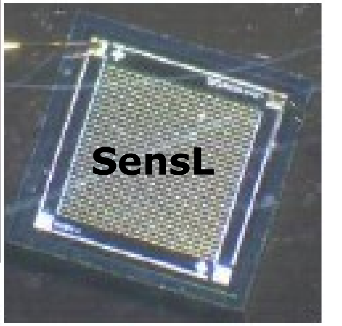

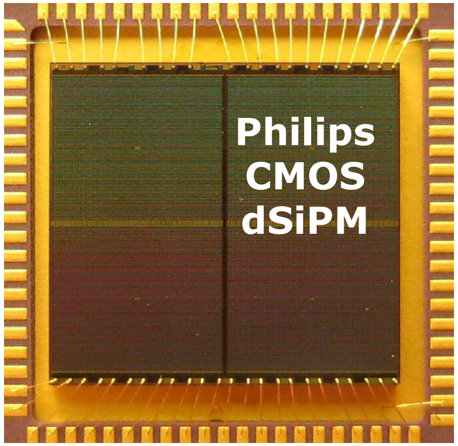

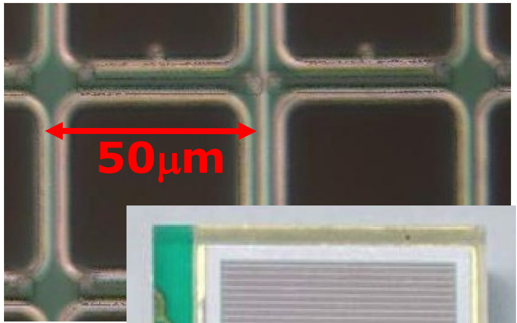

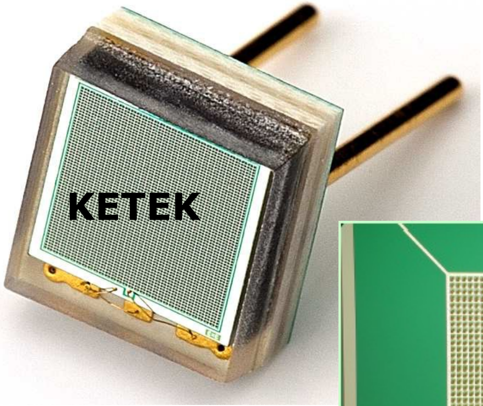

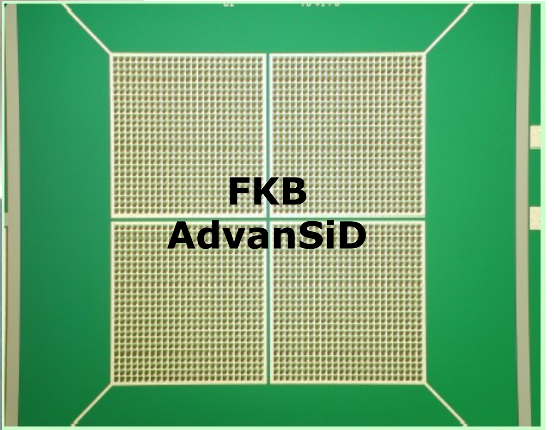

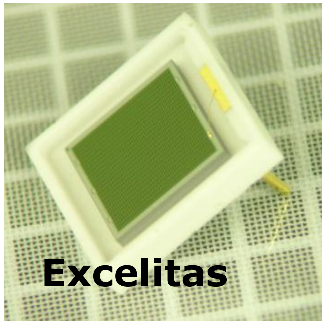

Amplification Technologies (DAPD)

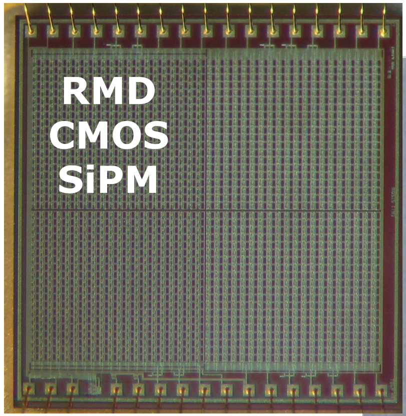

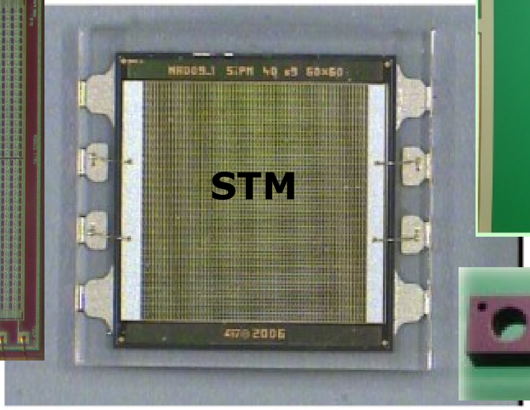

Recent samples among many

ZECOTEK MAPD-3N

FBK-AdvanSiD

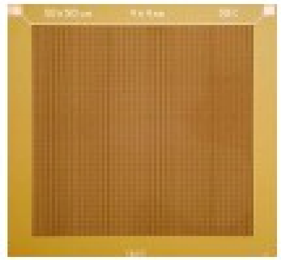

HAMAMATSU S10985

KETEK PM3350

STMicroelectronics

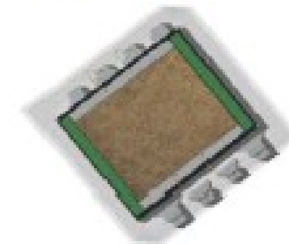

Producer	Reference	Area (mm^2)	PDE max @ 25 °C *	Dark Count Rate (Hz) @ 25°C *	Gain *
ZECOTEK	MAPD-3N	3 x 3	30% @ 480 nm	$9.10^5 – 9.10^6$	10^5
FBK - AdvanSiD	ASD-SiPM4S	4 x 4	30% @ 480 nm	$5.5\ 10^7$ - $9.5\ 10^7$	$4.8\ \ 10^6$
HAMAMATSU	S10985-50C	6 x 6	50% @ 440 nm (includes afterpulses & crosstalk)	$6.10^6– 10.10^6$	$7.5\ \ 10^5$
KETEK	PM3350	3 x 3	40% @ 420 nm	4.10^6	$2\ \ 10^6$
STMicrolectronics	SPM35AN	3,5 x 3,5	16% @ 420 nm	$7.5\ 10^6$	$3.2\ 10^6$

** datasheet data*

Ongoing R&D to increase the active area at KETEK, AdvanSiD, Excelitas (6 x 6 mm^2)
Other solution to get larger area : connection of several channels of a matrix

Discrete arrays

Producer	Device ID	Picture	Total area (mm^2)	SiPM area (mm^2/channel)	Nr. channels	μcell size
Hamamatsu	S11064-025P S11064-050P	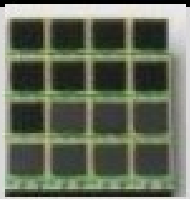	18 x 16.2	3x3	16(4x4) ch	25x25 μm 50x50 μm
Hamamatsu	C11206-0404DF	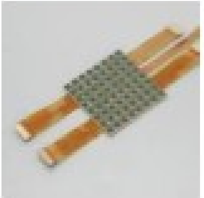		3x3	64(8x8) ch	
Hamamatsu	S11834-3388DF		72x64.8	3x3	256(16x16)ch	
FBK AdvanSiD	ASD-SiPM4s-P-4x4T-50 ASD-SiPM4s-P-4x4T-69	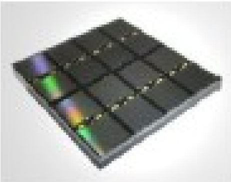	8.2 x 8.2	4x4	16(4x4) ch	50x50 μm 69x69 μm
FBK AdvanSiD	SiPM tile	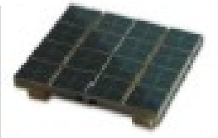	32.7x32.7	4x4	64(8x8) ch	
SensL	ArraySM-4P9 ArraySB-4P9 (blue sensitive)		46.3 x 47.8	3x3	144(12x12) ch (based on monolithic Array SM4)	35x35 μm

Monolithic Arrays

→ fill factor, uniformity, yield ...cost

Producer	Device ID	Picture	Effective area (mm^2)	SiPM area/channel (mm^2)	Nr. channels	μcell size
Hamamatsu	S10984-025P S10984-050P S10984-100P	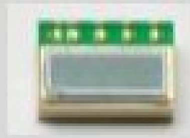	1 x 4	1x1	4(1x4)ch	25x25 μm 50x50 μm 100 x 100 μm
Hamamatsu	S10985-025C S10985-050C S10985-100C	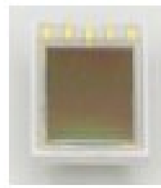	6 x 6	3x3	4(2x2)ch	25x25 μm 50x50 μm 100 x 100 μm
Hamamatsu	S11828-3344M	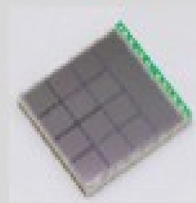	12 x 12	3x3	16(4x4)ch	50x50 μm
FBK AdvanSiD	ASD-SiPM1.5s-P-8X8A	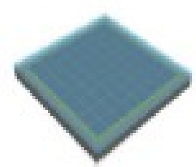	11.6 x 11.6	1.45x1.45	64(8x8)ch	50x50 μm
FBK AdvanSiD	ASD-SiPM3S-P-4X4A	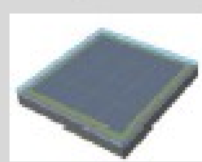	11.8 x 11.8	2.95x2.95	16(4x4)ch	50x50 μm
SensL	Array SM-4 Array SB-4 (blue sensitive)	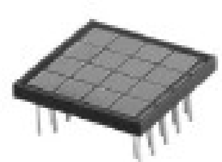	12 x 12	3x3	16(4x4)ch	35x35 μm

SPAD Arrays with electronics "integrated"

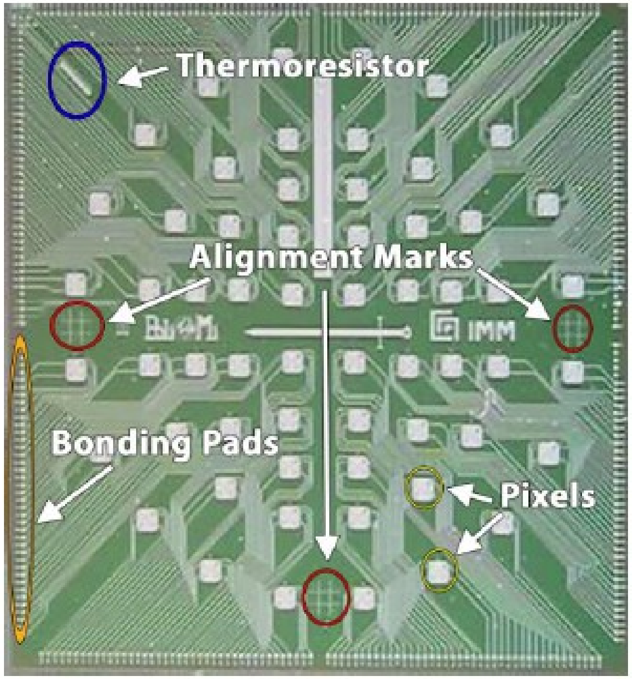

- quenching
- reset
- read-out

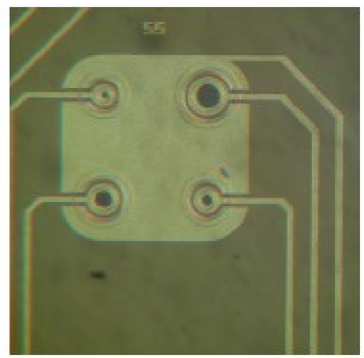

- Cova, Lacaita, Zappa et al since early 90-ies (Politecnico Milano group)

Guerrieri, NDIP 2008

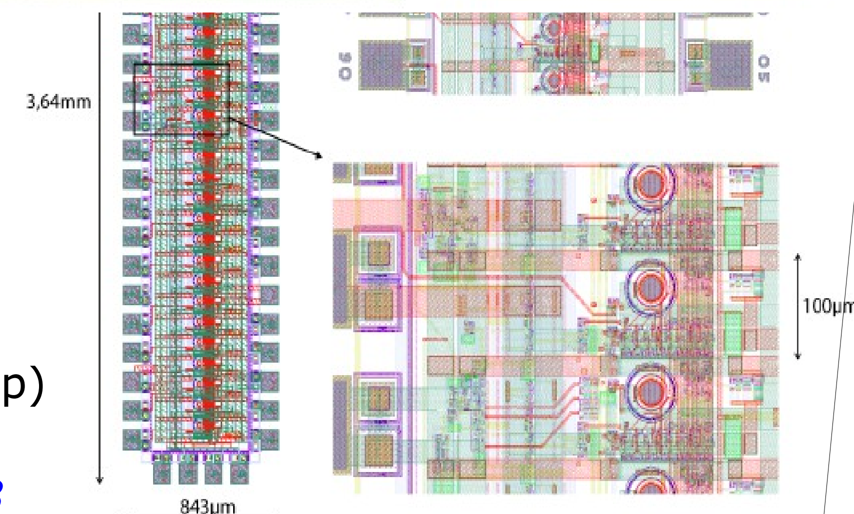

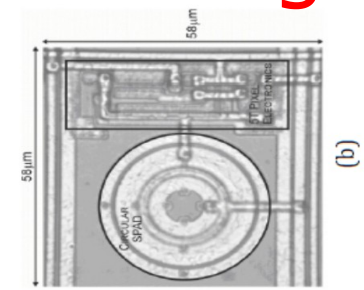

Niclass, PhD Thesis EPFL (2008)

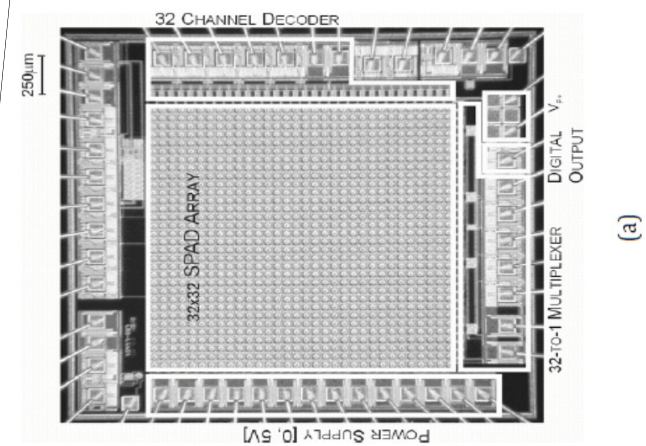

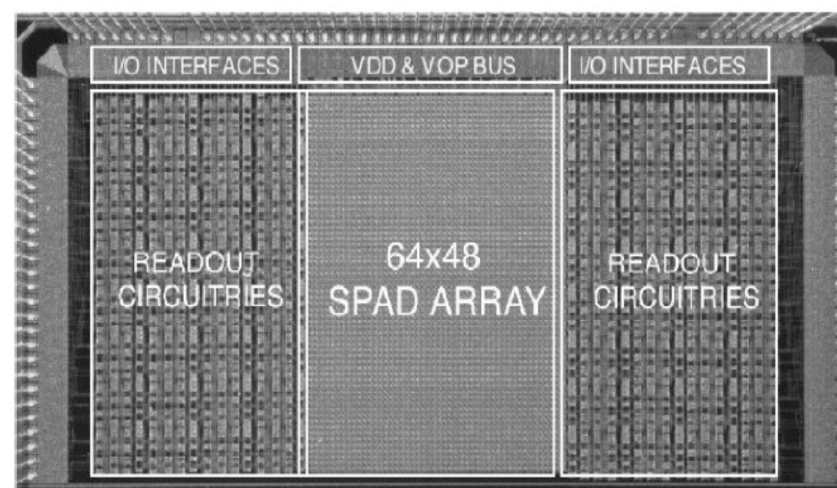

- *Charbon, Rochas, Niclass, et al (EPFL Lousanne group)*

See also:
- *Kindt et al*
- *Jackson et al*
- *Staples et al*

Today's fair competition: Analog vs Digital SiPM

Analog Silicon Photomultiplier Detector

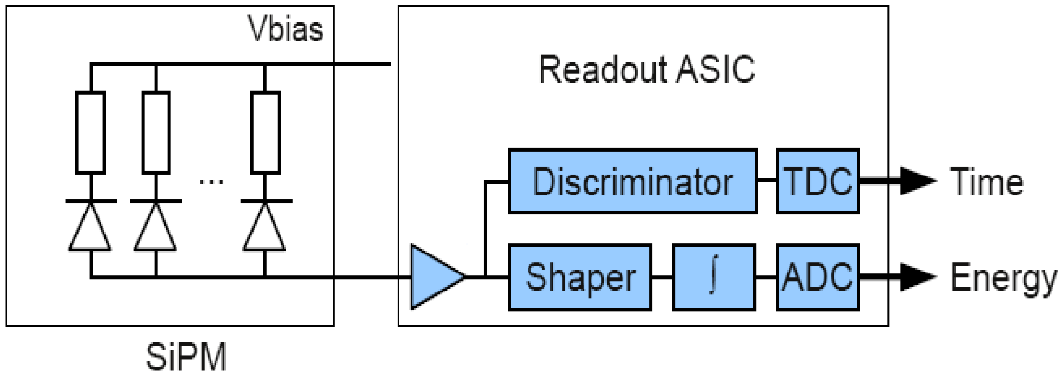

T.Frach - Heraeus Seminar 2013

Digital Silicon Photomultiplier Detector

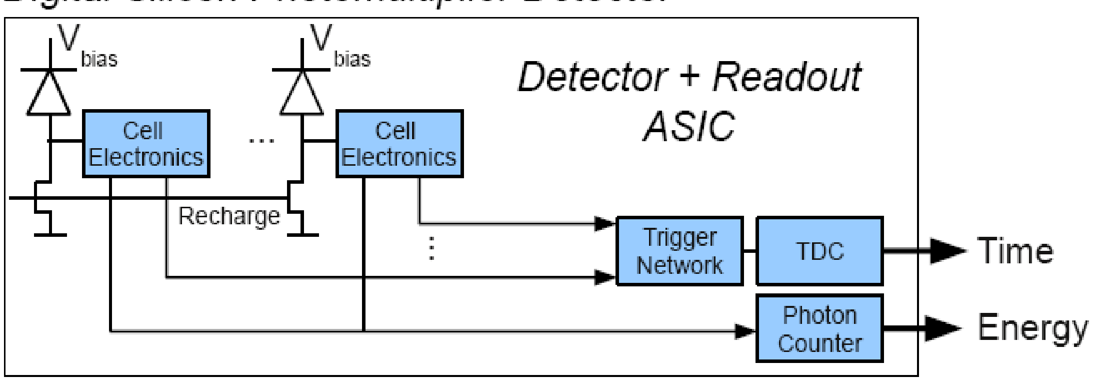

d-SiPM:
- for each light pulse → output is: time-stamp and number of photons
- control of individual cells
- O(500ns) RO dead time (upon trigger)

Analog SiPM

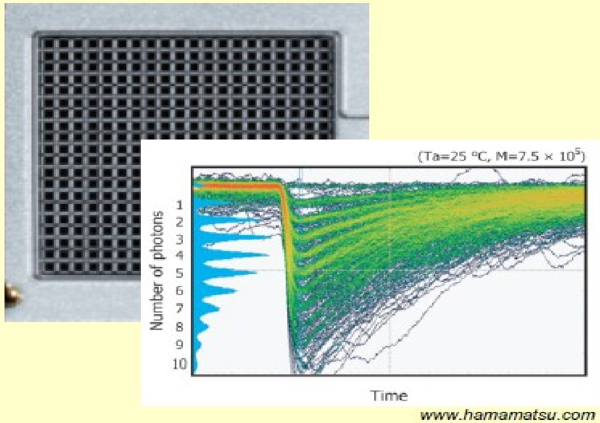

- Cells connected to common readout
- Analog sum of charge pulses
- Analog output signal

Digital SiPM

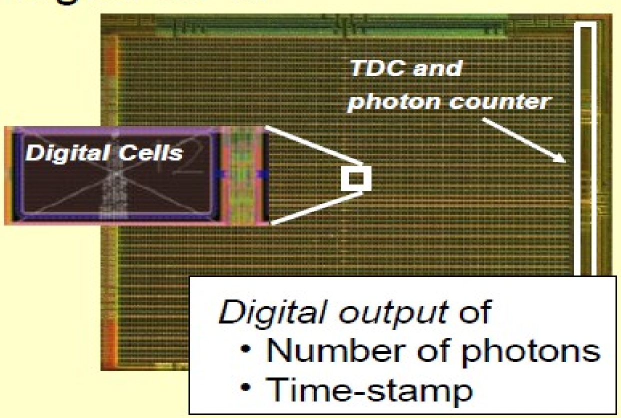

Digital output of
- Number of photons
- Time-stamp

- Each diode is a digital switch
- Digital sum of detected photons
- Digital data output

Key features: implementation

- GM-APD cells: **custom** (analog SiPM) vs **CMOS** (digital-SiPM)
- Quenching and Reset modes

Close up of a cell – custom process

Shallow-Junction APD

Example of implementation

C.Piemonte NIM A 568 (2006) 224

Optical window → Anti-Reflective Coating (ARC)
note: light absorption in Si, SiO_2

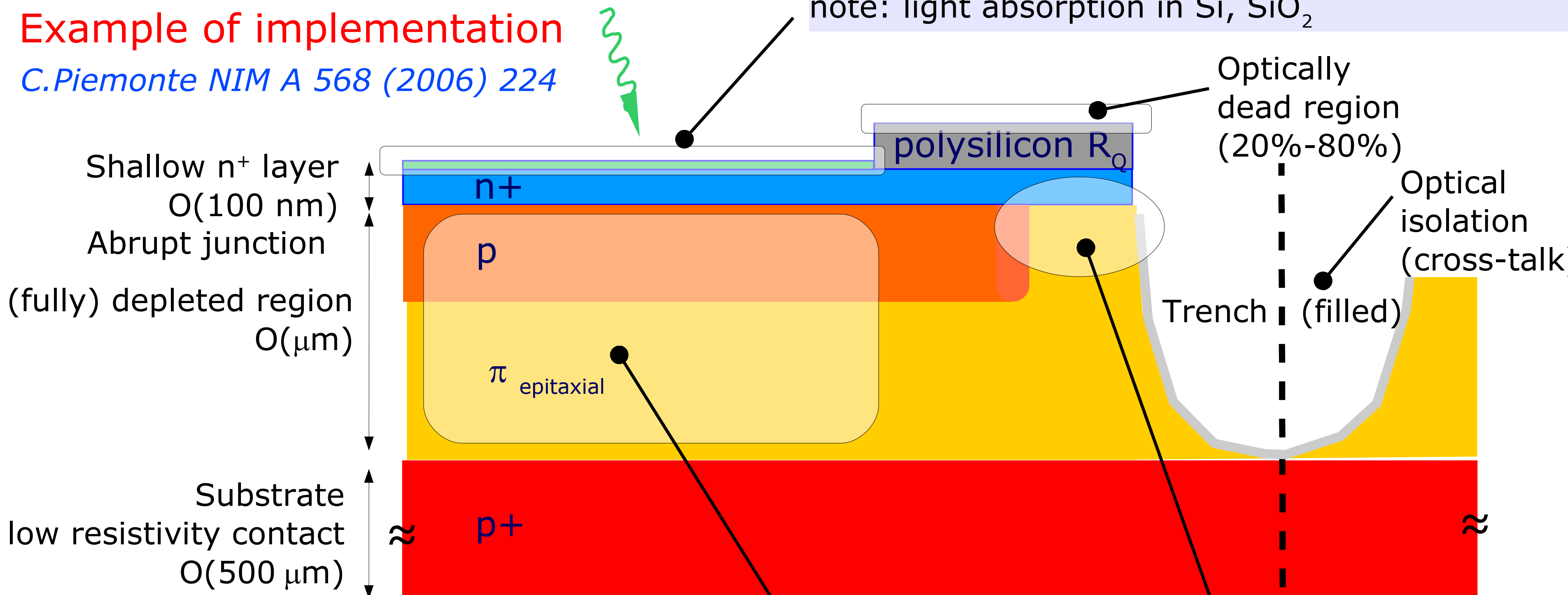

Active volume
- no micro-plasma's high quality epitaxial
- doping / E field profile engineering

Critical region
- Leakage current
- Surface charges
- **Guard Ring** for
  - preventing early edge-breakdown
  - isolating cells
  - tuning E field shape

→impact on Fill Factor

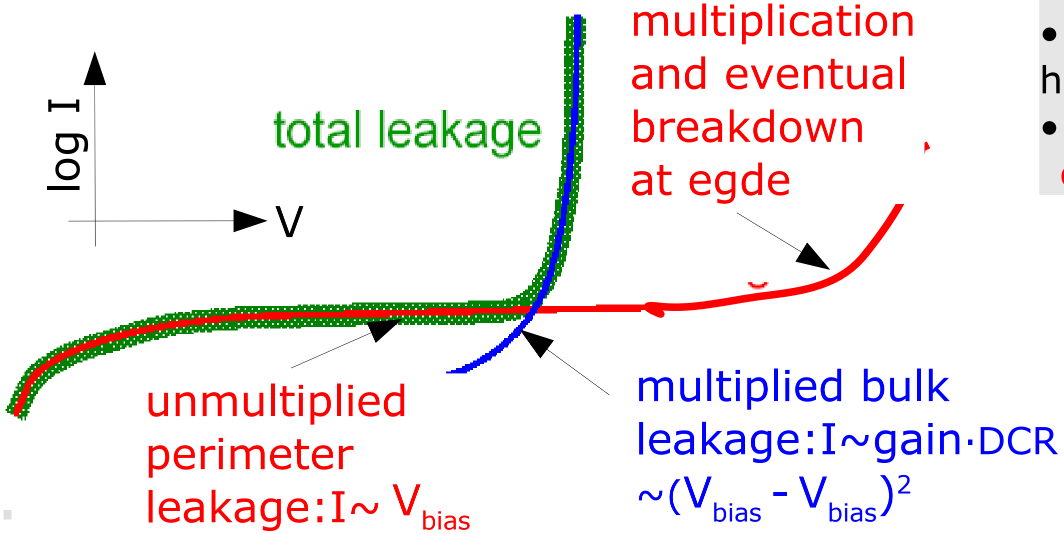

Close up of a cell - CMOS

Key elements for CMOS SiPMs
- **APD cell isolation** from CMOS circuitry
- **guard ring**
- **HV CMOS** extension against tunneling

APD integration into CMOS

Example of implementation *from T.Frach - US patent 2010/0127314*

Note
- extended CMOS processes exploited
- careful design of cell isolation and guard ring

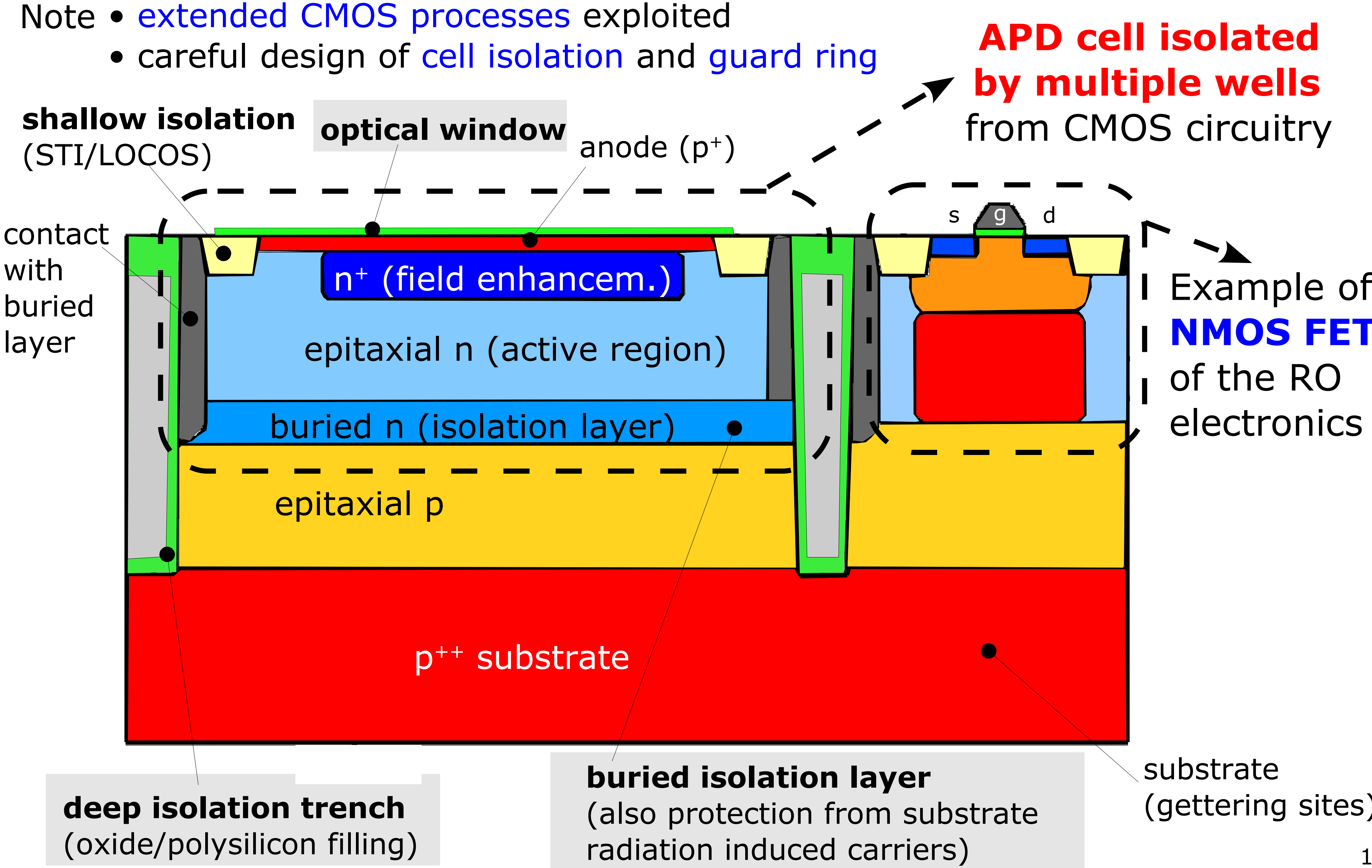

Passive / Active quenching and recharge

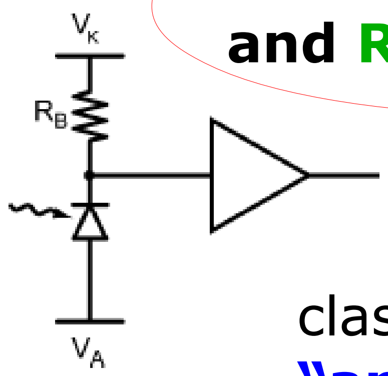

Passive Quenching and Reset

classical
“analog” SiPM

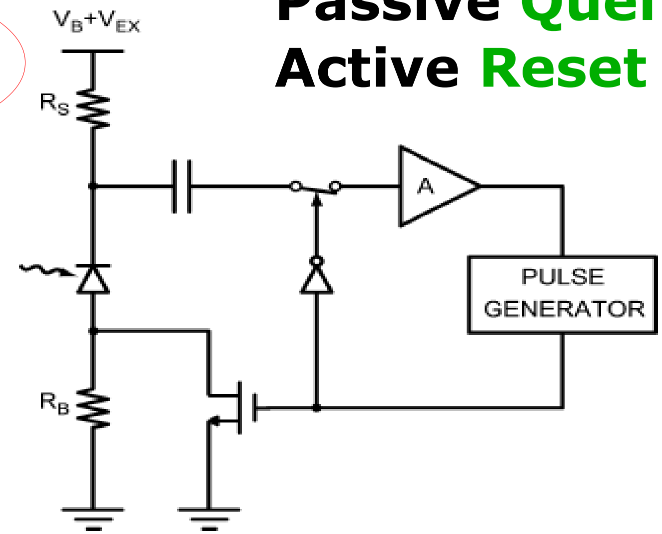

Passive Quenching
Active Reset

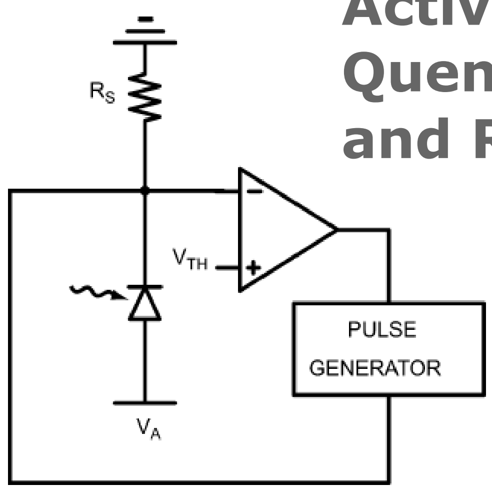

Active Quenching and Reset

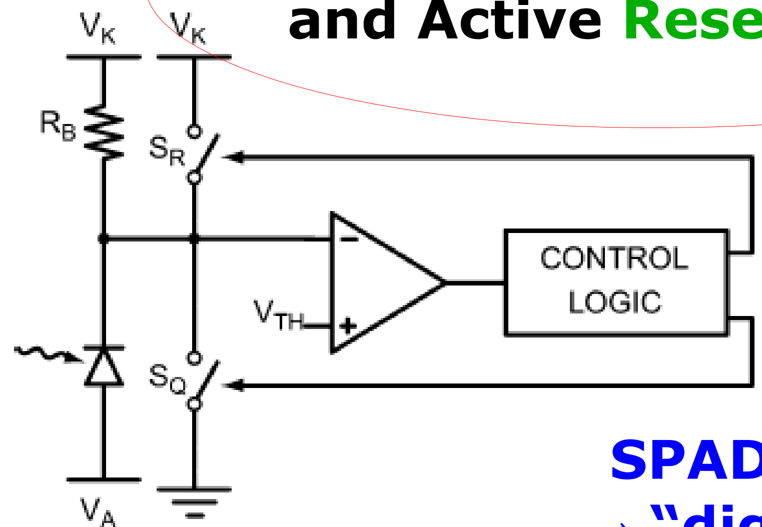

Active/Passive Quenching and Active Reset

SPAD arrays →
→ “digital” SiPM

Gallivanoni et al IEEE TNS 57 (2010) 3815

Passive mode: quenching resistor

Rq~ few 100kΩ

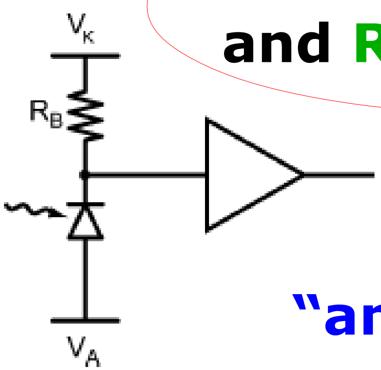

Passive Quenching and Reset

"analog" SiPM

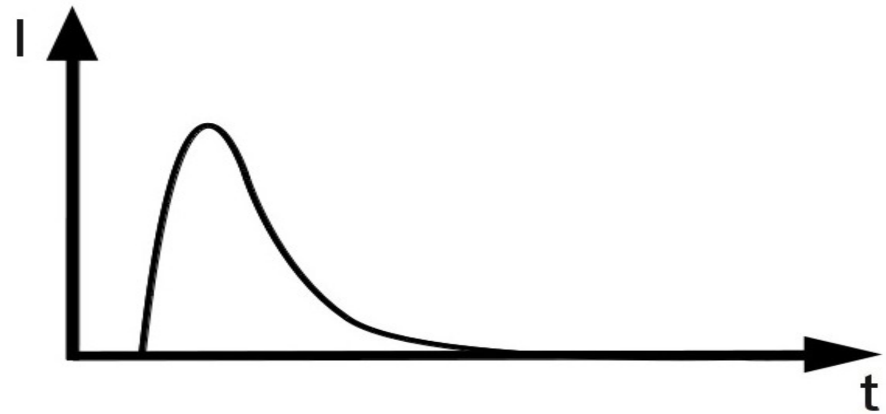

- "Quenching resistor" regulates both **quenching** and **recharge**
- Simple concept but tricky to implement (high-ohmic resistors needed)
- Allows easy implementation of summation
- **Constraints due to passive mode**: latch current level (20μA)
  → large charge developed before quenching
  → limited recharge current (R$_q$ ~ ΔV/20μA for safe quenching → I$_r$ < 20μA)
  ("long" recovery time: τ_r~ Rq x Cd)
- Output signal compatible with that of PMTs → re-use of readout infrastructure

Active mode: transistors to Quench and Reset

- Sense the voltage at the diode terminal
- Use transistors to actively **discharge/recharge** the diode
  → controlled amount of charge → reduced after-pulsing and cross-talk
  → controlled (fast) recovery
- Flexibility: programmable timing possible, disabling of faulty cells
- Electronics area not active (unless 3D integ.): higher cost & lower fill factor
- Electronics exposed to radiation: hardness ?
- Fast digital signals (gate delays of ~30ps, rise/fall times ~90ps), low parasitics

Separation of **photon number**, **time of arrival** and **position** information right **at the detection element** might potentially enable new detector concepts

Active/Passive Quenching and Active Reset

SPAD arrays - - "digital" SiPM

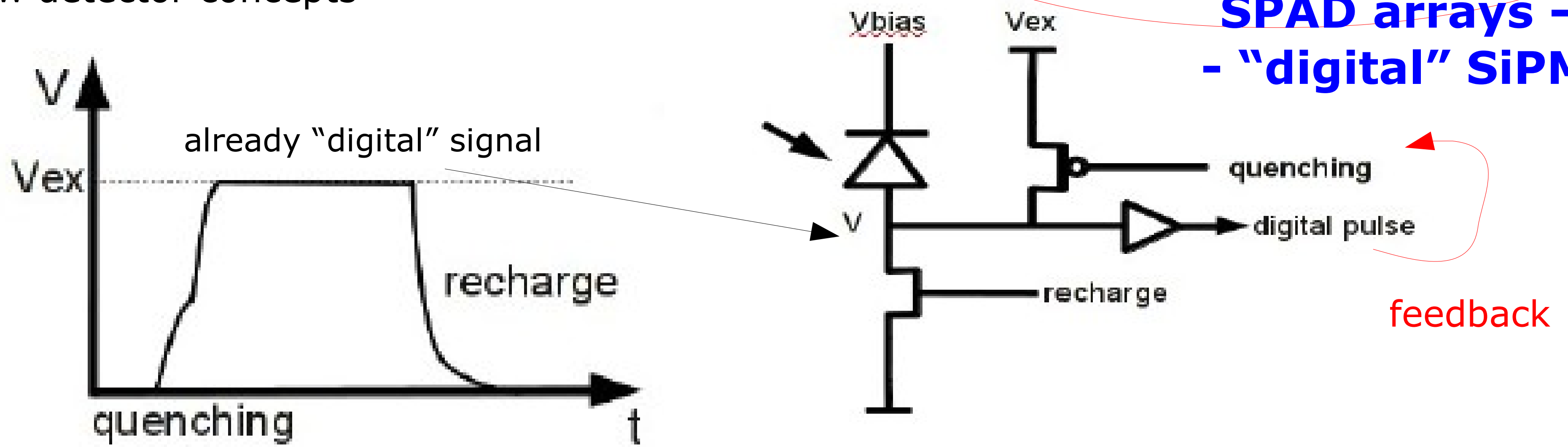

Active mode → "digital" SiPM

Philips Digital SiPM
APD cells & integrated electronics

- Cell area ~ 30x50μm^2
- Fill Factor ~ 50%

T.Frach at LIGHT 2011

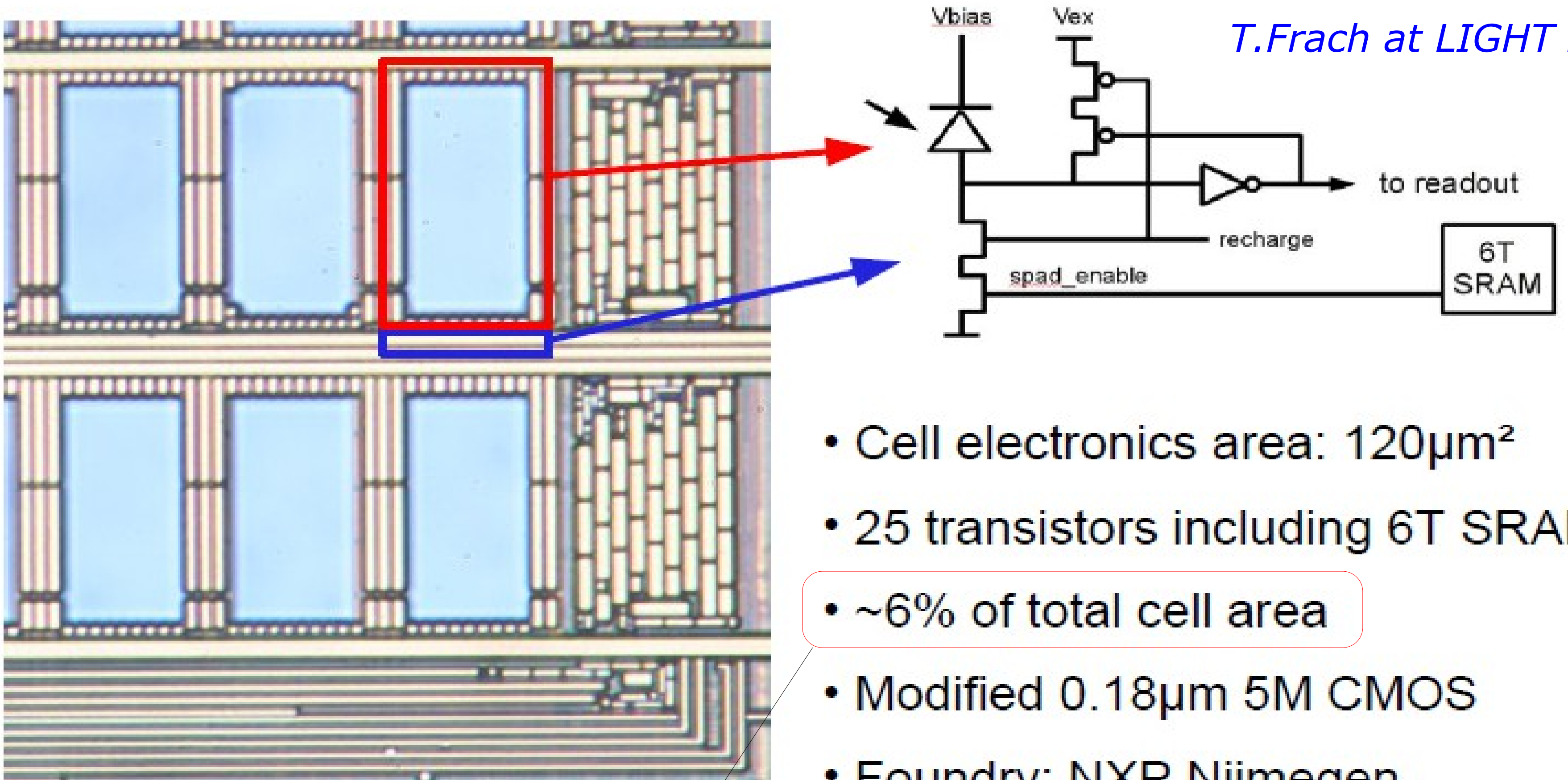

- Cell electronics area: 120μm^2
- 25 transistors including 6T SRAM
- ~6% of total cell area
- Modified 0.18μm 5M CMOS
- Foundry: NXP Nijmegen

- reduced Fill Factor
- electronics exposed to radiation
  → additional radiation weakness

Passive quenching + active recharge

Passive Quenching and Reset

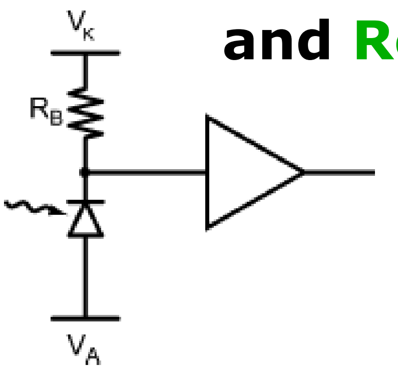

Passive Quenching Active Reset

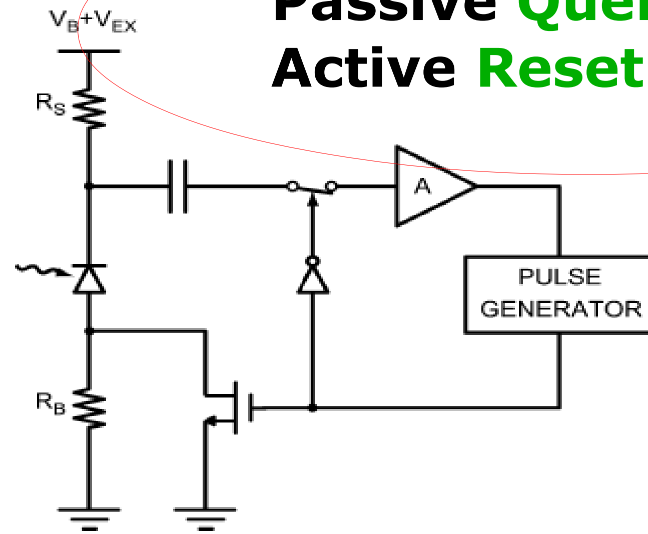

MOS-SiPM

Active Quenching and Reset

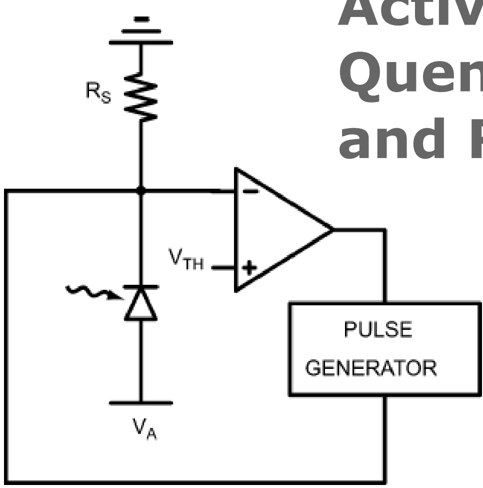

Mixed Active/Passive Quenching and Active Reset

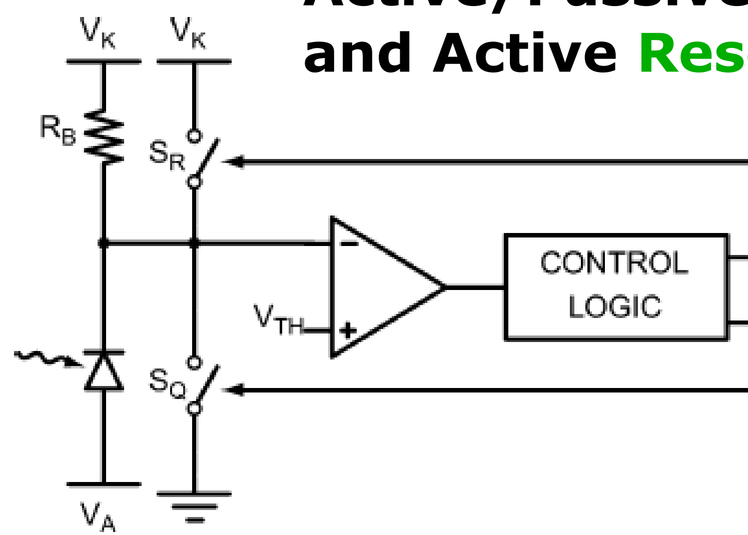

Gallivanoni et al IEEE TNS 57 (2010) 3815

MOS-SiPM (new "analog" SiPM structure)

Passive quenching + active recharge

Gola, Piemonte, Acerbi IEEE NSS 2013 (FBK-Advansid)

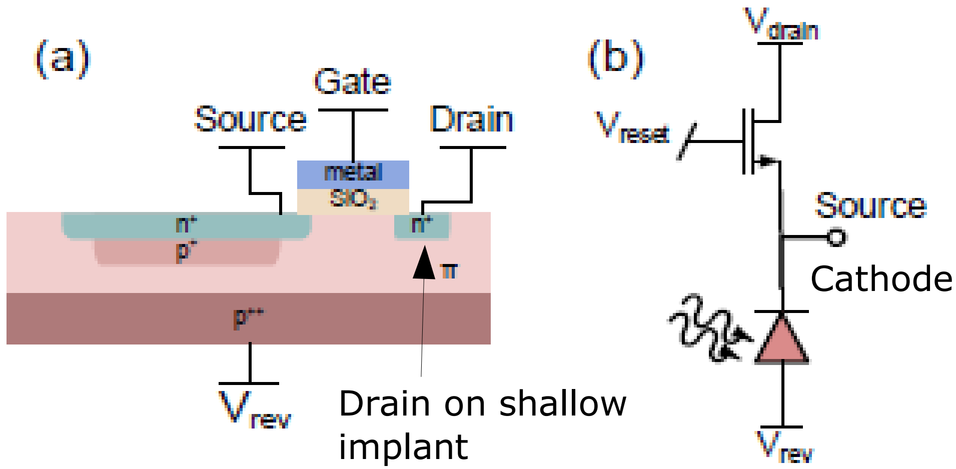

Fig. 1: (a) Structure of the MOS-SiPM cell, showing the transistor partially merged with the SPAD. (b) Schematic circuit of the microcell.

- **MOSFET transistor** replaces quenching R
- custom process
- **no losses** in Fill Factor
- **cheaper** than standard analog SiPM

- **Operation** : periodic reset

- **Features**

→ "hottest" cells self-disabled (like in d-SiPM)
 → low Dark Count device
→ After-pulsing suppressed almost completely
→ Very fast signal ~2ns width
 (AC coupling to Cathode)

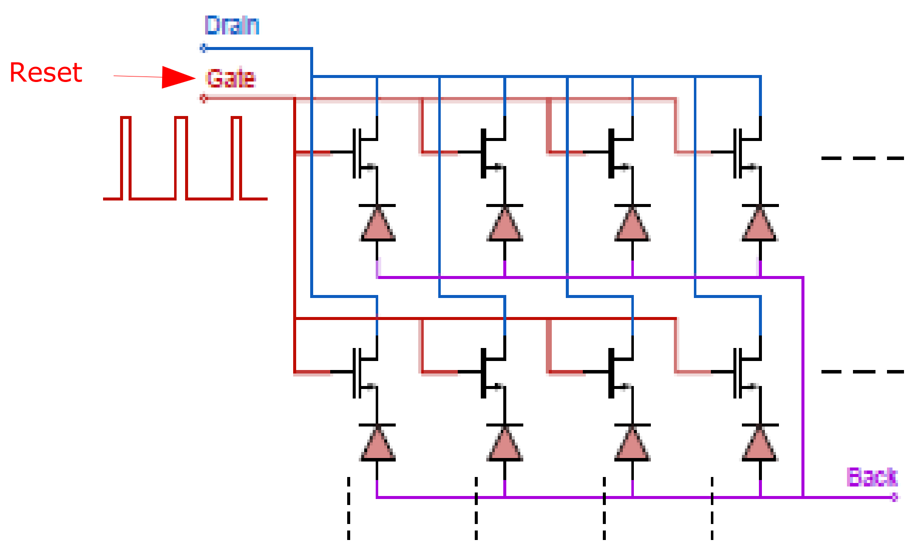

Fig. 2: Schematic circuit of the MOS-SiPM, showing the connections of the microcells.

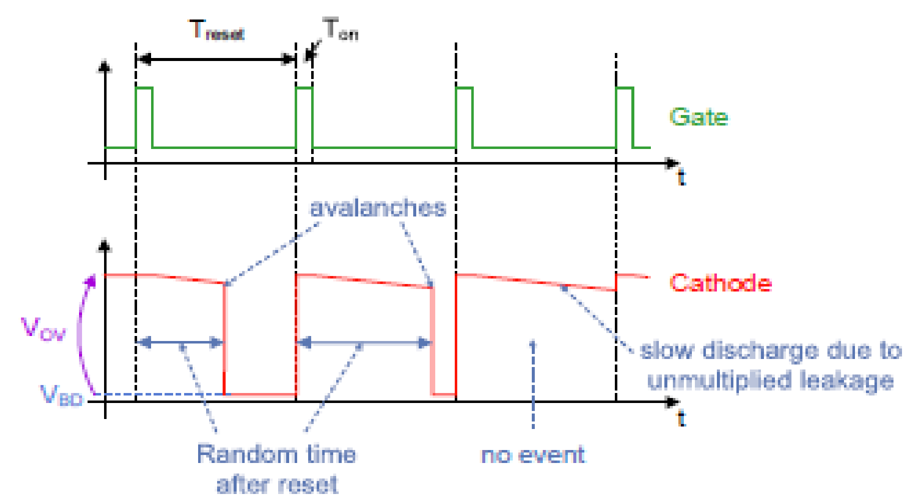

Fig. 3: Working principle of the MOS-SiPM, which is operated in a periodic pulsed reset mode.

!!! developement to be followed

Key features: main parameters

Gain, Pulse shape,
Dynamic Range, Linearity

related to the recharge of the diode capacitance from V_{bd} to V_{bias} during the avalanche quenching time after I_{latch} is reached

pulses triggered by non-photo-generated carriers (thermal / tunneling generation in the bulk or in the surface depleted region around the junction)

Primary noise:
→ thermally generated
Correlated noise:
→ after-pulses, cross-talk

carriers can be trapped during an avalanche and then released triggering another avalanche

photo-generation during the avalanche discharge. Some of the photons can be absorbed in the adjacent cell possibly triggering new discharges

PDE = QE * P_{01} * ε

QE = quantum efficiency
P_{01} = avalanche triggering prob.
ε = geometrical fill factor

Photo-detection efficiency

Related to the photo-generation and to the avalanche propagation

Time resolution

Gain and Response (passive mode)

- Gain and its fluctuations
- Response non-linearity
- New Tiny cell devices

GM-APD Operation model – passive quenching

Diode (capacitor) fast discharge
and slow recharge

charge stored defines Gain
→ Gain ~ C ΔV
$\Delta V = V_{bias} - V_{bd}$ "Over-Voltage"

currents internal / external

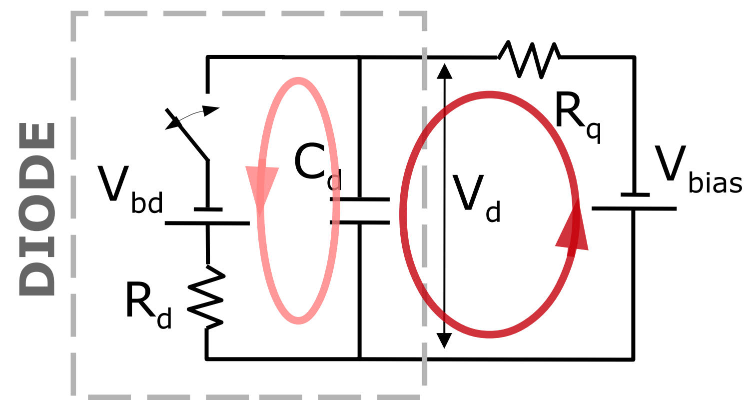

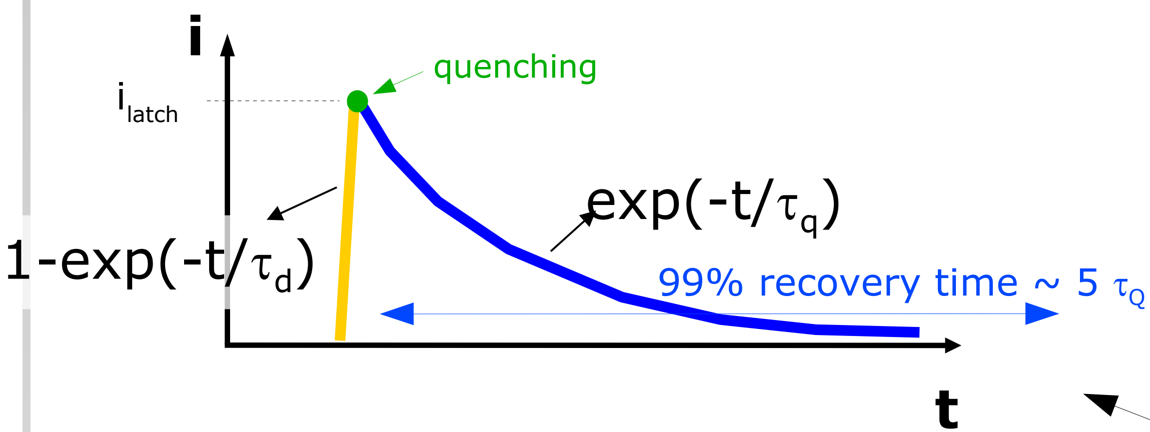

Rise time — Fall time (recovery)

$\tau_d = R_d C_d \ll \tau_q = R_q C_d$

pulse shape (ideal)

Gain → linear with ΔV (≠ APD)
→ no intrinsic fluctuations !!! (≠ APD)
→ independent of T at fixed ΔV (≠ APD)

Rise time T dependence (weak) due to R_d

Recovery time T dependence (strong) due to R_q
C_d is independent of T

Waveform, charge spectrum and gain

Pulse shape

1. fast component
(parasitic transient)

2. slow component due to
(99% recovery time ~100ns)

Waveform (Dark noise)

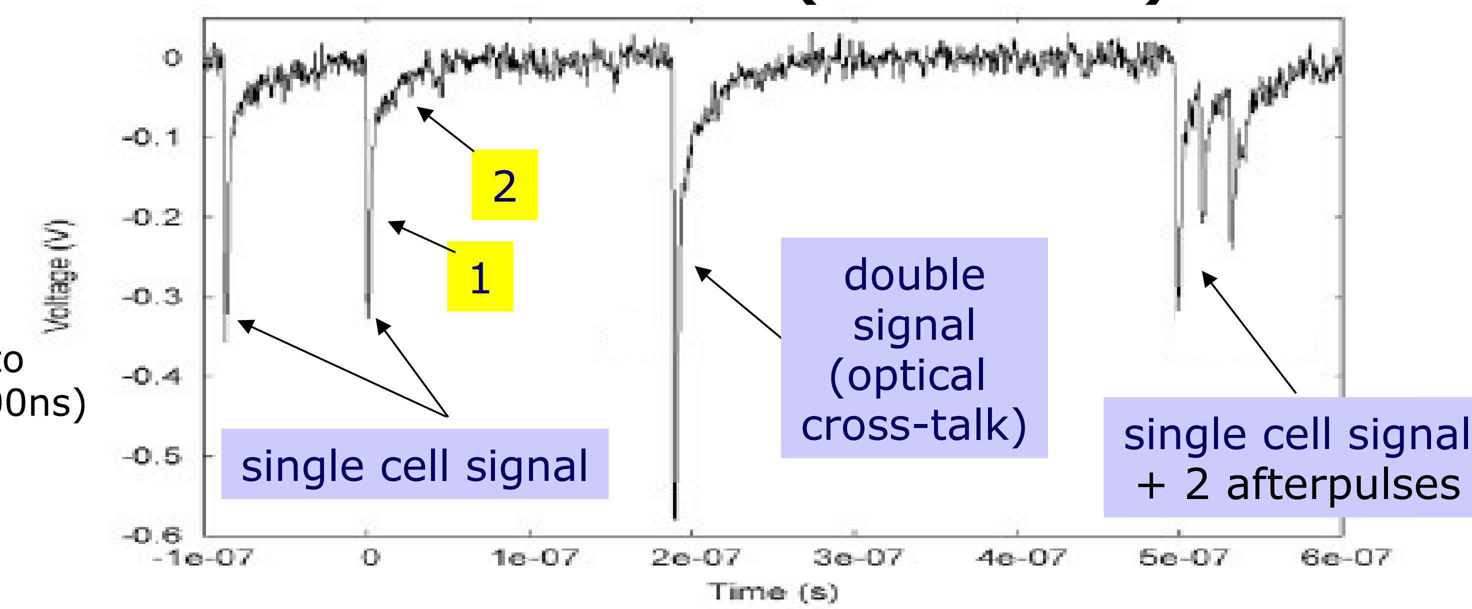

Charge spectrum

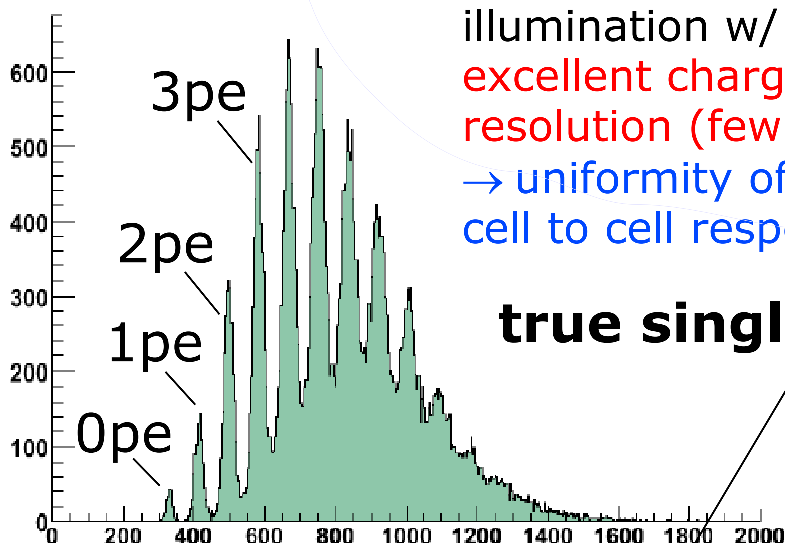

illumination w/ LED
excellent charge resolution (few%)
→ uniformity of cell to cell response

true single ph.e

NOTE: gain easily measured
… better if integrate all charge

Gain

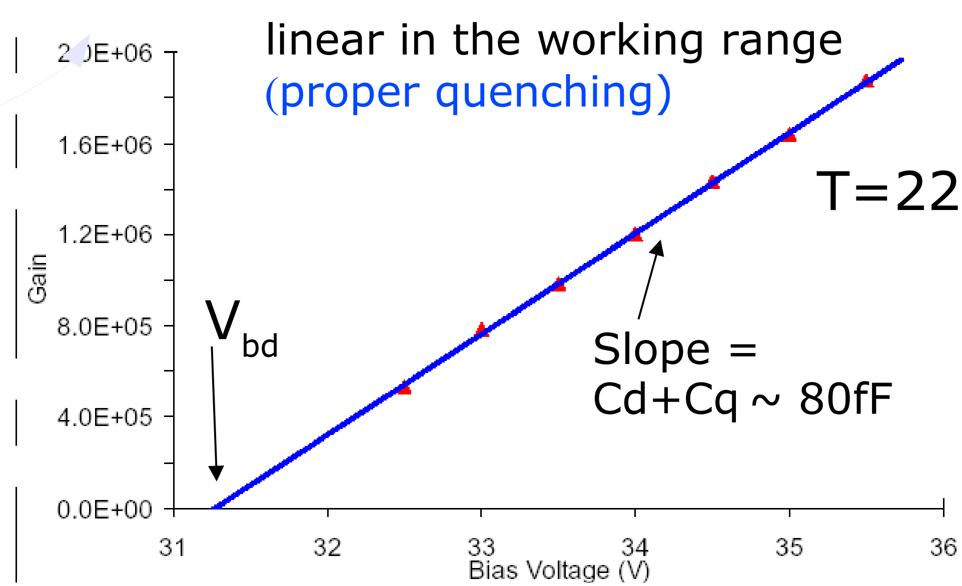

Gain fluctuations (Single Electron Resp.)

$$G = \Delta V (C_q + C_d)/q_e \longrightarrow \frac{\delta G}{G} = \frac{\delta V_{bd}}{V_{bd}} \oplus \frac{\delta C_{d,q}}{C_{d,q}}$$

- uniformity of cell geometry (active area and volume → $C_{d,q}$) control at % level

SiPM gain fluctuations (intrinsic) differ in nature compared to APD where the statistical process of internal amplification shows a characteristic fluctuations

- intrinsic: local doping densities (Poisson): $\delta V_{bd} \sim O(0.1V)$ *Shockley, Sol. State Ele. 2 (1961) 35*

- doping, epitaxial, oxide (processing): $\delta V_{bd} \sim O(0.1V)$

- Additional δG due to fluctuations of
  - quenching time (Rq)
  - charge (after-pulses)

SES MEPhI/PULSAR APD, U=57.5V, T=-28 C

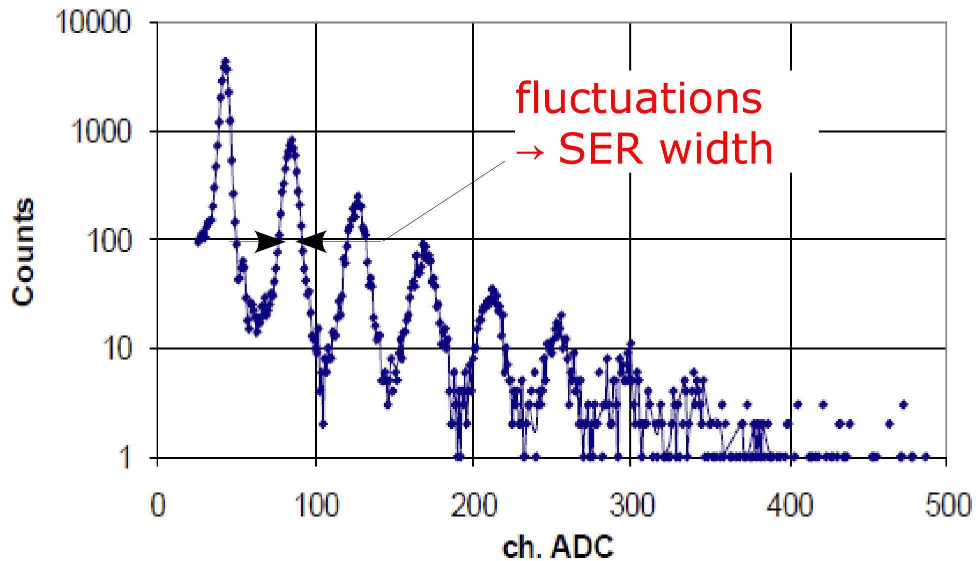

G.Collazuol - RICH 2013

Recent improvements in V_{bd} uniformity

Engineering high electric field & depletion/drift layer profiles

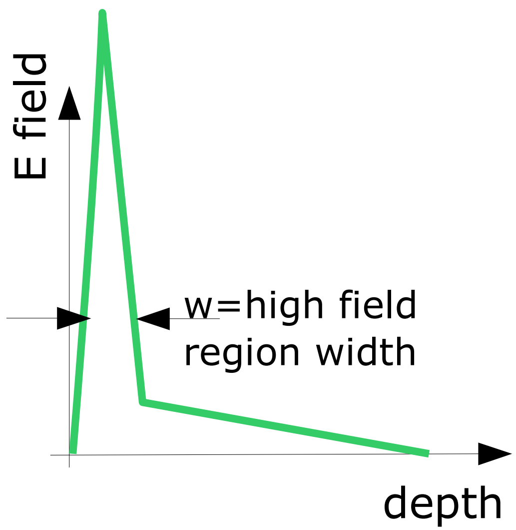

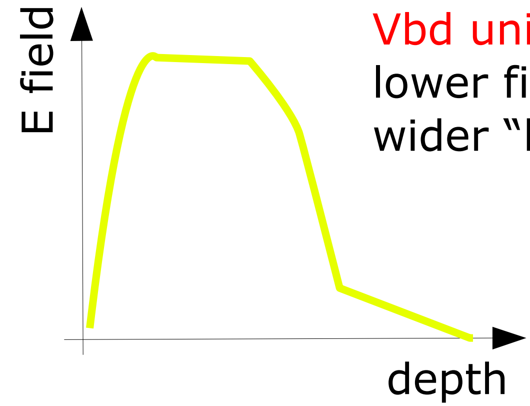

Vbd uniformity easier with lower field over a wider "high field" region

Recent progresses in FBK-Advansid devices

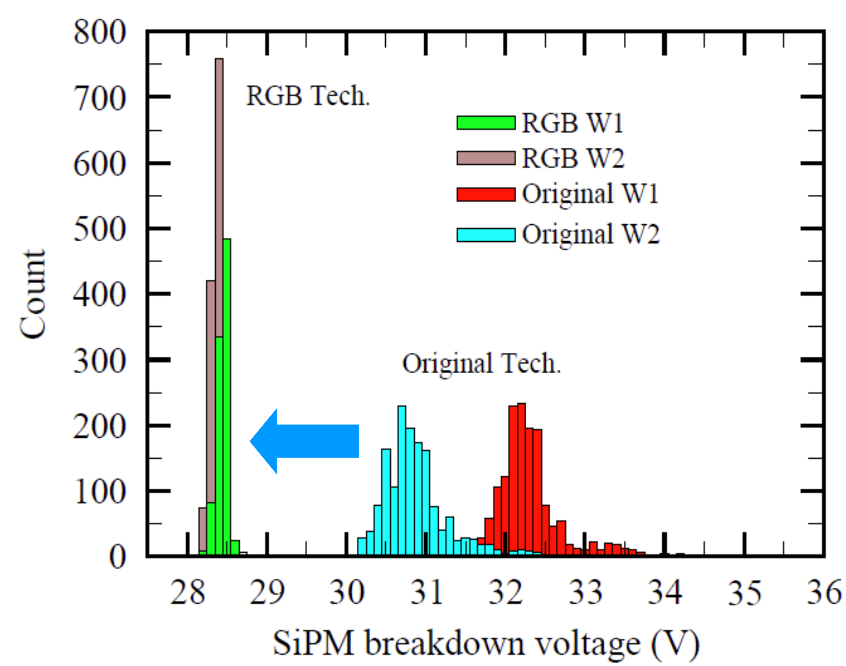

→ Improved break-down voltage uniformity
- at wafer level
- among wafers

N.Serra: "Characterization of new FBK SiPM technology for visible light detection", JINST 2013 JINST 8 P03019

Note: also improvement on T coefficient of V_{bd} → stability

Response Non-Linearity

Non-proportionality of charge output w.r.t. number of photons (i.e. response) at level of several % might show up even in quenching regime (negligible quenching time), depending on ΔV and on the intensity and duration of the light pulse.

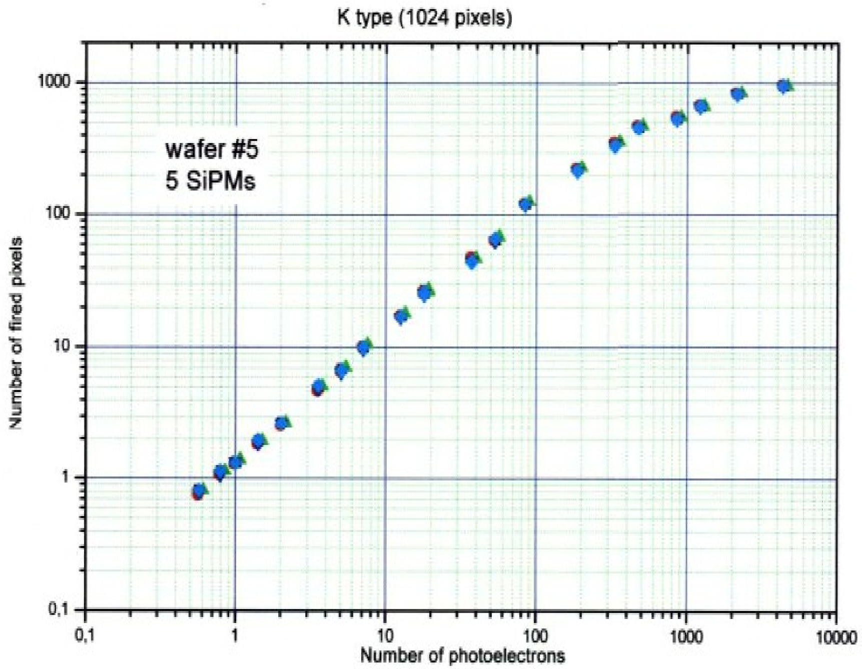

Main sources are:

- finite number of pixels
- finite recovery time
- after-pulses, cross-talk
- drop of ΔV during the light pulse

in case of large signal current on series (ballast) resistances

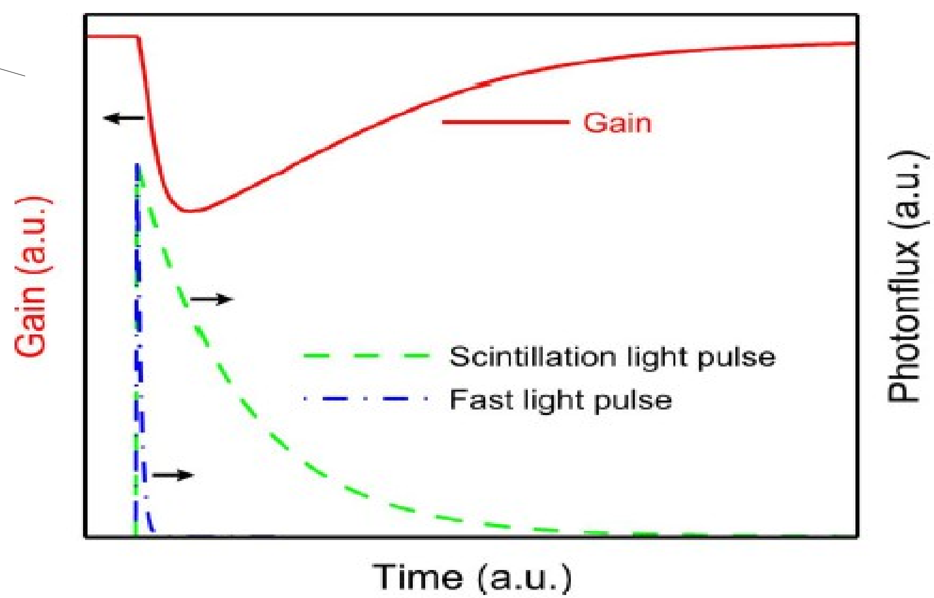

T.van Dam IEEE TNS 57 (2010) 2254

Detailed model to estimate non-lin. corrections

Finite number of cells is main contribution in case number of photons ~ O(number of cells) (dynamic range not adequate to application)

→ saturation $n_{fired} = n_{all}\left(1-\mathrm{e}^{-\frac{n_{phot.}PDE}{n_{all}}}\right)$

→ loss of energy resolution

see Stoykov et al JINST 2 P06500 and Vinogradov et al IEEE NSS 2009 N28-3

G.Collazuol - RICH 2013

Tiny cell → better performance

Many small cell SiPM types available
→ **Fill Factor improving** (> 50%)

- tiny cells (→ 10-15μm)
  → HPK, FBK-Advansid, NDL, MPI-LL, …
- micro cells (→ μm)
  → Zecotek, AmplititionTechn.

tiny cell MPPC (2012) by Hamamatsu

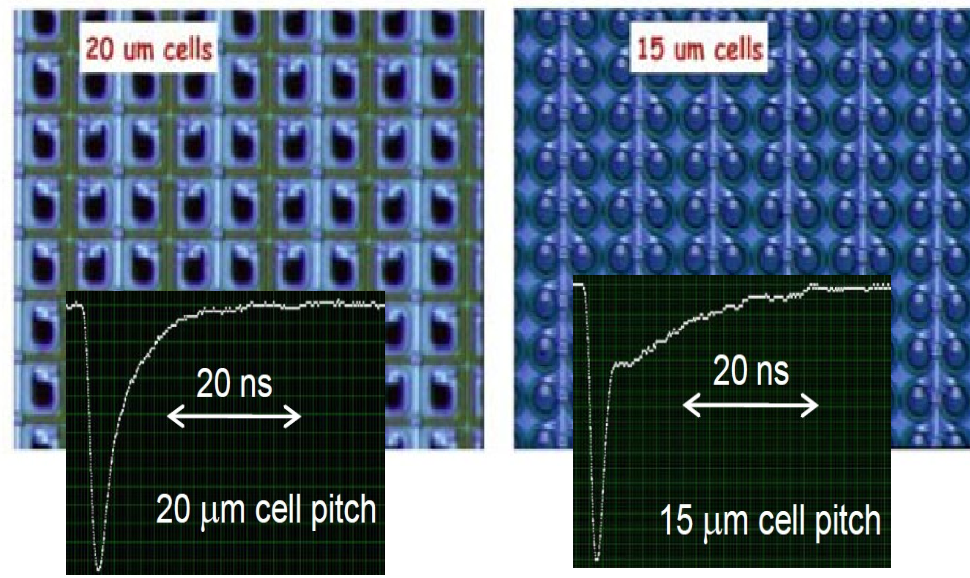

SiPMs NDL (Bejiing)

Zhang et al NIM A621 (2010) 116
Han at NDIP 2011

- type: n-on-p, Bulk Rq
- high cell density (10000/mm²)
- fast recovery (5ns)
- low gain
- **better timing**

→ **dynamic range**

→ **less after-pulsing**
→ **less cross-talk**
→ **mitigate effects of radiation damages**

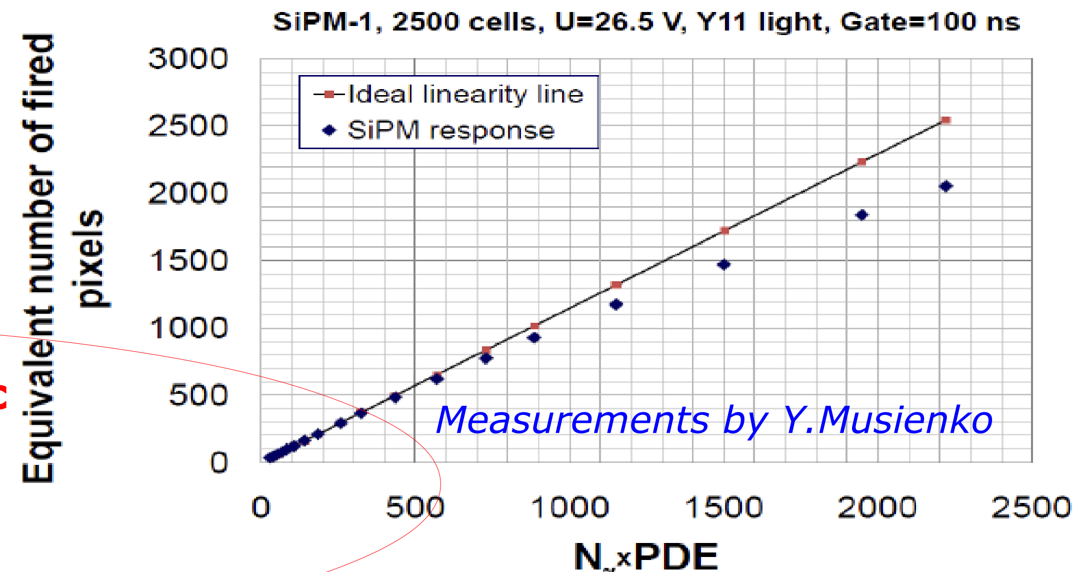

Noise sources → recent improvements

pulses triggered by non-photo-generated carriers (thermal / tunneling generation in the bulk or in the surface depleted region around the junction)

Primary noise

→ dark counts

Correlated "excess" charge:

→ After-pulsing

→ Cross-Talk

"optical"

carriers can be trapped during an avalanche and then released triggering another avalanche

photo-generation during the avalanche discharge. Some of the photons can be absorbed in the adjacent cell possibly triggering new discharges

Dark current vs T

- Two sources (SHR-TAT, BBT)
- Affecting mainly the high field region

Noise mainly comes from the high E Field region (no whole depletion region)

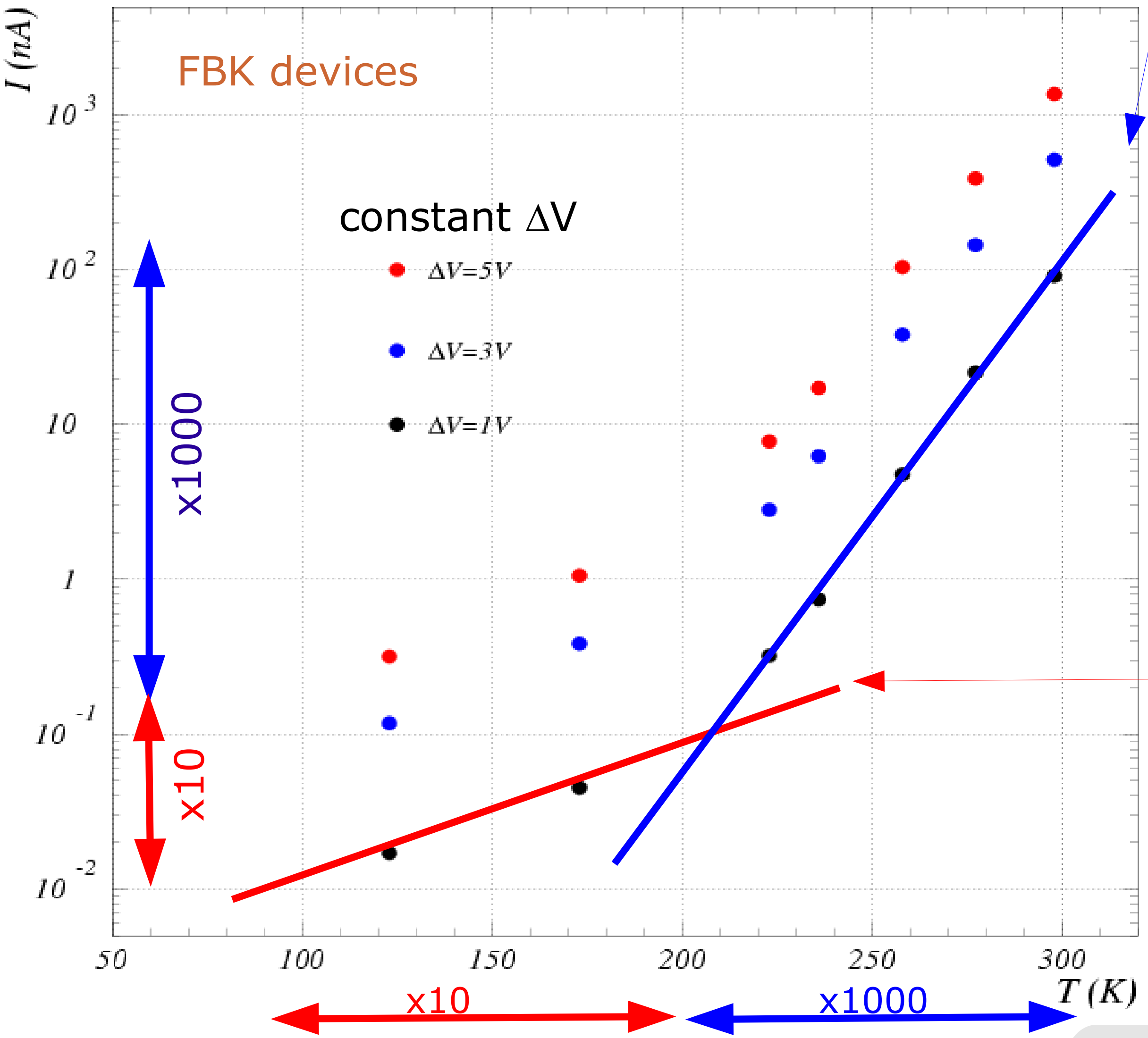

1) Generation/Recombination SRH noise (enhanced by trap assisted tunneling)

$$I_{reverse} \sim T^{1.5} \exp \frac{-E_{act}}{K_B T}$$

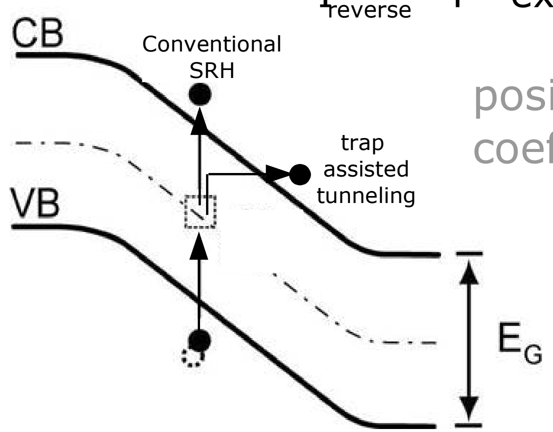

positive T coefficient

2) Band-to-band Tunneling noise (strong dependence on the Electric field profile)

negative T coefficient

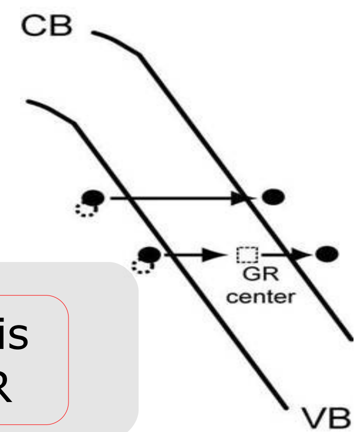

Tunneling noise dominating for T<200K (sharp high E field region → higher noise)

E field engineering is crucial for min. DCR

Recent improvements against Dark Counts

Engineering high electric field & depletion/drift layer profiles

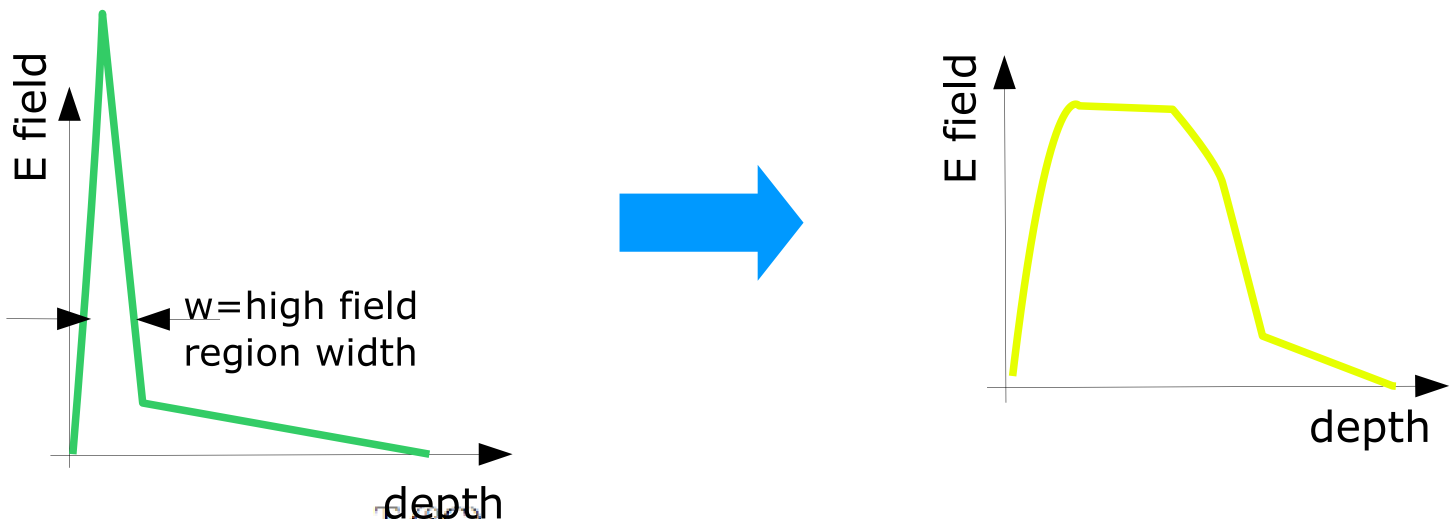

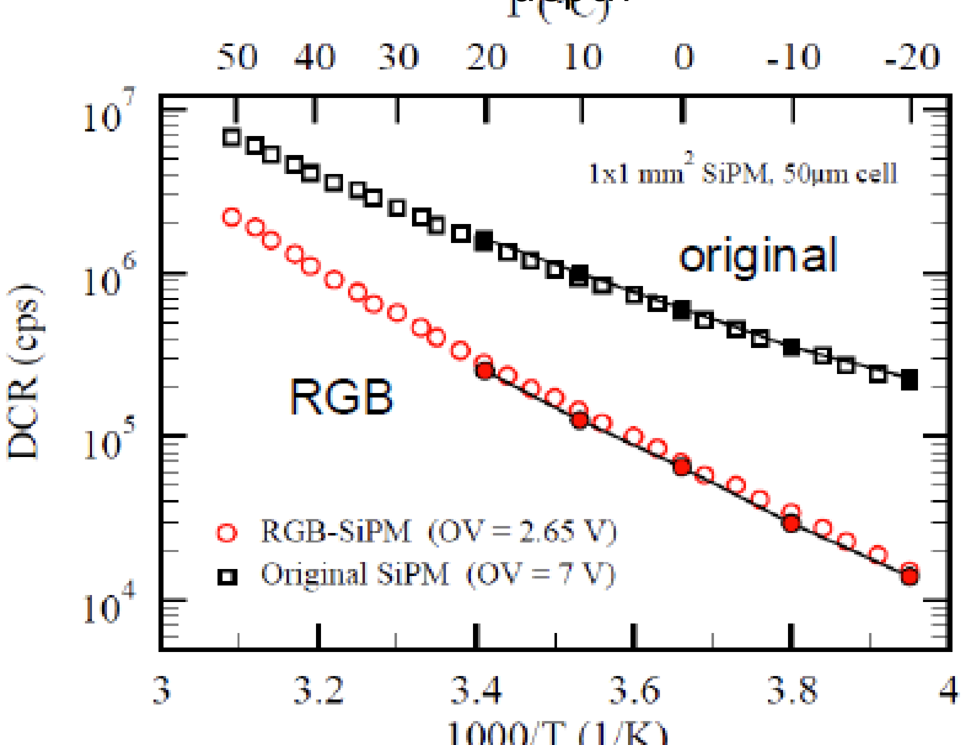

RGB has a much lower noise and a steeper temperature dependence:

→ **less tunneling**

Recent progresses in FBK-Advansid devices

Recent improvements against Dark Counts

KETEK PM 3350 (p^+-on-n, shallow junction)
$3x3mm^2$ active area pixel size $50x50\ \mu m^2$

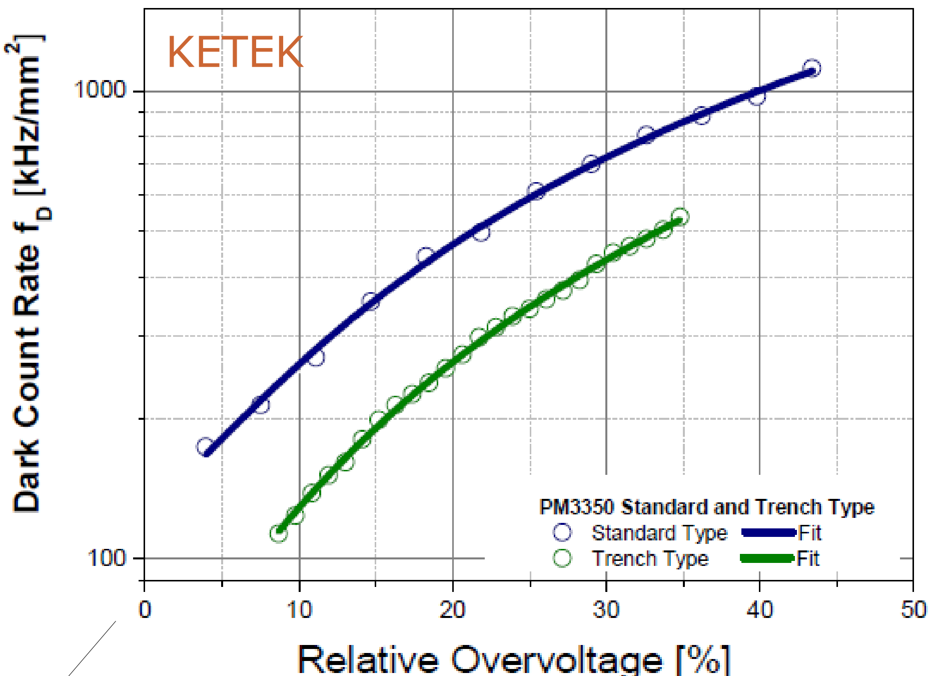

V_{bd} ~ 25V

F.Wiest – AIDA 2012 at DESY

Critical issues:
- quality of epitaxial layer
- gettering techniques
- Electric field → tunneling

Exelitas 1st generation SiPM 2011
(p^+-on-n) $1x1mm^2$

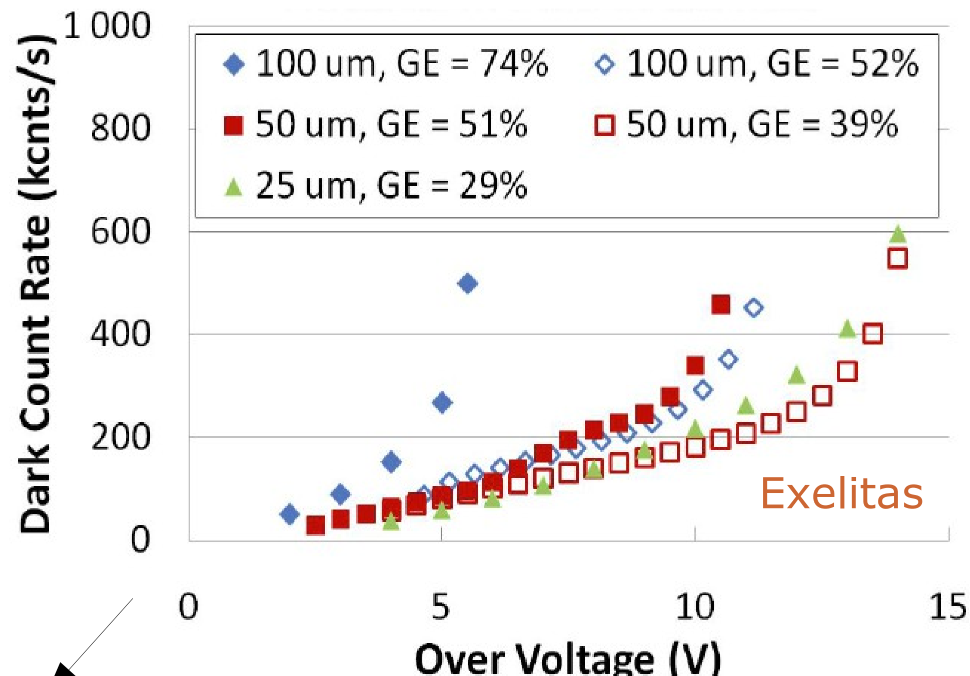

V_{bd} ~ 140V

P.Berard – NDIP 2011

Various devices show
DCR below ~$100kHz/mm^2$
in extended over-voltage range

DCR – comparison of recent devices

Hamamatsu most recent devices (2013) work at very low Dark Count Rate (few x 10kHz)

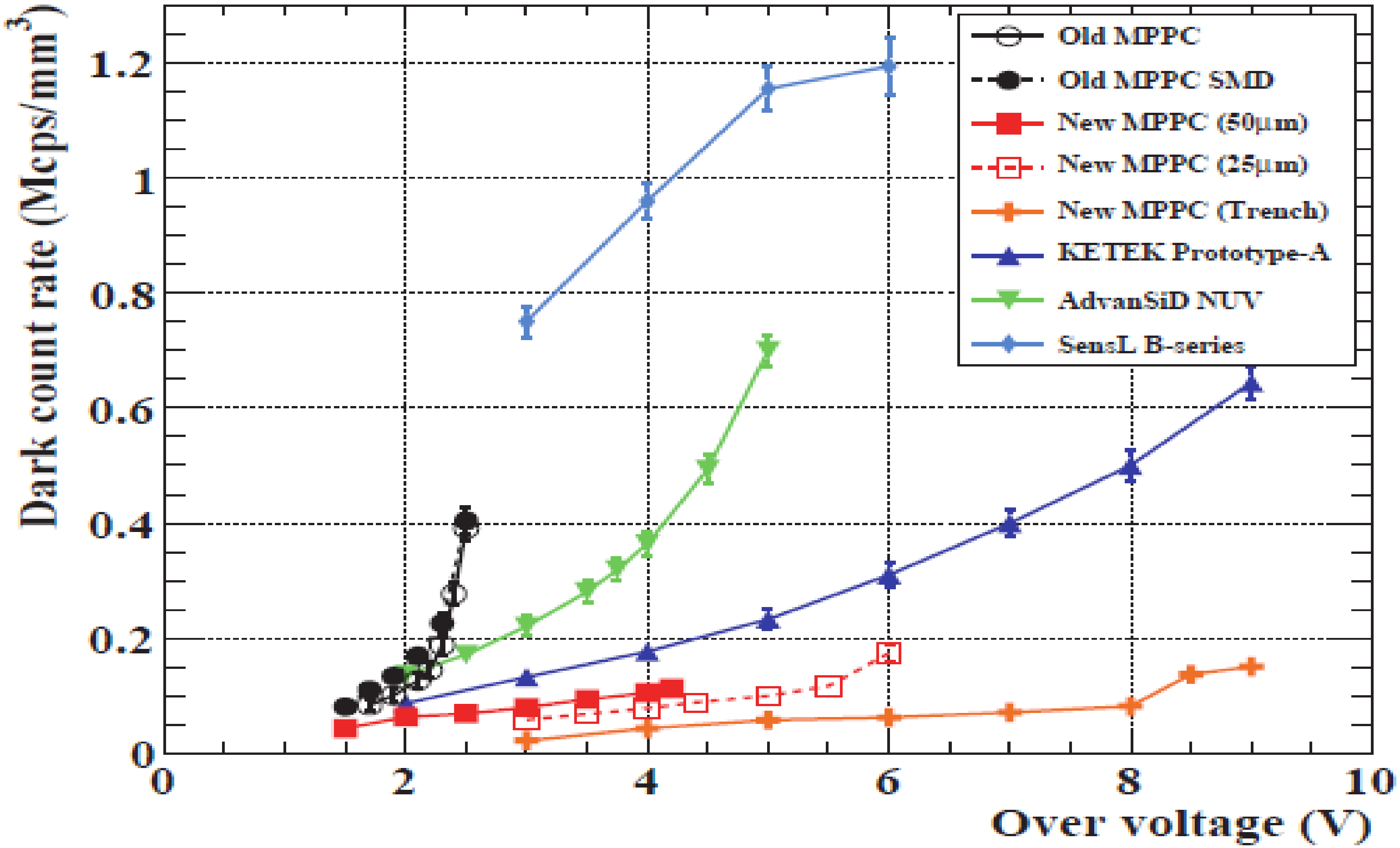

Y.Uchiyama et al
IEEE NSS 2013

Note: DCR depends on Over-voltage, as well as PDE
→ plotting DCR vs PDE yields fairer comparison

DCR - digital-SiPM (Philips)

Control over individual SPADs enables detailed device characterization

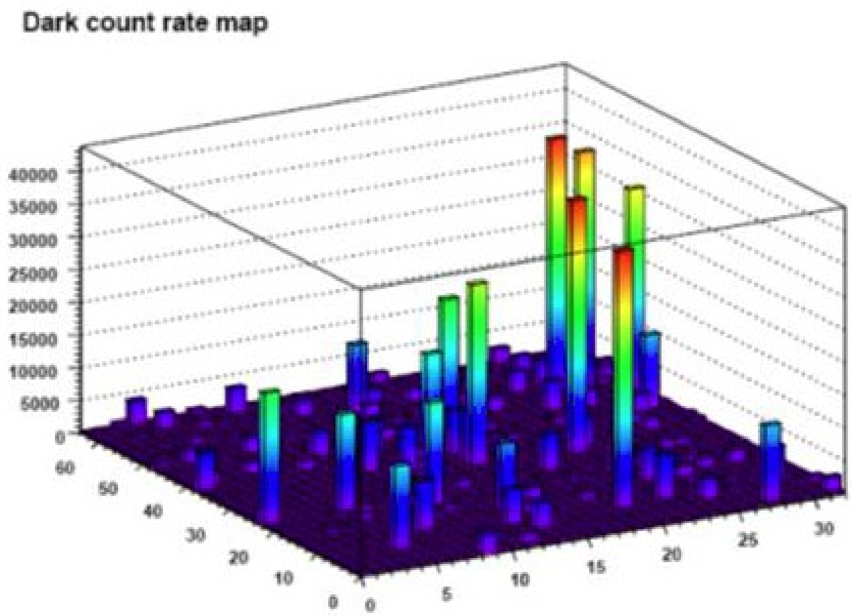

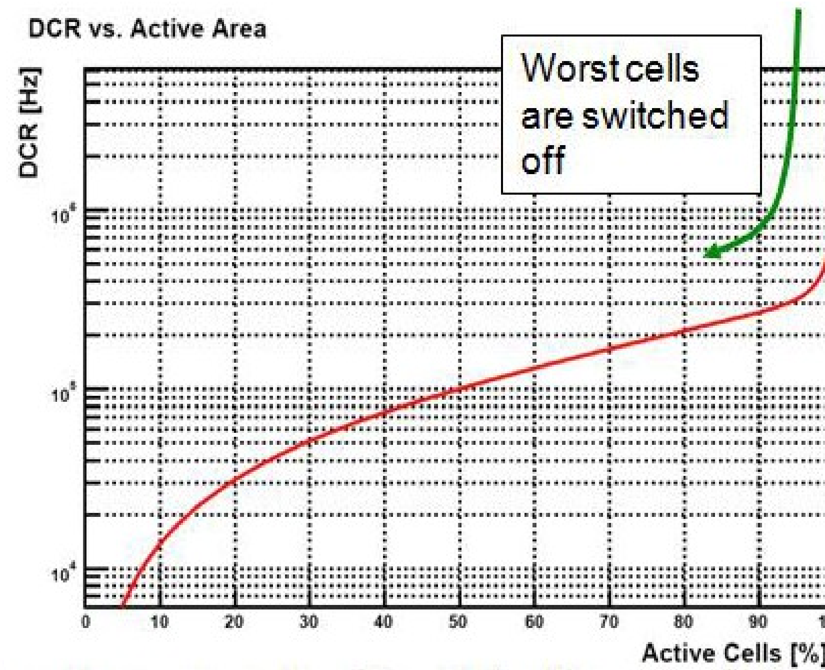

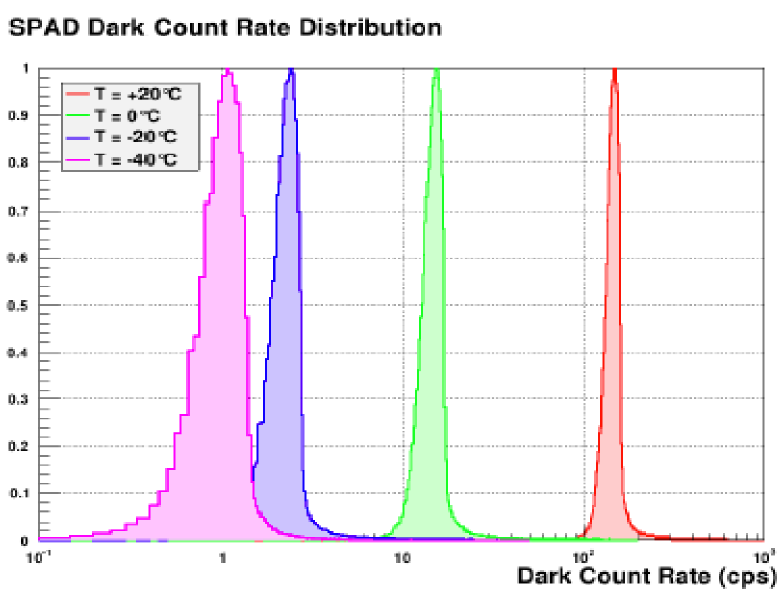

- Over 90% good diodes (dark count rate close to average)
- Typical dark count rate (DCR) at 20°C and ΔV=3.3V ~150Hz / diode
- Low DCR ~1-2Hz/diode at -40°C

T.Frach at Heraeus Seminar 2013

After-Pulsing Carrier trapping and delayed release

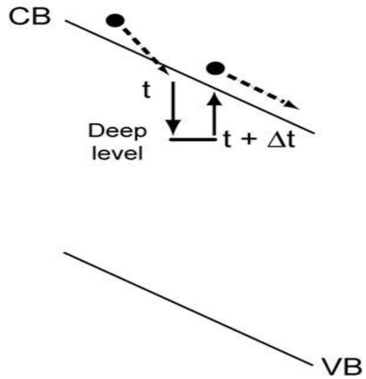

$$P_{afterpulsing}(t) = P_c \cdot \frac{\exp(-t/\tau)}{\tau} \cdot P_{01} \quad \propto \Delta V^2$$

~Few % level at 300K

avalanche triggering probability
$\propto \Delta V(t)$

τ : trap lifetime
depends on trap level position

P_c : trap capture probability
$\propto$ carrier flux (current) during avalanche $\propto \Delta V$
$\propto$ N traps

quadratic dependence on ΔV

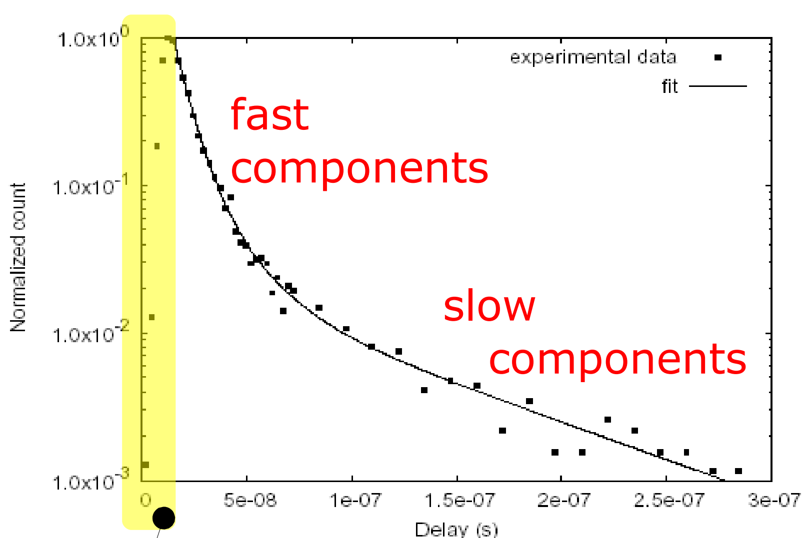

Fig. 10. Spectrum of the delay time from the primary pulse to the after-pulse.

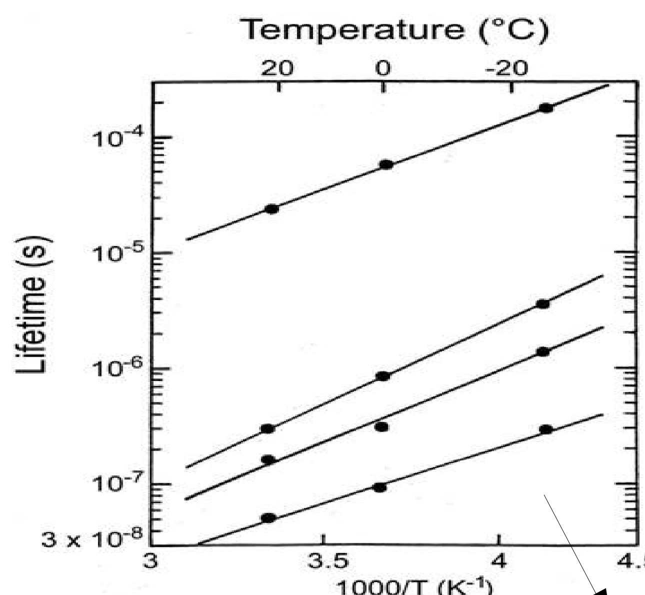

S.Cova, A.Lacaita, G.Ripamonti, IEEE EDL (1991)

not trivial dependence on T

Only partially sensitive to after-pulsing during recovery
ie recovery hides After-pulses (does not cancel them)

Optical cross-talk

Avalanche luminescence (NIR)

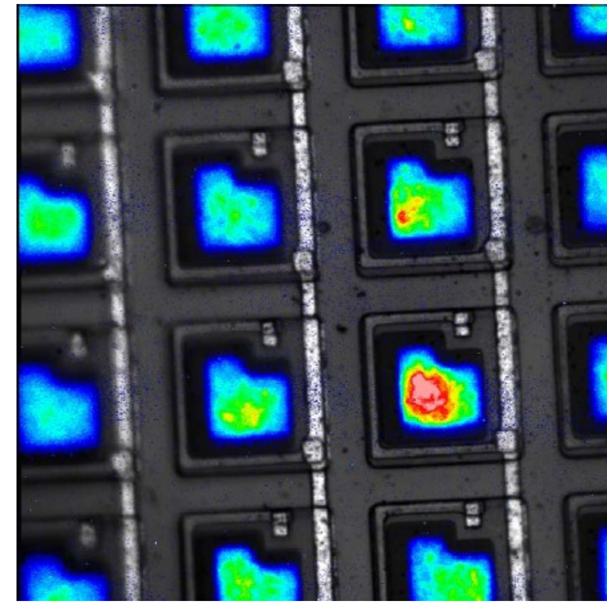

N.Otte, SNIC 2006

Carriers' luminescence (spontaneous direct relaxation in the conduction band) during the avalanche: probability 3.10^{-5} per carrier to emit photons with E> 1.14 eV

A.Lacaita et al. IEEE TED (1993)

Photons can induce avalanches in neighboring cells. Depends on distance between high-field regions

ΔV^2 dependence on over-voltage:
- carrier flux (current) during avalanche $\propto \Delta V$
- gain $\propto \Delta V$

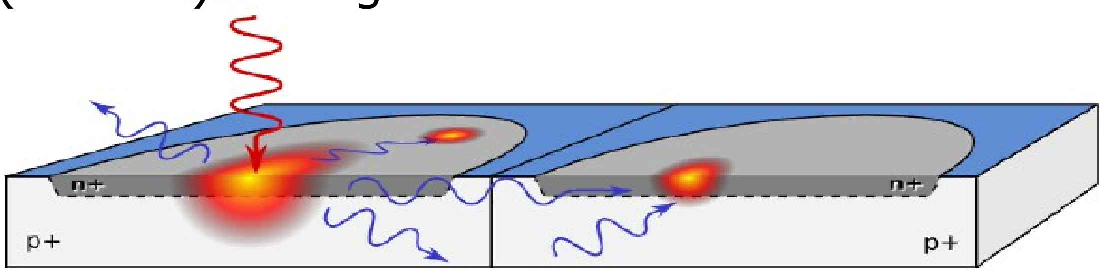

Counteract:
- optical isolation between cells

by trenches filled with opaque material
- low over-voltage operation helps

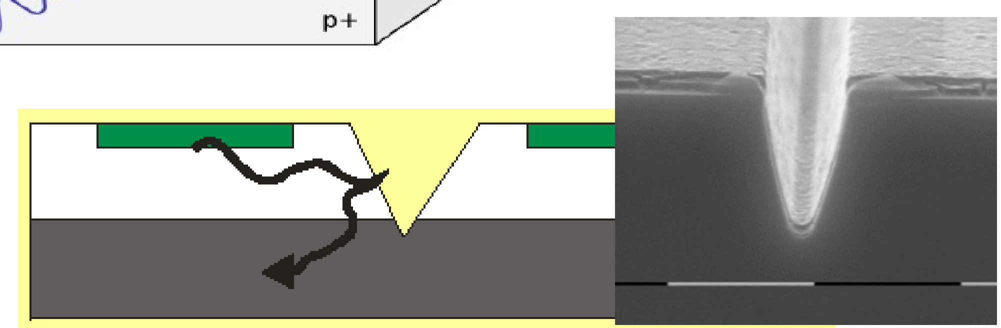

It can be reduced to a level below % in a wide ΔV range

Correlated noise sources

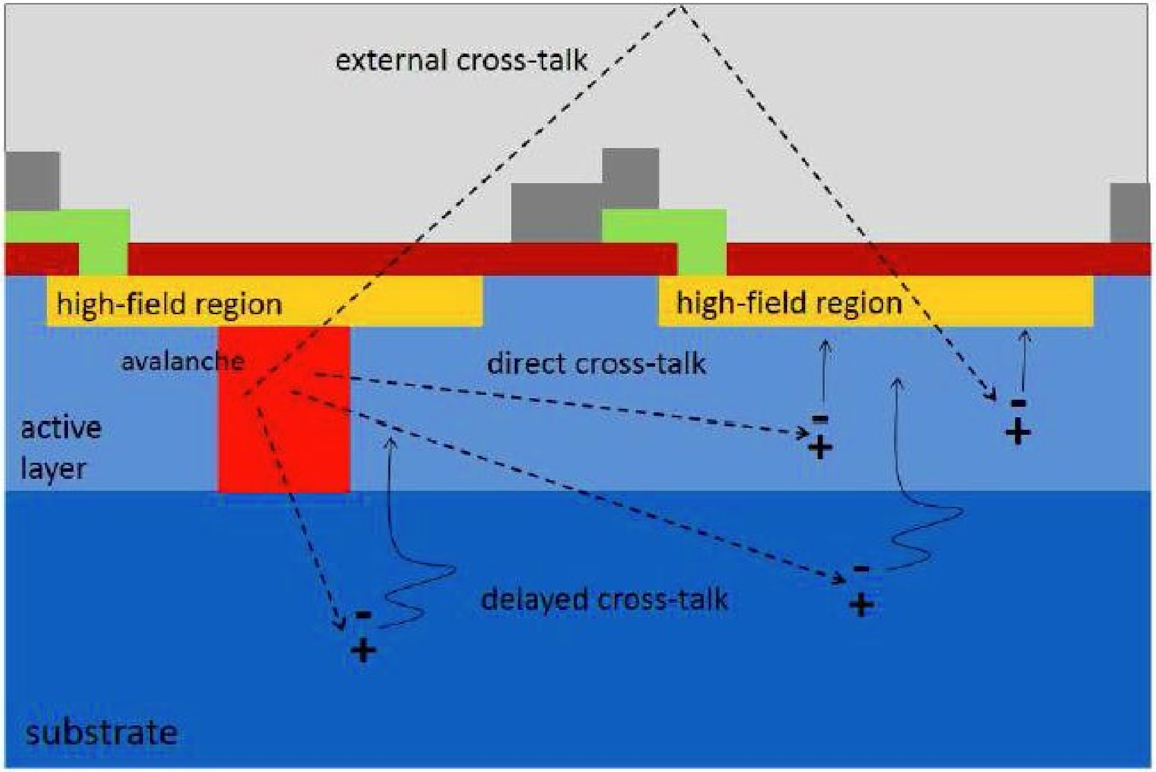

...many paths for optical cross-talk

A.Ferri IPRD 2013

Note:
C.Piemonte et al at IEEE NSS 2012 propose an interesting method for disentangling the various noise components (correlated and not, AP, XT, ...)

- Trenches to avoid direct and delayed cross-talk...
- buried junction to avoid out-diffusion...

- lower gain → use tiny cells (passive quenching)
(ie less charge) → or active quenching devices

Recent devices from Hamamatsu (2013)

Reduced After-pulsing or Cross-Talk rates...
(… not simultaneously in the same device)

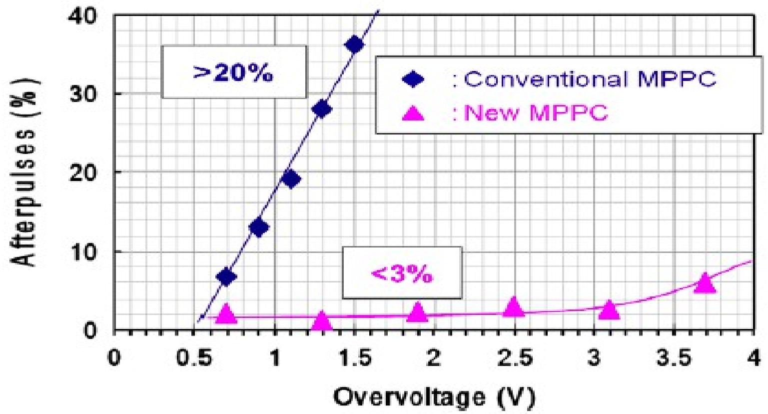

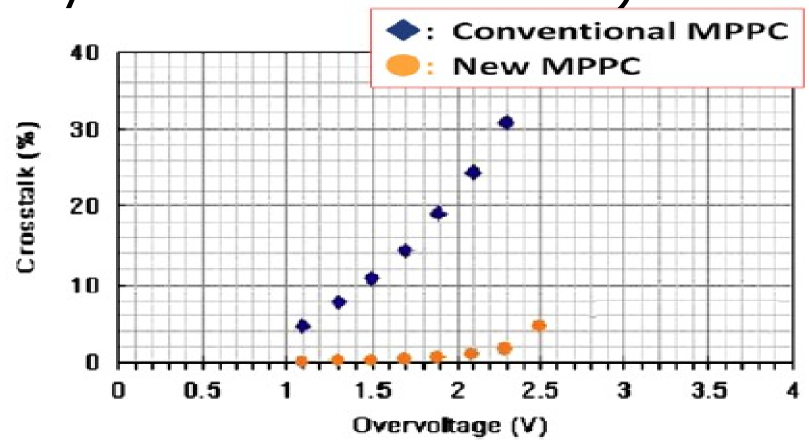

trench type device

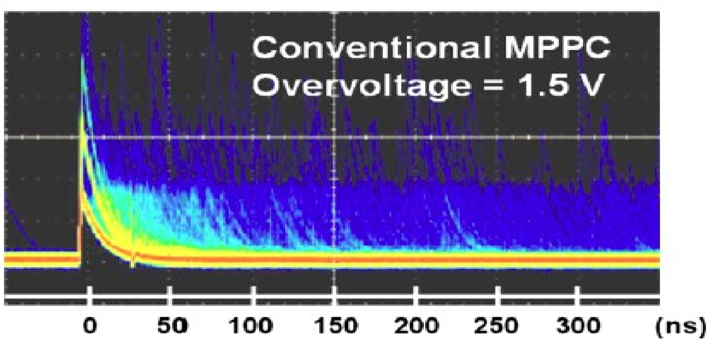

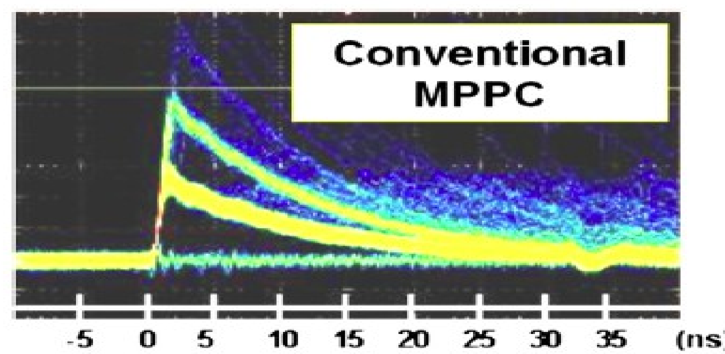

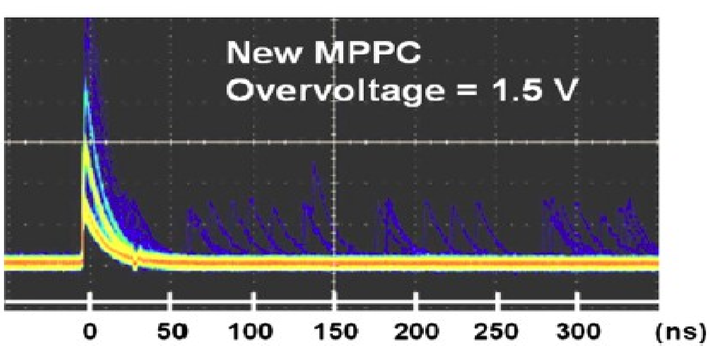

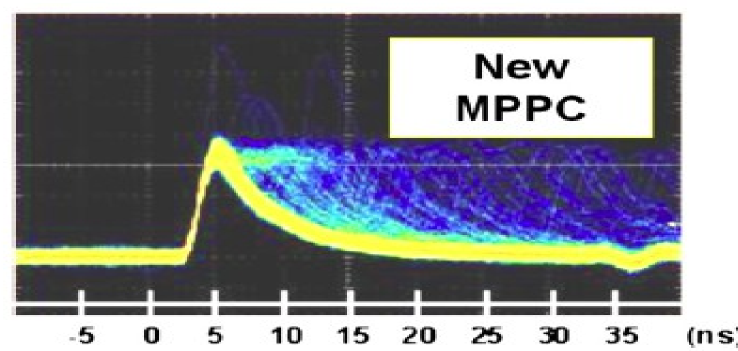

K.Sato et al Vienna Conference on Instrumentation 2013

Cross talk in most recent devices

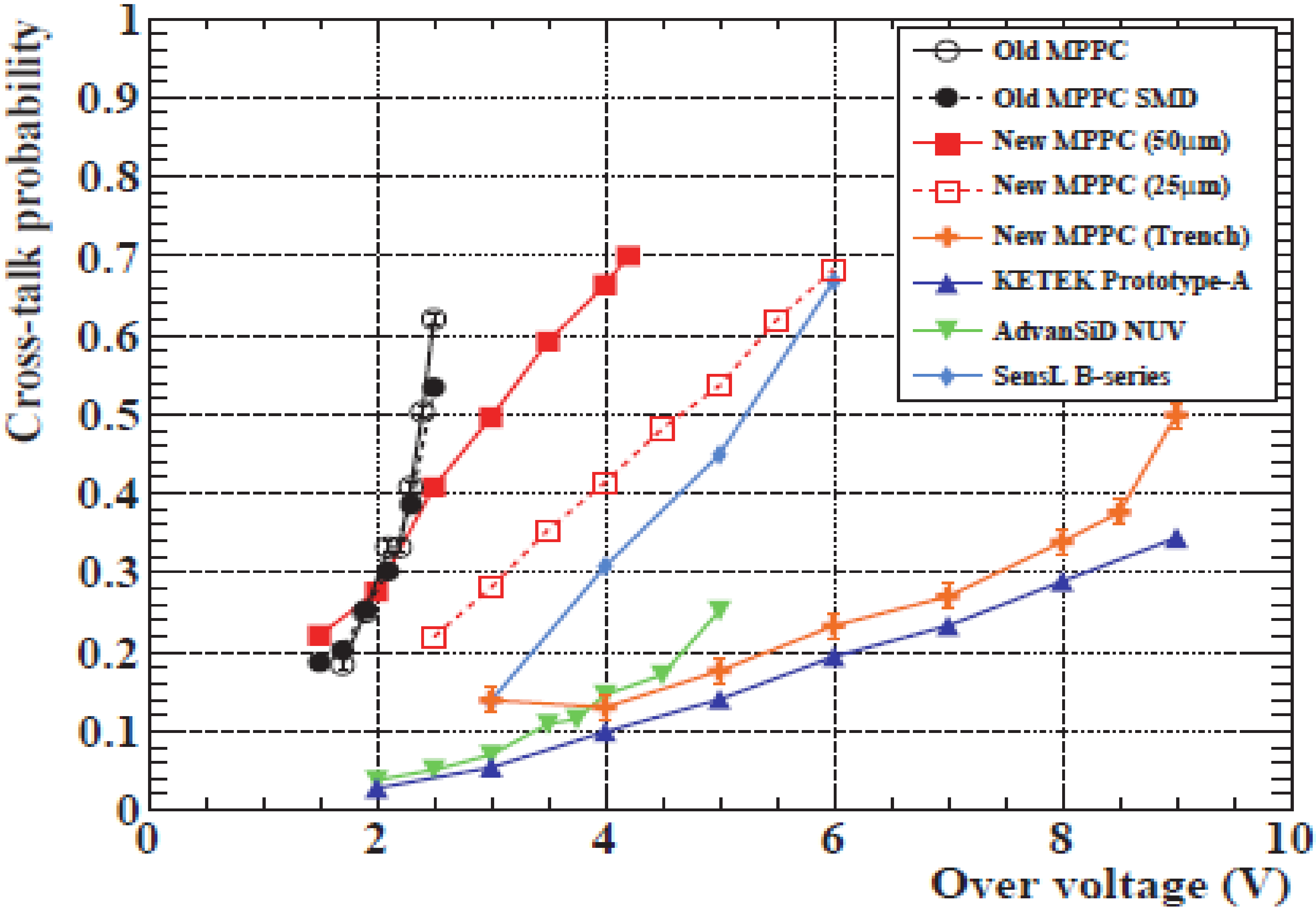

Y.Uchiyama et al IEEE NSS 2013

Photo-Detection Efficiency - PDE

- PDE dependence on wavelength
  (tuning to match application requirements)
- Recent improvements on peak PDE
- UV and VUV enhanced devices

Photo-Detection Efficiency (PDE) – 3 factors

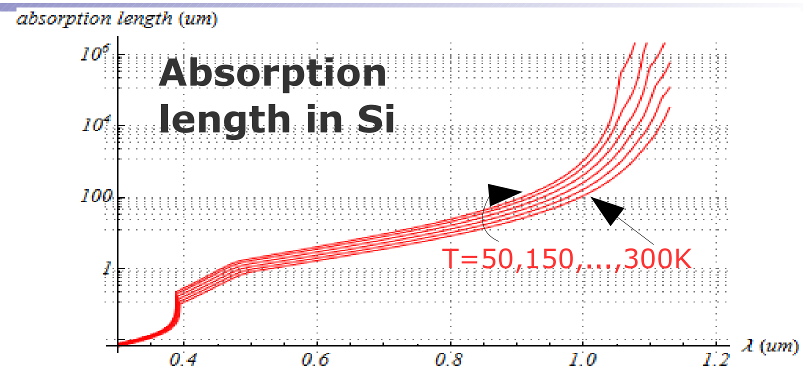

QE: carrier Photo-generation

probability for a photon to generate a carrier
(in the **active region**) that reaches the high field region

→ λ and T dependent
→ ΔV independent if full depletion at V_{bd}

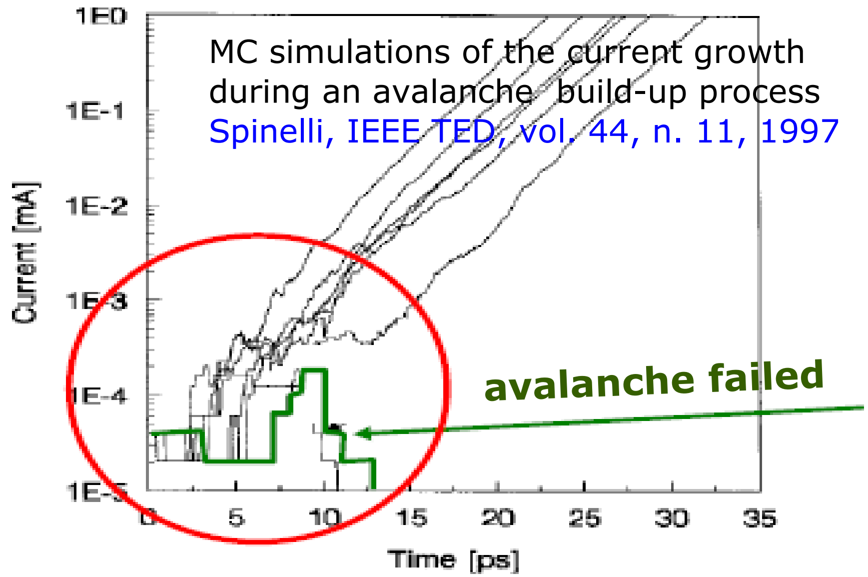

P_{01} : avalanche triggering probability

probability for a carrier traversing the
high-field to **generate the avalanche**

→ λ, T and ΔV dependent

FF: geometrical Fill Factor

fraction of dead area due to structures
between the cells, eg. guard rings, trenches

→ negligible ΔV dependence (cell edges)

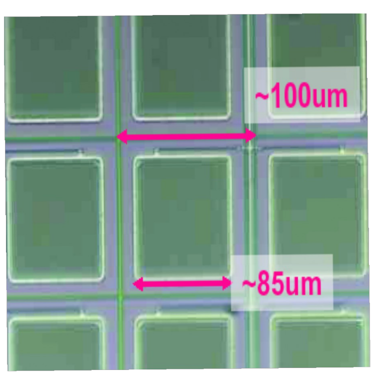

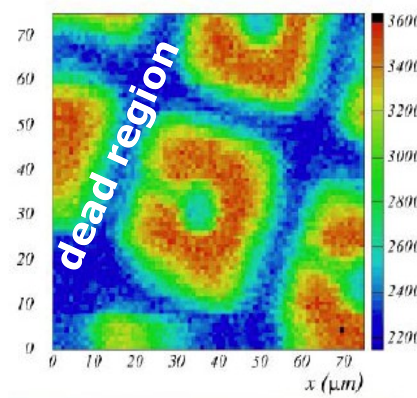

Aval. Triggering Probability → PDE shape vs λ

Tuning PDE spectrum:
(matching applications)

- junction depth (shallow → reach trough)
- junction type (p-on-n or n-on-p)

main PDE absolute scale differences due to Fill Factor

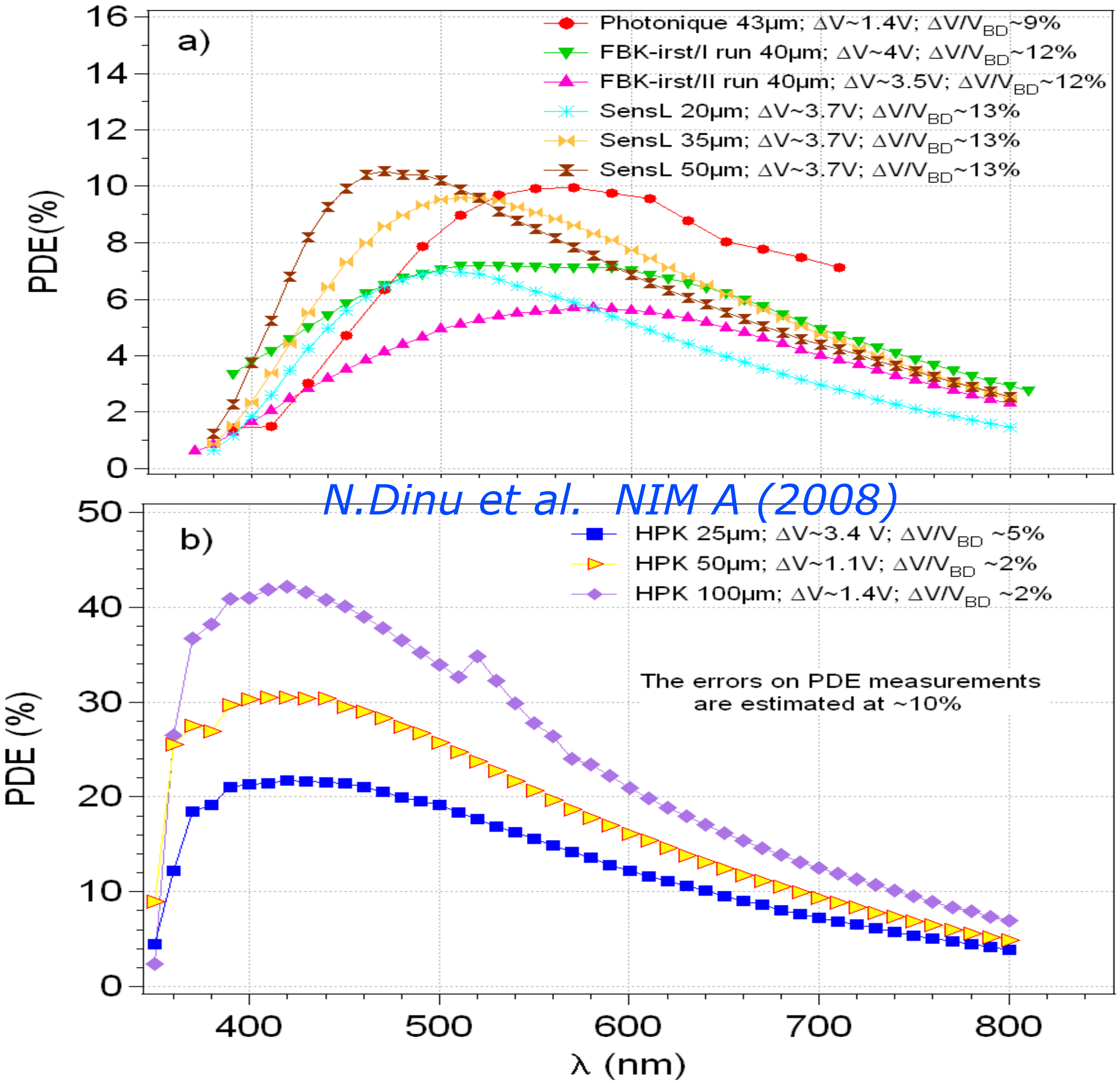

N.Dinu et al. NIM A (2008)

n-on-p structures

sensitivity peak → green-red

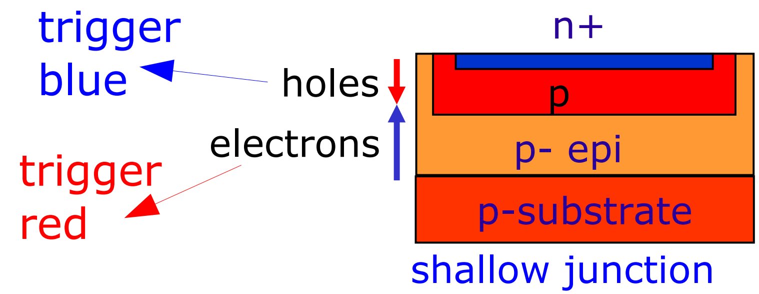

Ionization rate in Silicon

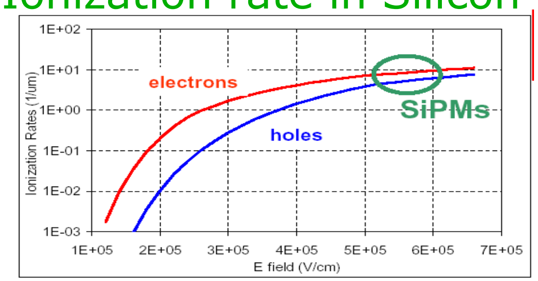

p-on-n structures

sensitivity peak → blue

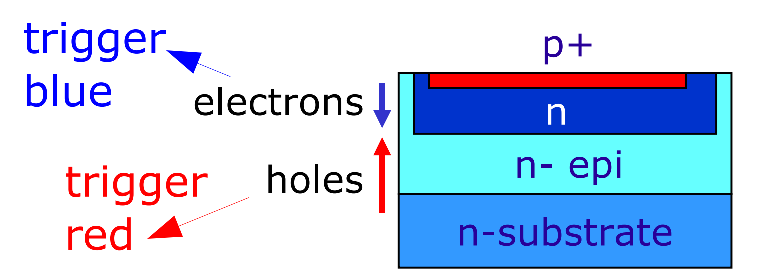

Aval. Triggering Probability → PDE shape vs λ

main PDE absolute scale differences due to Fill Factor

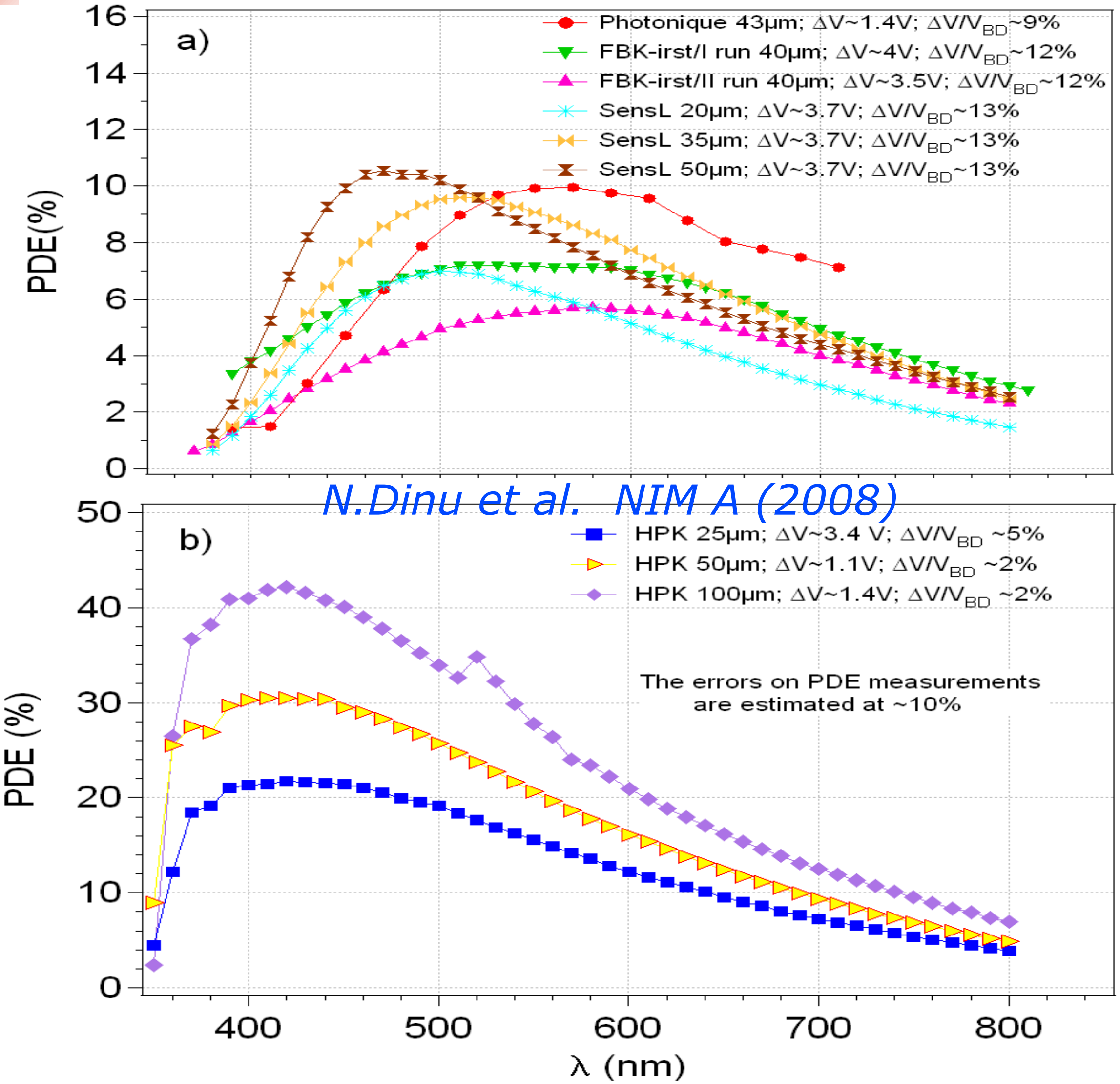

N.Dinu et al. NIM A (2008)

n-on-p structures

sensitivity peak → green-red

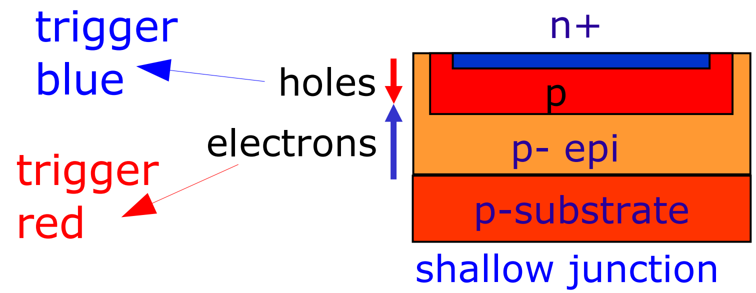

Ionization rate in Silicon

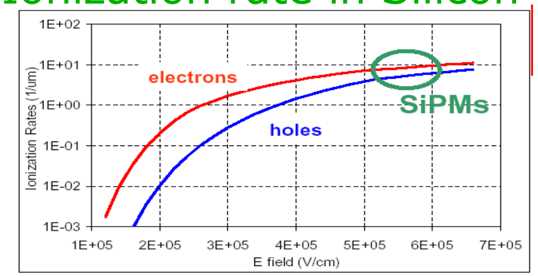

p-on-n structures

sensitivity peak → blue

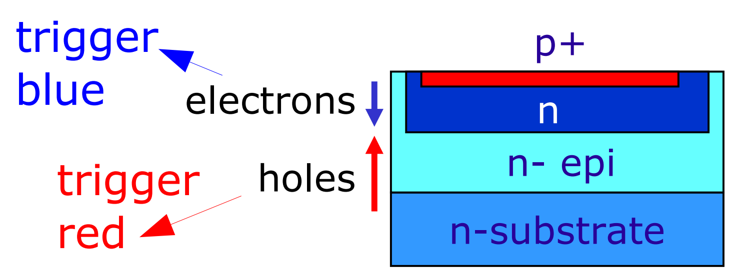

Tuning PDE spectrum: (matching applications)

- structure type (shallow or reach trough)
- junction type (p-on-n or n-on-p)

Recent improvements in PDE

Barlow – LIGHT 2011

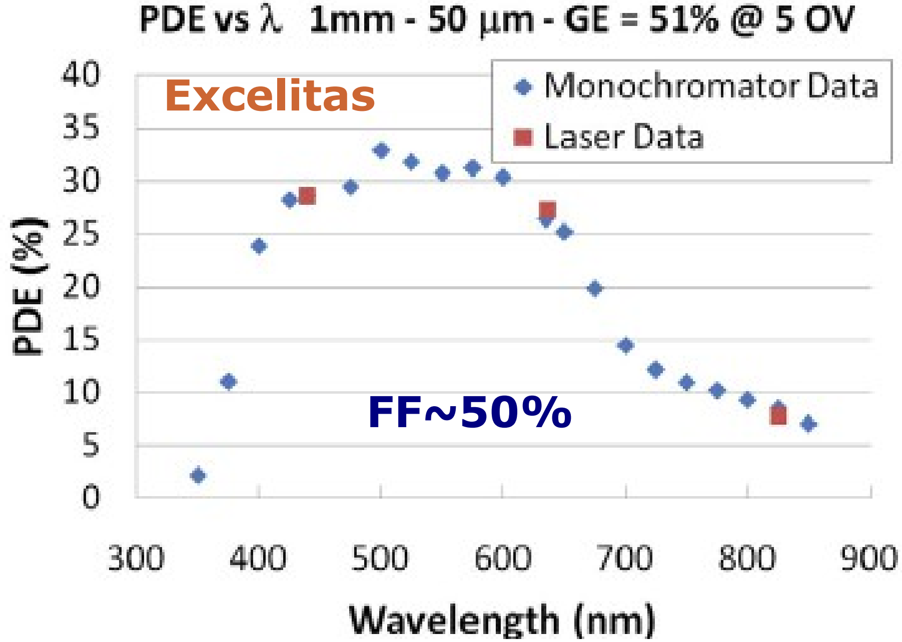

→ PDE peak constantly improving for many devices
→ every manufacturer shape PDE for matching target applications

F.Wiest – AIDA 2012 at DESY

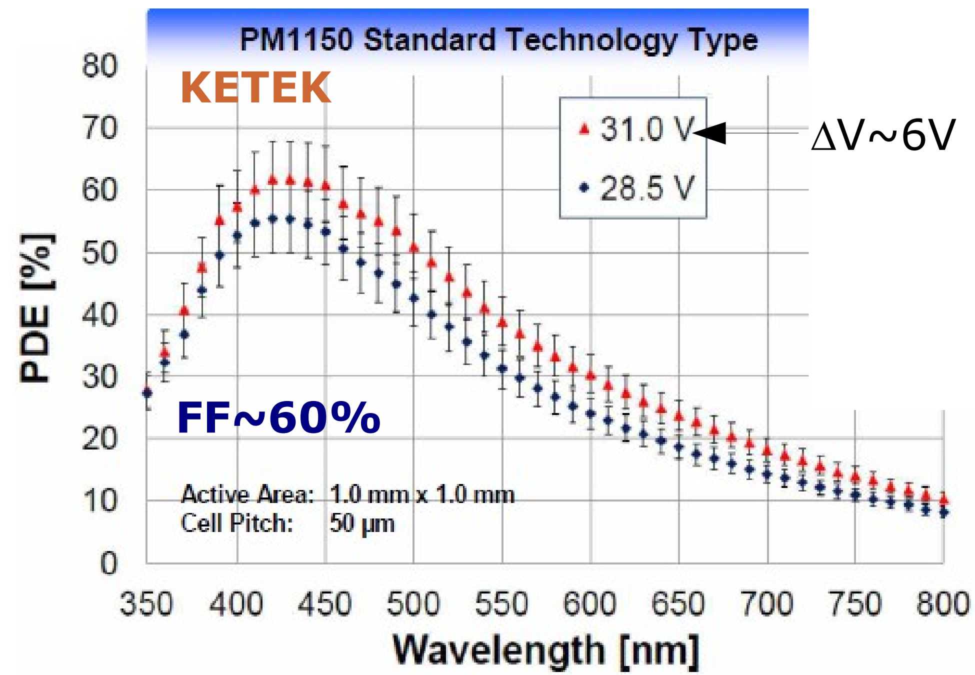

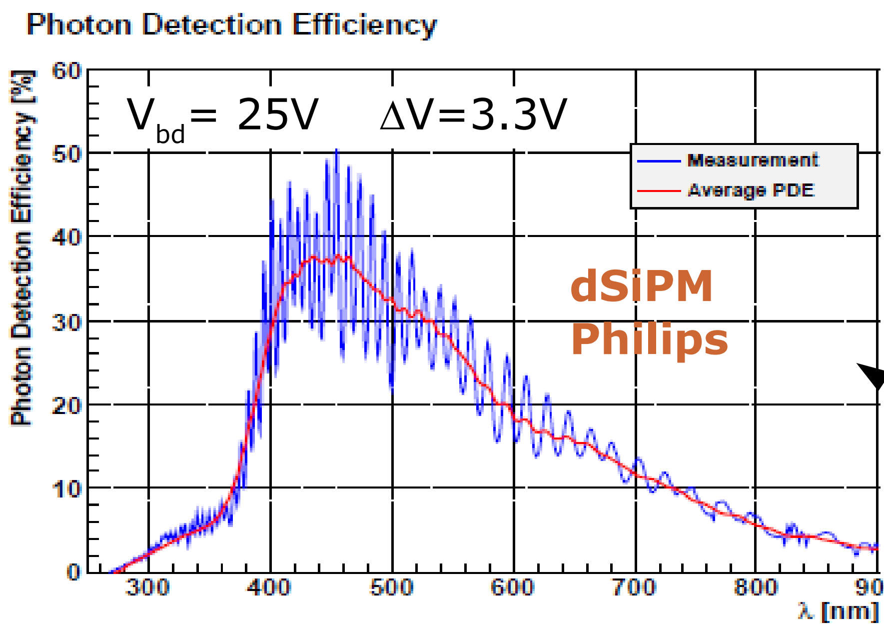

T.Frach 2012 JINST 7 C01112

dSiPM (latest sensor 2011)
→ up to now no optical stack optimization
→ no anti-reflecting coating
→ potential improvement up to 60% peak PDE (*Y.Haemish at AIDA 2012*)

UV and VUV SiPM development

FBK - Advansid
NUV-SiPM (Near-UV)

- PDE (350nm) ~ 27 % (FF = 45 %)
- DCR = 200 kHz @ 20°C (ΔV = 5V)

A.Ferri et al at IDPASC 2013

Other UV developements:
→ *E.Popova at PhotoDet 2012*

ripple is etalon effect on prototype devices

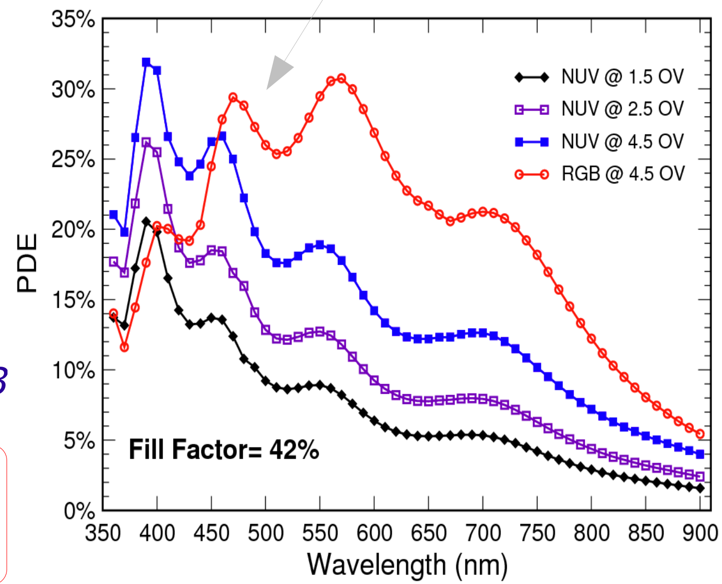

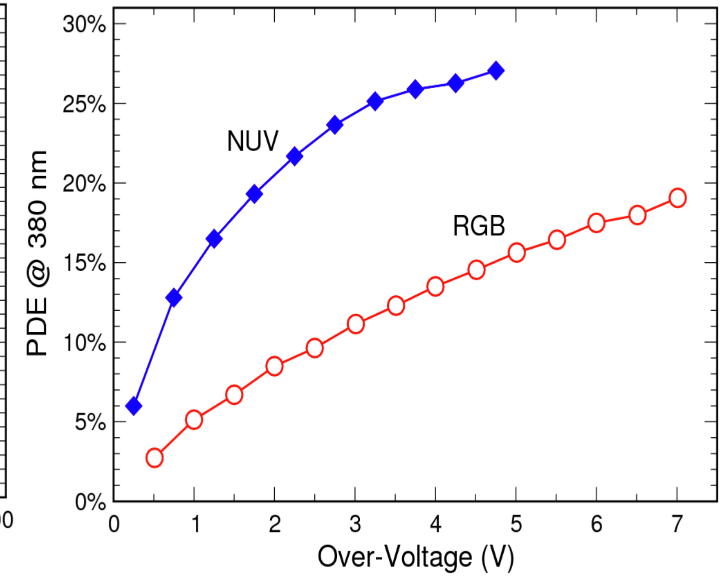

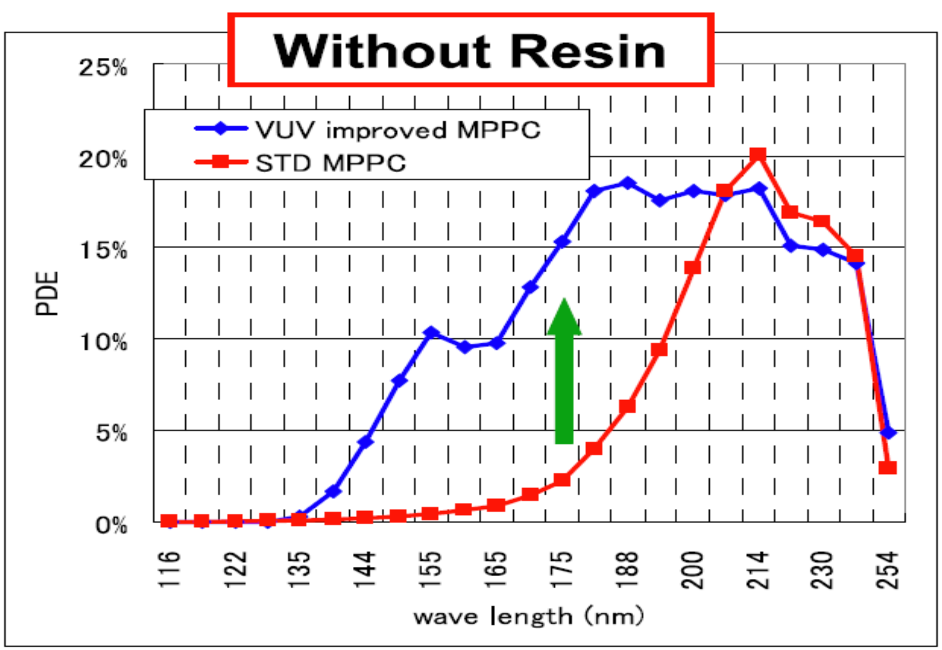

Sato et al - Vienna Conf. on Instr. 2013

Hamamatsu
VUV-enhanced MPPC

→ removal of protection coating
→ optimization of the parameters
- thinner junction
- optimized superficial layers

...

New windows for applications in fundamental Physics experiments
- Dark matter detection
- ν-less double beta decays
- Rare decay modes (MEG)

Timing fluctuations

1) SiPM are intrinsically very fast

Two timing components (related to avalanche developement)

- prompt → gaussian time jitter below **100ps** (depending on ΔV, and λ)
- delayed → non-gaussian tails up to **few ns** (depending on λ)

see G.C. at IDPASC school 2013 - Siena

2) Factors affecting practical timing measurements

→ digital filtering for best timing

→ ARC/CFD ok; ToT to be avoided (for single photon)

3) Optimization of devices for timing

→ enhancing the fast signal component

→ trade-off PDE vs Timing

Discharge transverse size in SiPM and pulse shape simulation

Still too few studies of avalanche development in SiPM
(lots about SPADs instead)

→ Interesting measurements and hybrid model of avalanche development and signal formation by R.Mirzoyan et al (*see E.Popova at IEEE NSS 2013*)

Geiger discharge light

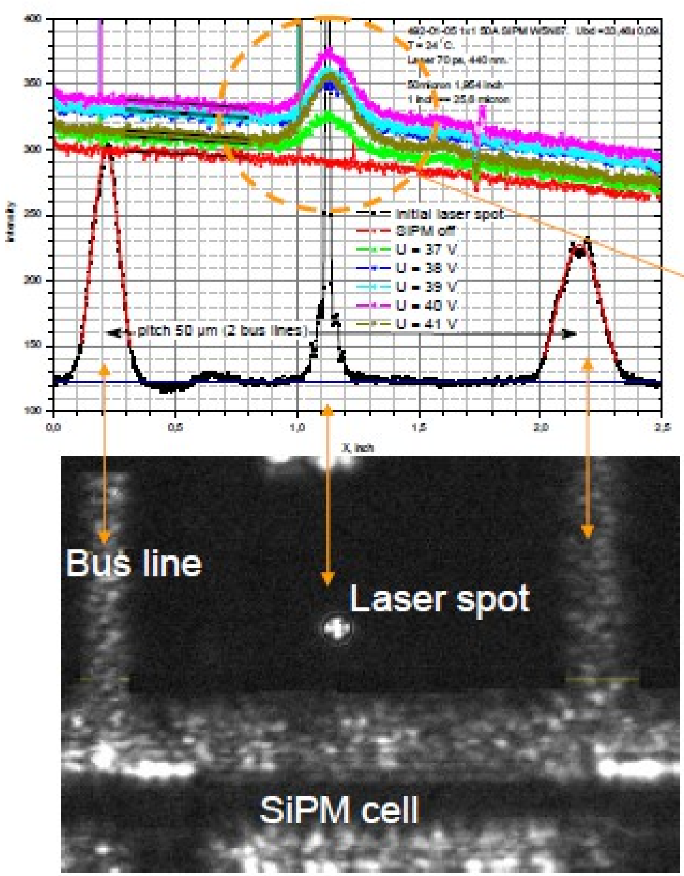

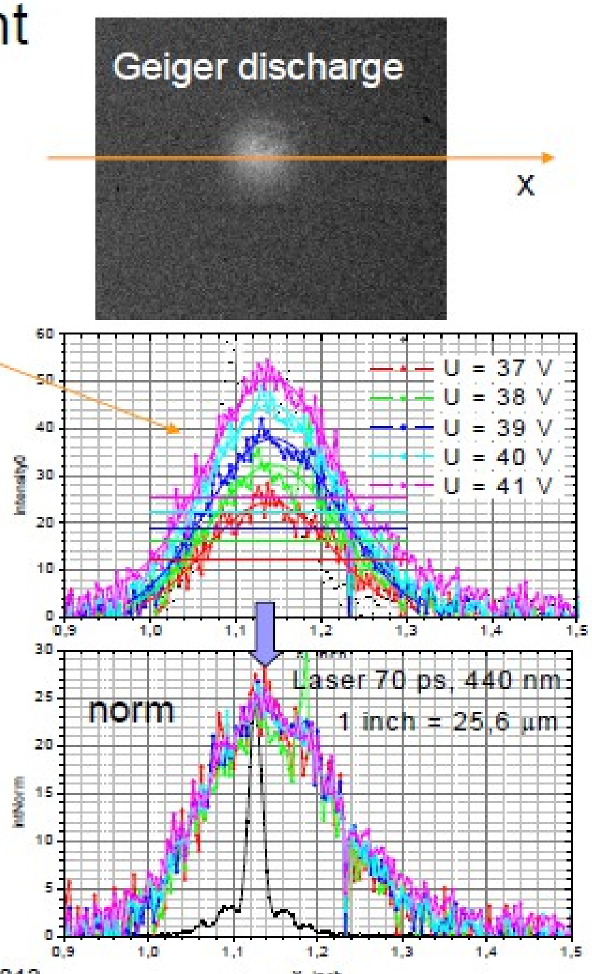

Spot size of Avalanche

1) O(10)μm

2) independent of over-voltage

3) mild dependence from cell size

Factors affecting timing measurements

- **Front edge signal shape** depends on **ΔV**, **T** and **impact position:**
  1) ARC/CFD partially effective in canceling time walk effects
  2) **digital timing filter** might account for shape variations (ΔV, T)

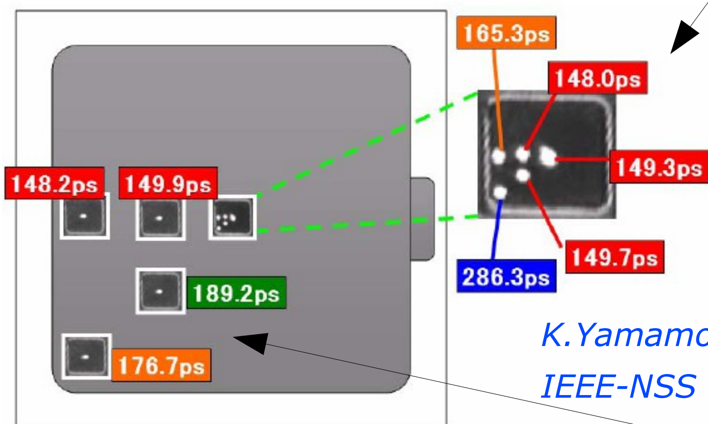

K.Yamamoto IEEE-NSS 2007

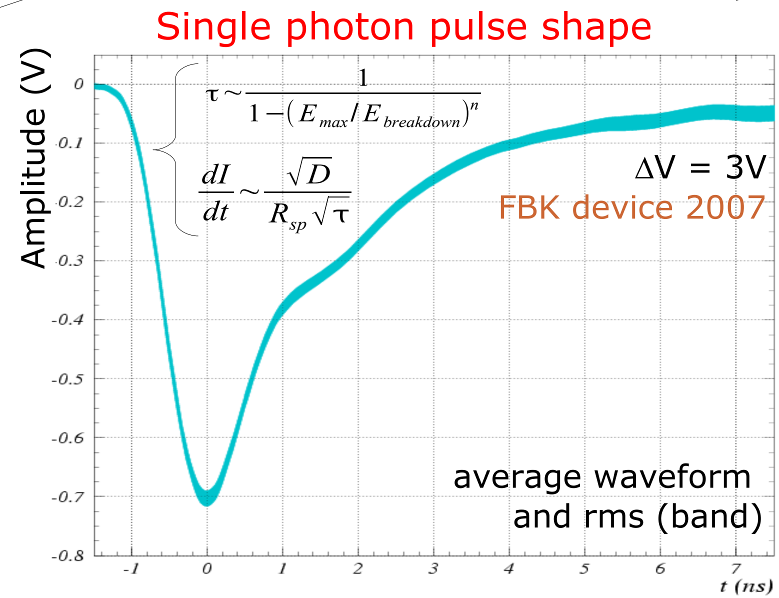

Due to:
1) slower propagation of avalanche front

2) lower E field at edges

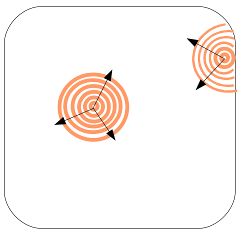

- Additional fluctuations of signal front from non-**uniformity** among cells in terms of:
  1) electric field profile
  2) break-down voltage
  3) quenching Rq
  5) parasitic capacitance parallel to Rq
  4) inductive trace lines from cell to signal pad
     (see improvements by using Trough Silicon Vias in Hamamatsu devices → *Sato et al IEEE NSS 2013*)

- **trailing edge shape** fluctuates (after-pulses) and **Pulse width** depends on **ΔV:**
  → falling signal part not useful for timing (detrimental)
  → better not to use Time-over-Threshold (for single photon)

- Additional contribution from **baseline fluctuations** (dark pulses, afterpulses)
- Very often **electronics contribution dominates**

Example of Single Photon Timing Res. ("intrinsic")

timing measurement with femto-second laser, 2GHz voltage amplifier, 2GHz/20GSs sampling and digital time filtering optimized for SiPM pulse

FBK devices 2007
shallow junction

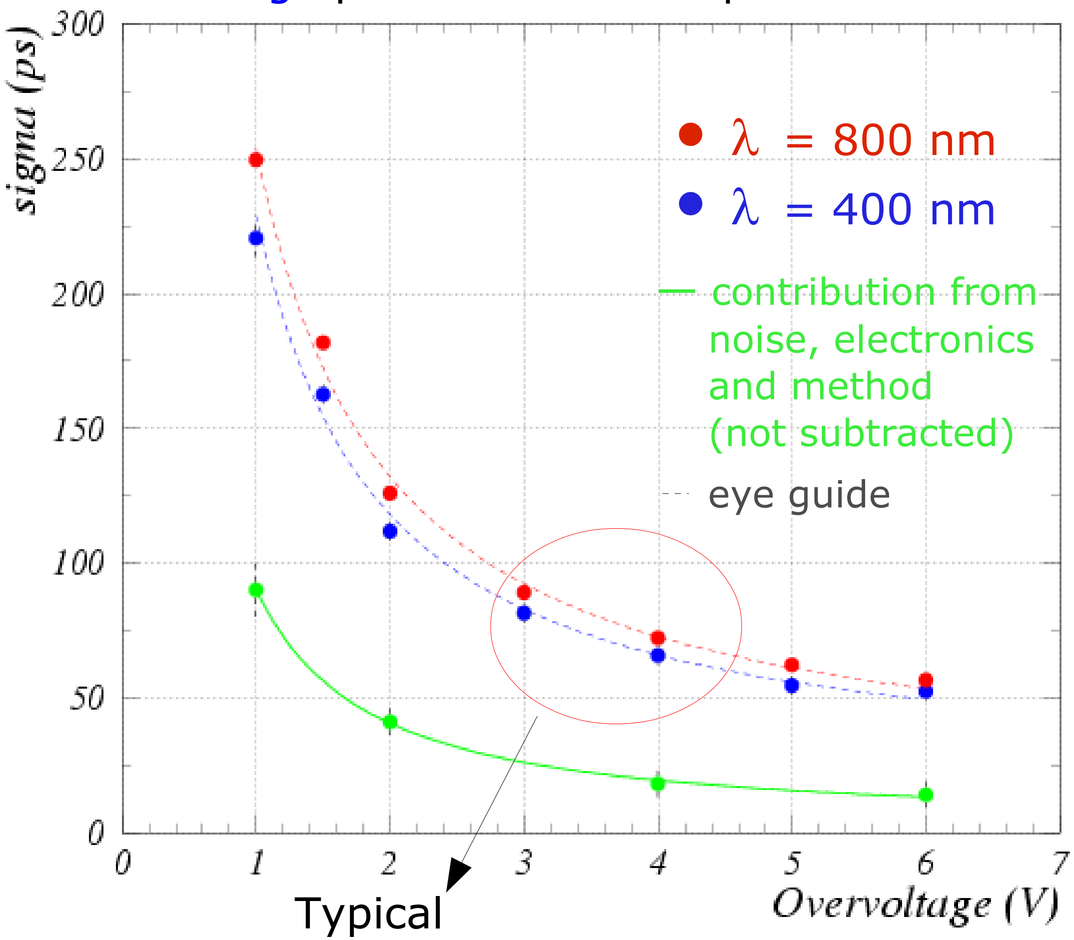

Typical working region

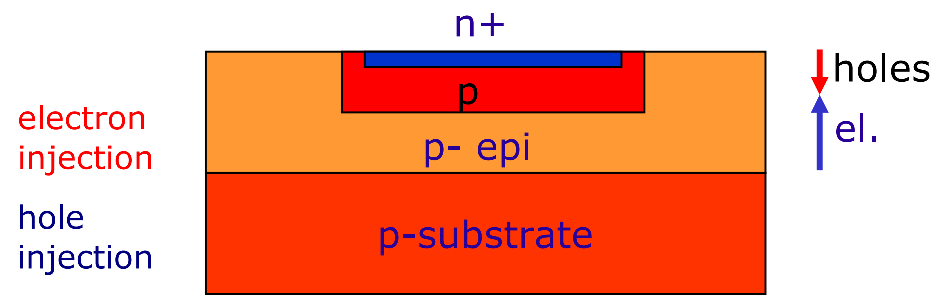

In general due to drift, resolution differences

1) high field junction position
- shallow junction: $\sigma_t^{red} > \sigma_t^{blue}$
- buried junction: $\sigma_t^{red} < \sigma_t^{blue}$

2) n^+-on-p smaller jitter than p^+-on-n due to electrons drifting faster in depletion region (but λ dependence)

3) above differences more relevant in thick devices than thin

G.C. et al NIMA 581 (2007) 461

NOTE: good timing performances kept up to 10MHz/mm^2 photon rates

Interesting comparative timing measurements:
see work in progress by *Brunner etal at DIRC 2013*
! at the moment I don't think they reach the ultimate timing resolution for the SiPM samples under study

SPTR comparison - various SiPM types

A.Rohzin – PhotoDet 2012

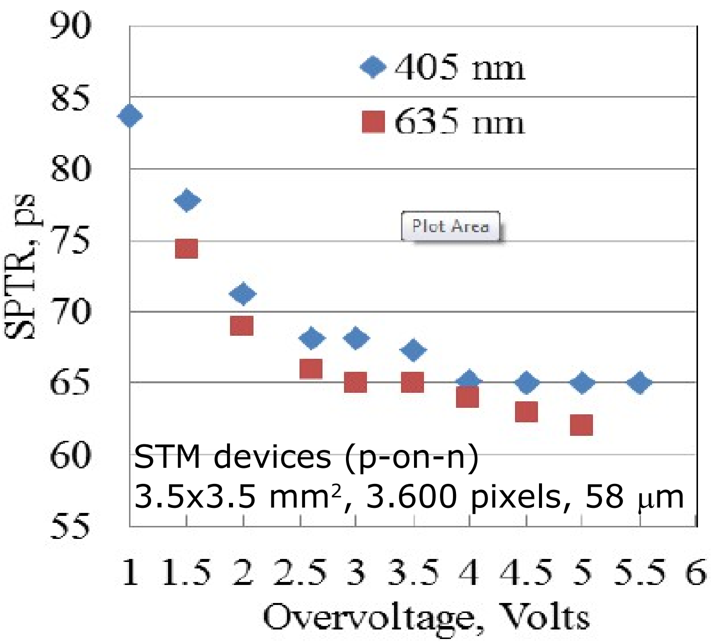

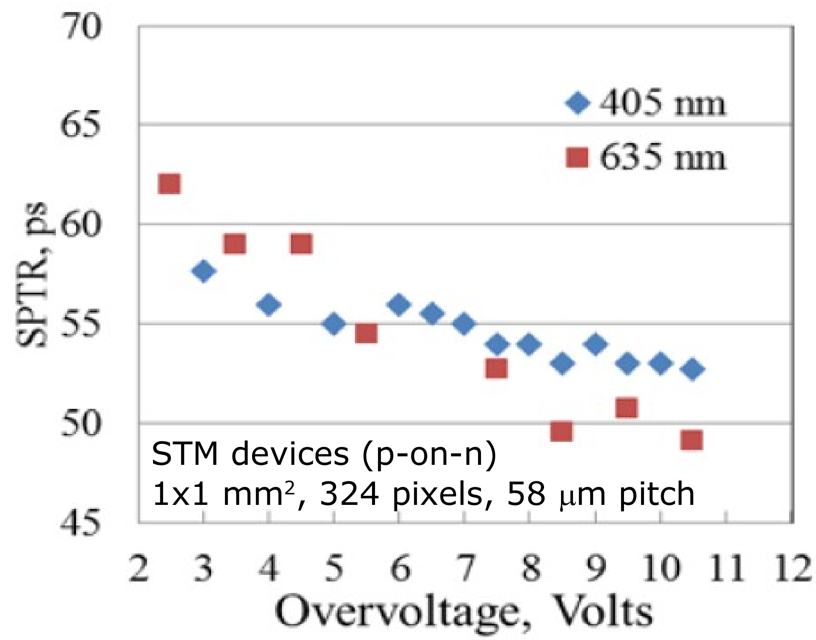

- PiLas (ps) laser

- DRS4 waveform digitizer

- optimized timing algorithms (library of traces, for each SiPM type and light source)

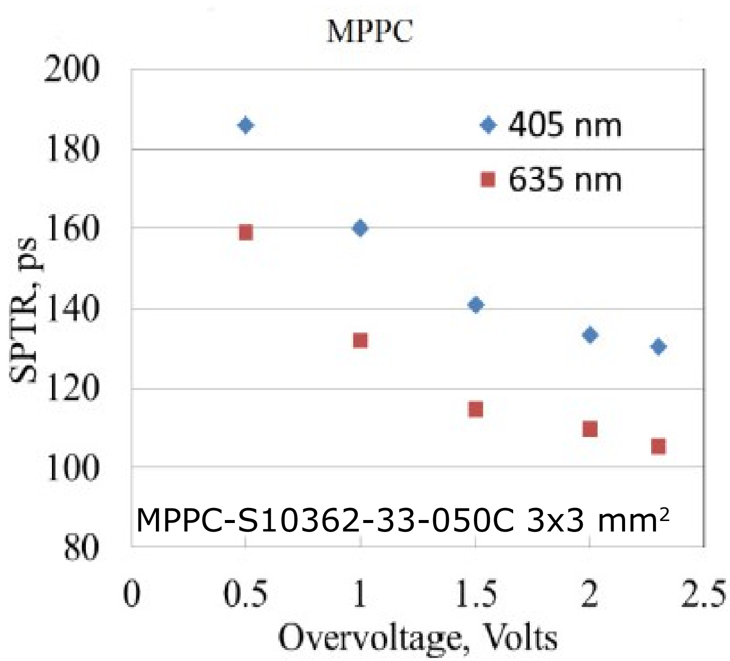

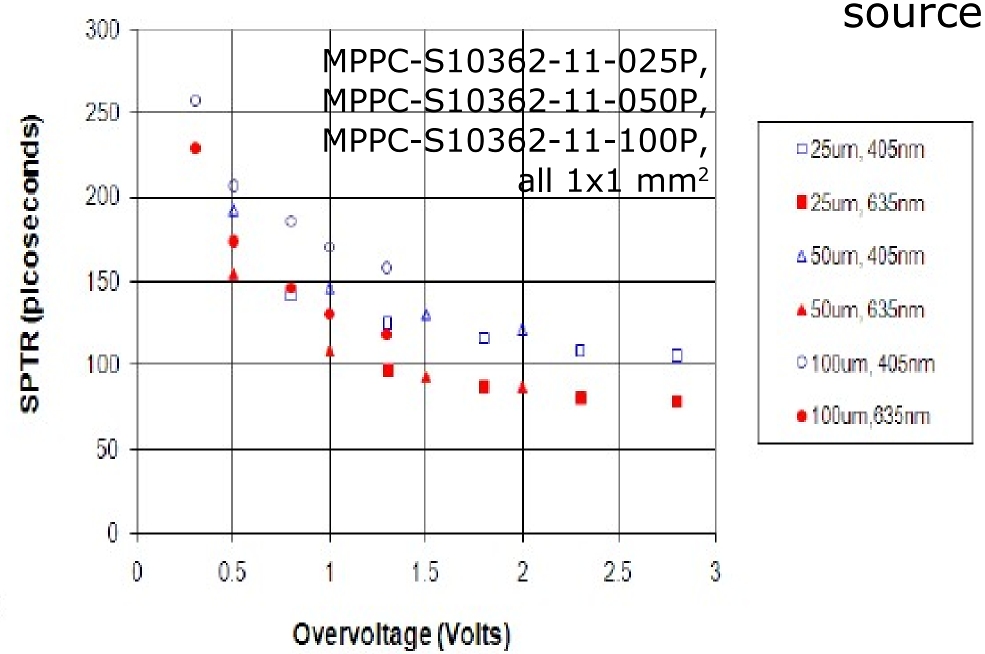

digital- SiPM timing resolution

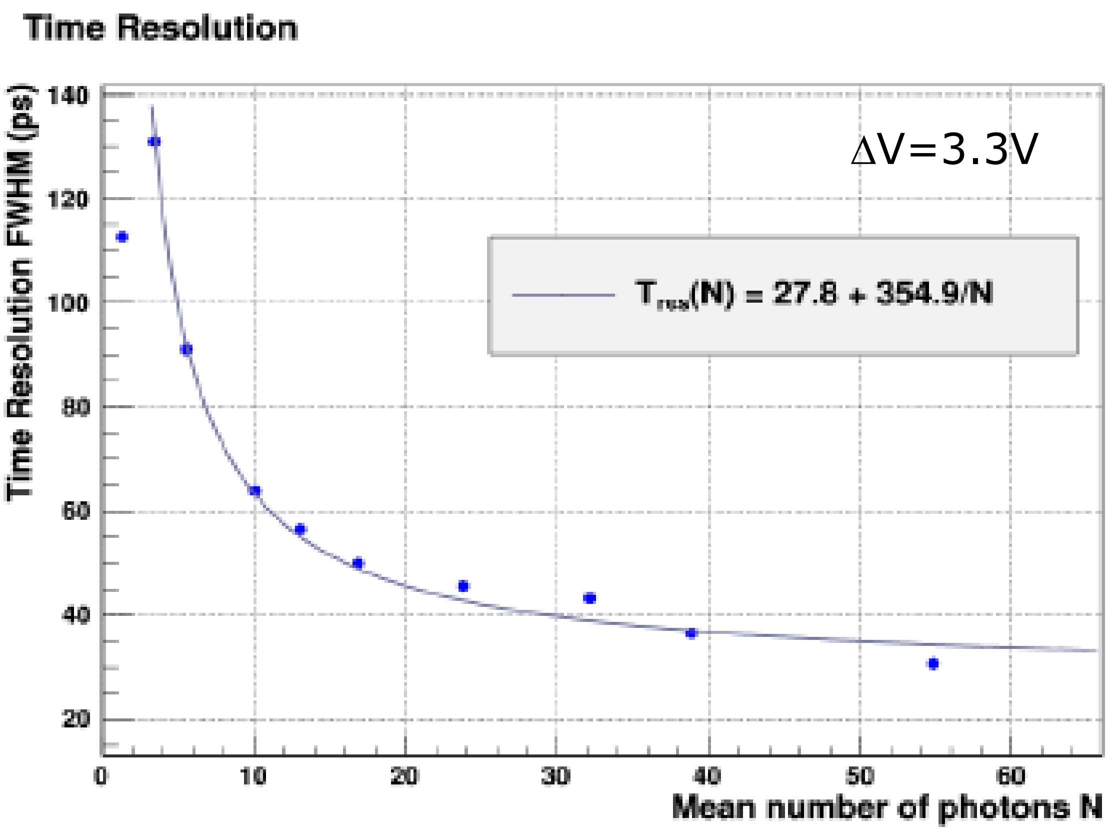

T.Frach at LIGHT 2011

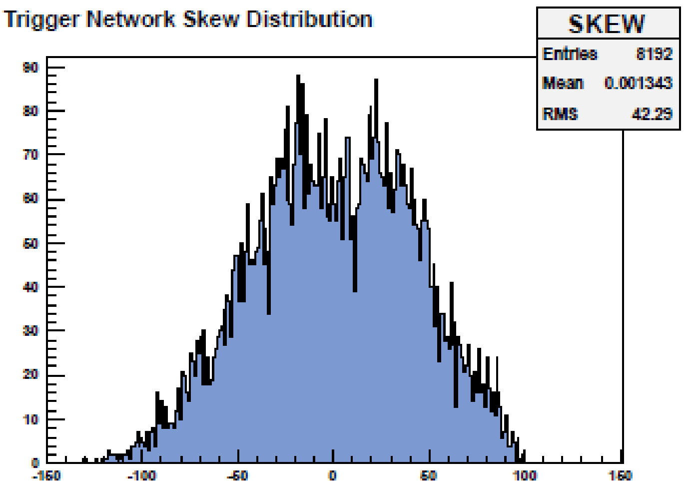

- Sensor triggered by attenuated laser pulses at first photon level
- Laser pulse width: 36ps FWHM, λ = 410nm
- Contribution to time resolution (FWHM):

SPAD: 54ps, trigger network: 110ps, TDC: 20ps

- Trigger network skew currently limits the timing resolution

Optimizing signal shape for timing

It can be shown that there are 2 signal components: fast + slow (recovery) (*see eg C. de La Taille at PhotoDet 2012*)

$$\frac{V^{max}_{fast}}{V^{max}_{slow}} \sim \frac{C_q^2 R_q}{C_d C_{tot} R_{load}}$$

Increasing C_q/C_d or/and R_q/R_{load}
→ spike enhancement → better timing
→ slow recovery tail suppressed
→ reduced baseline fluctuations

Among new (2013) Hamamatsu structures

- trench insulation (against cross-talk)
- metal resistor

→ enhanced and well controlled amount of "parasitic" Cq

1) enhanced fast pulse amplitude
2) suppressed slow pulse amplit.

1) better timing with fast component
2) lower sensitivity to baseline fluctuations
→ further improve timing by using higher gain

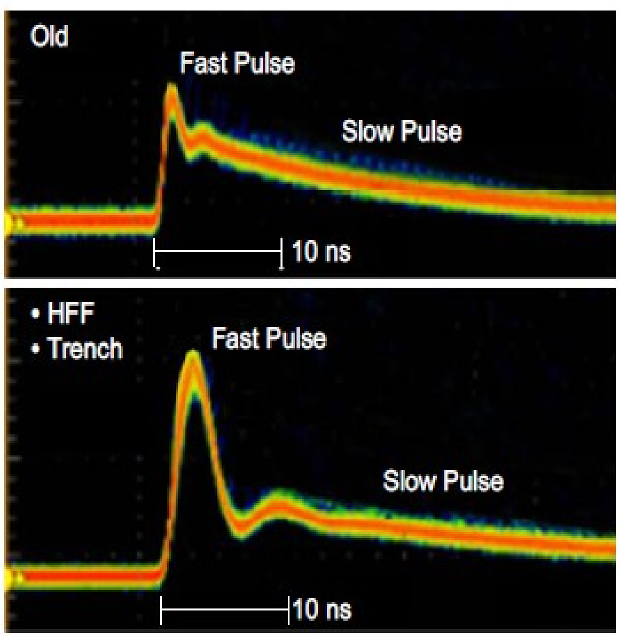

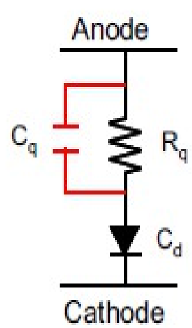

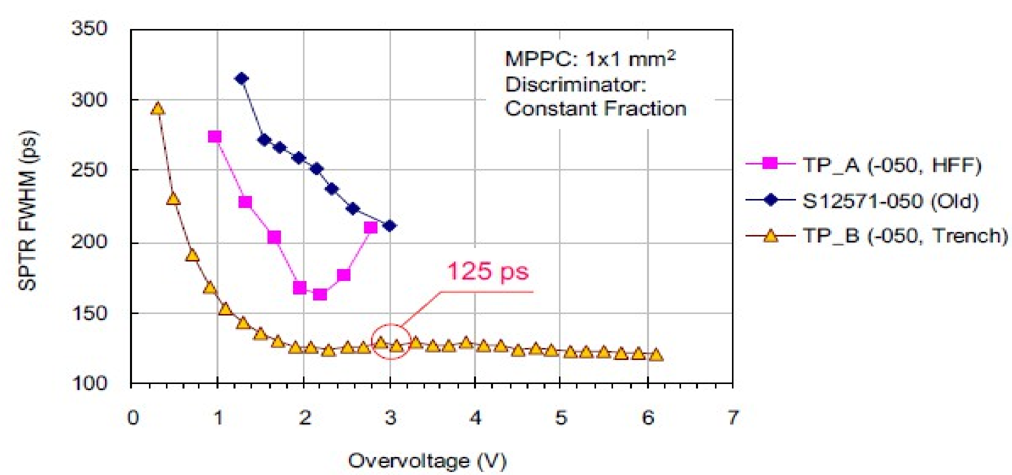

T.Nagano et al IEEE NSS 2013

Optimizing signal shape for timing

SensL new SiPM architecture for fast timing

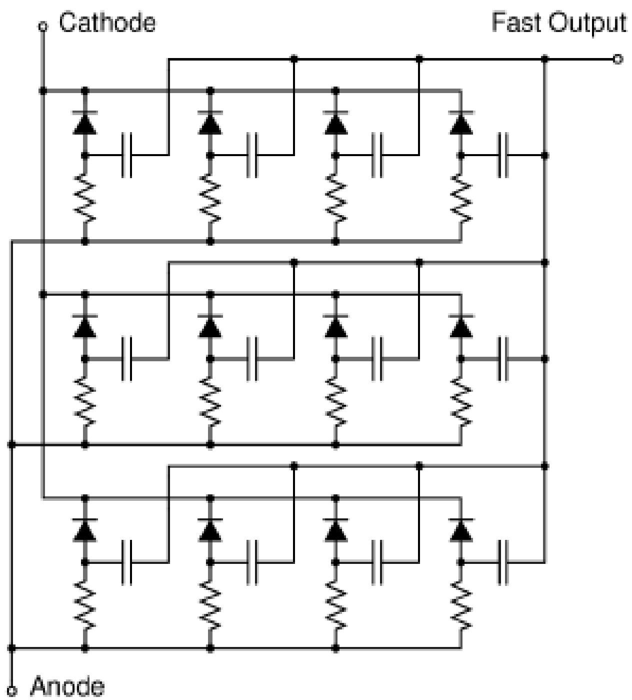

Figure 2: Concept schematic of the SensL fast output SiPM shown as an array of microcells connected in parallel (Courtesy of SensL [9].) Each diode symbol represents an individual p-n junction microstructure. Unlike standard SiPMs, each junction in the SensL device has a connection to a third electrode with a low capacitive coupling.

see also O'Neill et al - PhotoDet 2012

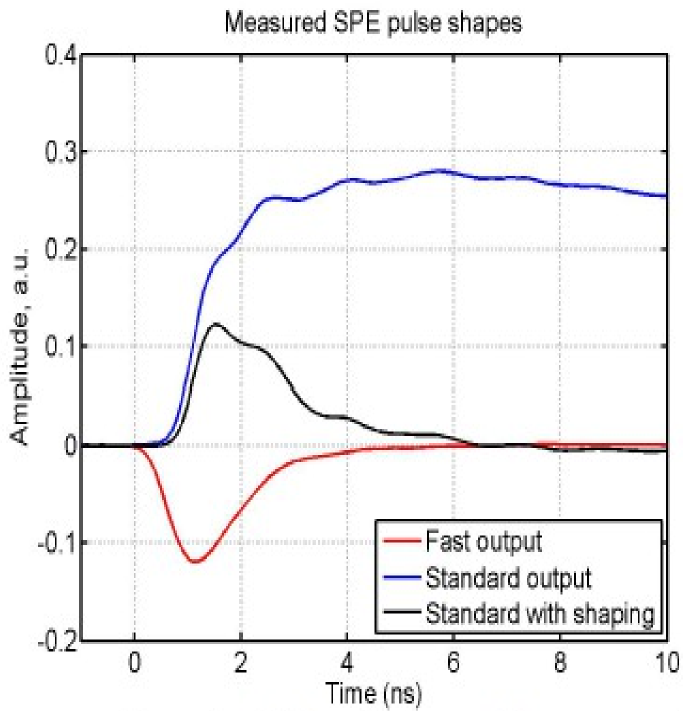

Figure 9: Measured SPE signals from the SensL MicroFB-30035 device (3×3 mm2 area with 35 μm microcells): fast output (red), standard output (blue), and (black) standard output connected to an external C-R shaping circuit (τ = 2 ns).

Dolinsky et al – IEEE NSS 2013

Additional **Fast timing output** is shown to be equivalent to external high-pass filtering (clipping) but of more practical use (many photons applications)

For a comparison of timing performances with many photons see *Y.Uchiyama et al IEEE NSS 2013*

Hybrids → large area

- HAPD (multi-pixel / 1 pixel very large area)
- VSiPMT (prototype, 1 pixel)

APD is not suited for single photon… BUT

APD biased for **low gain** M < 1/k

- fast exponential growing due to only electrons
- high number of carriers in high field region at given time:
  → small gain fluctuations
- Timing fluctuations are small: limited only by the length of depletion region
  → time resolution limited by electronics
  (high Amplification for low light signals)

APD biased for **high gain** M > 1/k

- hole ionization events contribute
  → increase of gain is the result of small number of large pulses due to one or more hole ionization initiated secondary avalanches (ENF)
- low number of carriers in high field region at given time and hole ionization near cathode resulting in larger pulses
  → large gain fluctuations
- **slow buildup** and long pulse due to many carriers over long time
  → large timing fluctuations

Hayat et al J. Lightwave Tech. 24 (2006) 755
Fox et al Rev. Sci. Instr. 70 (1999) 1951

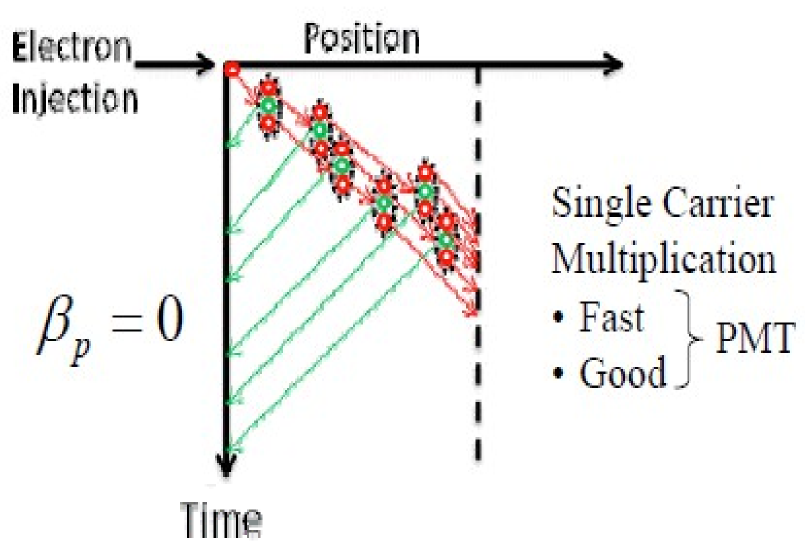

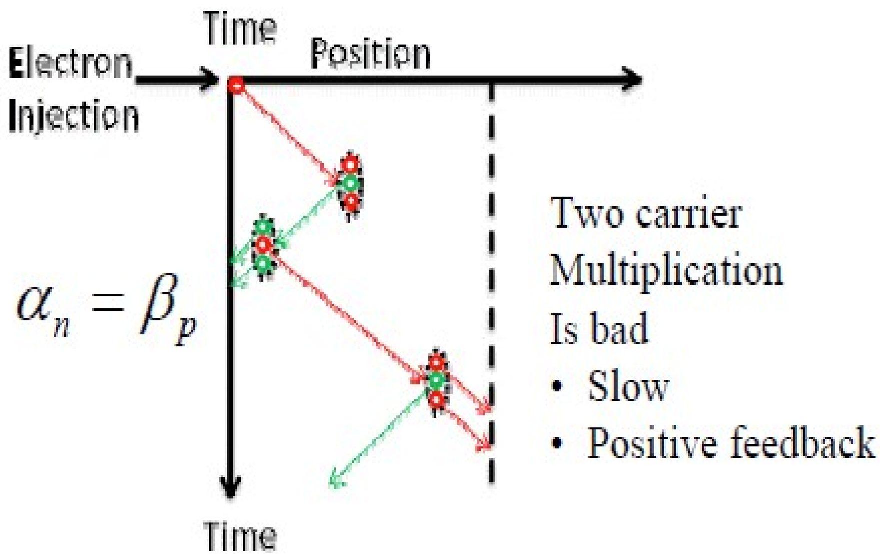

Large Area Photo-Detectors → H-APD

moderate "Bombardment" gain + low avalanche gain

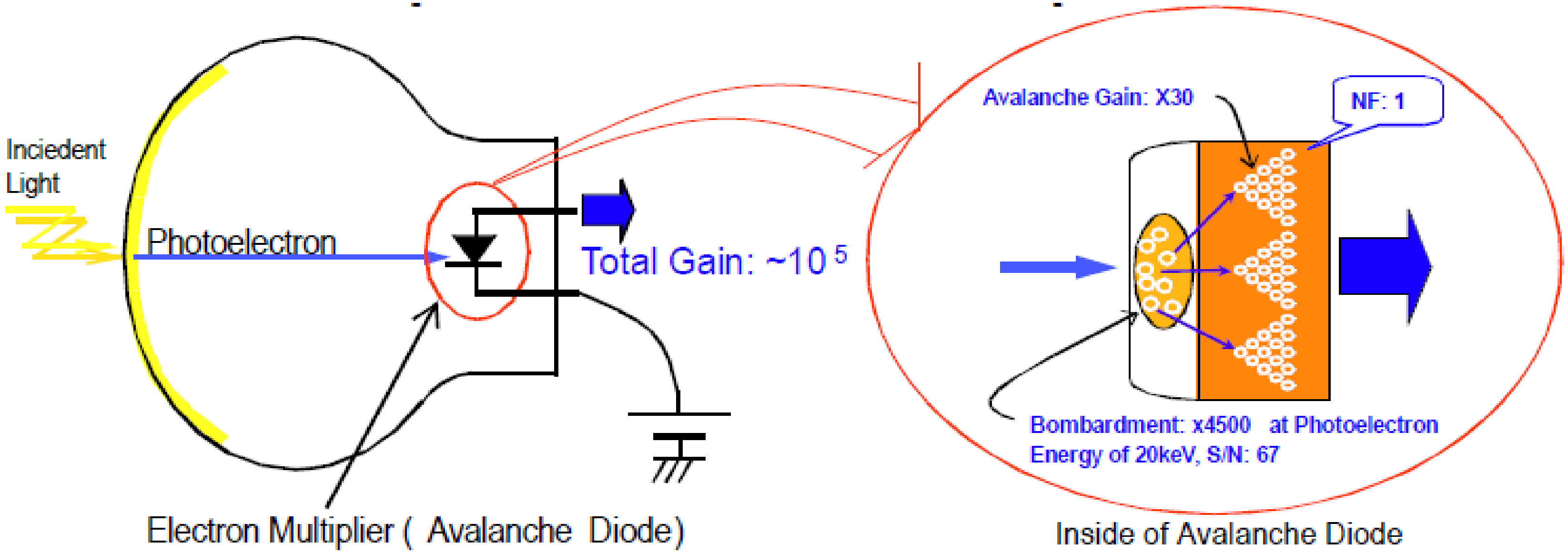

HPD
✓ has a simpler structure
✓ is expected to save production costs
✓ have better S/N but lower gain.

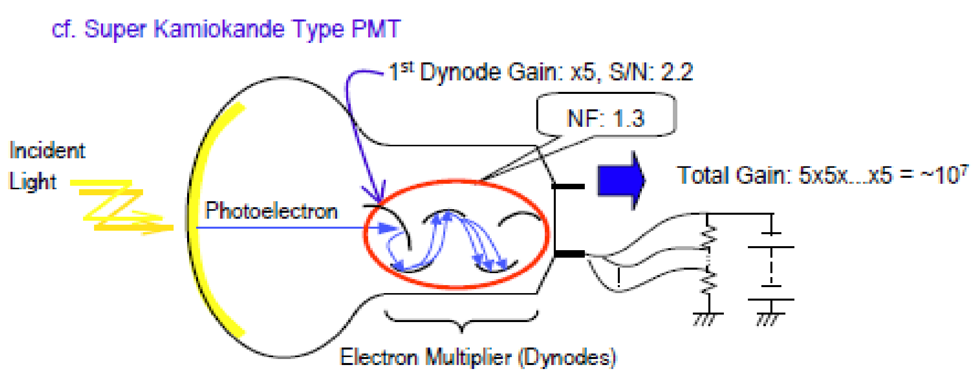

Developements (Hamamatsu) for various Cherenkov based detectors
→ Belle II ARICH (baseline) *see talk by S.Nishida at this Conference*
→ Hyper-Kamiokande (option) *see talk by S.Hirota at this Conference*

Large Area Photo-Detectors → HAPD

Total Gain ~ 7 10^5

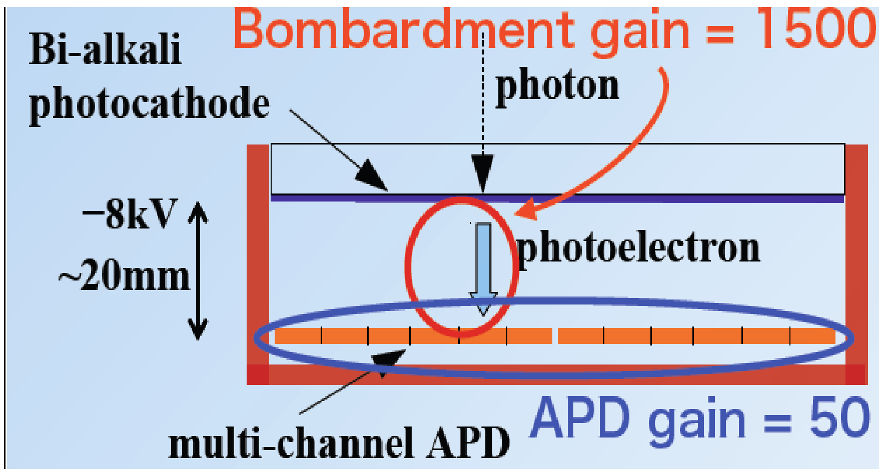

Dedicated APD layout for
- kinematic E threshold
- protection against alkali
- HV insulation
- mitigate radiation effects

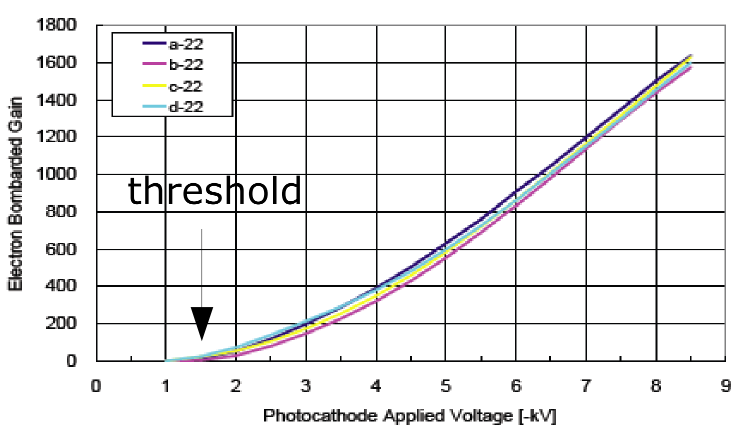

see talk by S.Korpar at this Conference

Single photon sensitivity

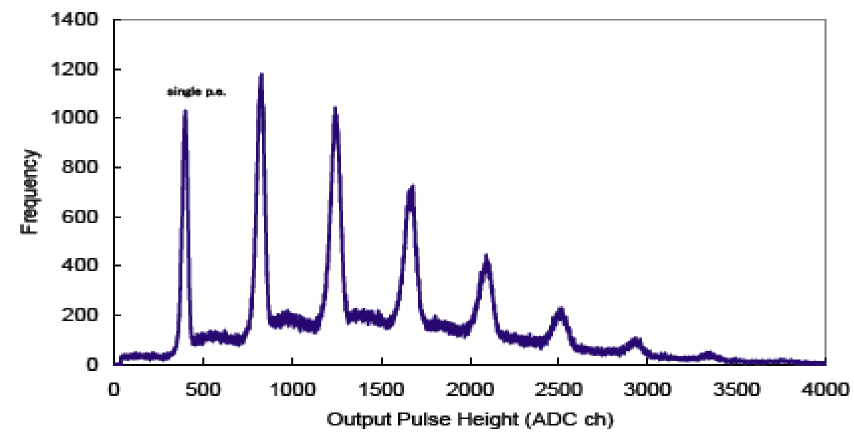

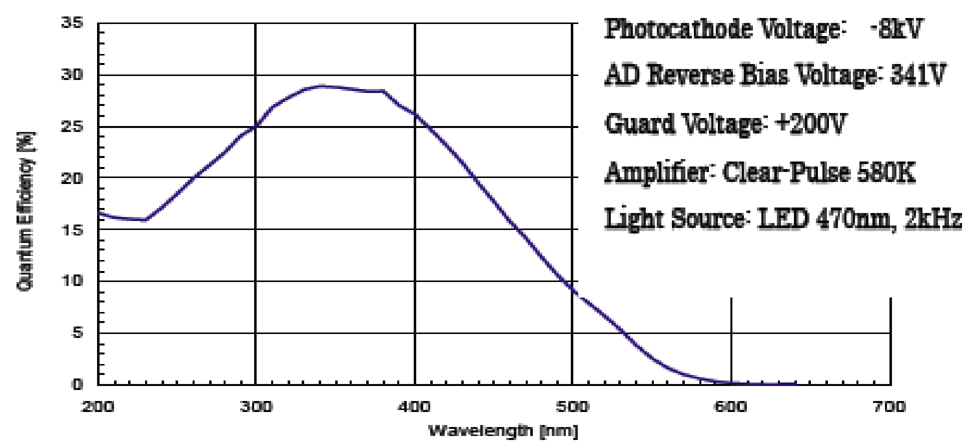

Y.Yusa at EPS 2013

Note: expected improvement in timing resolution compared to same geometry PMT tubes (in particular for 8'' and 20'' devices
→ *poster by Y.Suda at this conference*)

Large Area Photo-Detectors → VSiPMT

see talk by D.Vivolo and poster by C.M. Mollo at this Conference

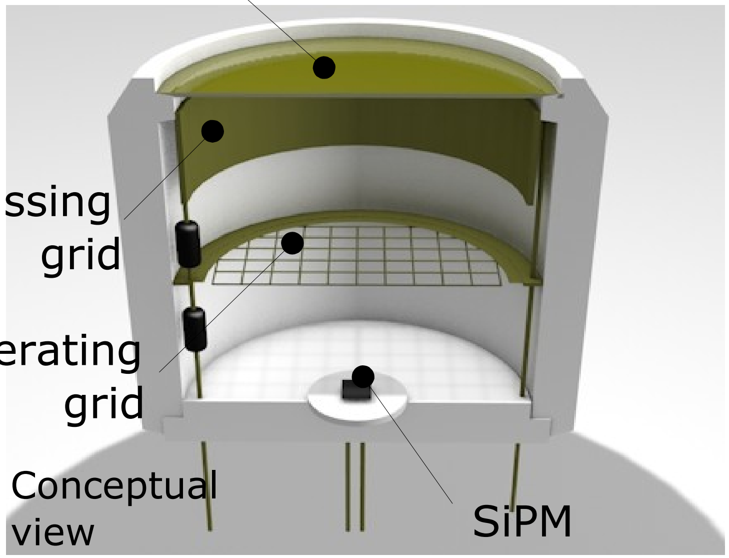

INFN Napoli – Barbarino et al and Hamamatsu Collaboration

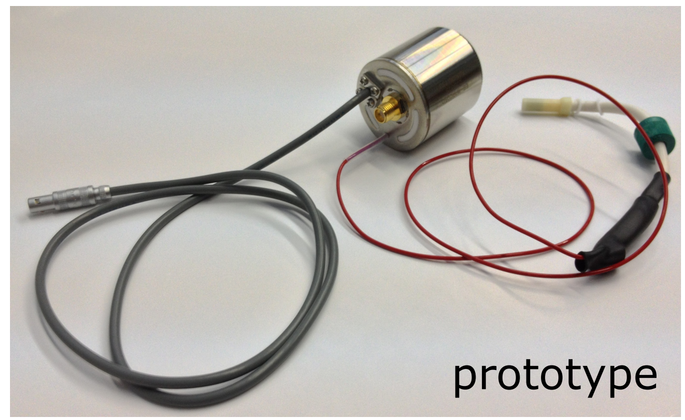

SiPM (MPPC Hamamatsu)
- 1×1 mm^2
- No epoxy layer
- Thin SiO2 layer
- p-on-n structures

Photocathode
- NEA (GaAsP) (higher PDE, while SiPM noise dominates)
- diameter 3 mm

First measurements (2013)

Single photon sensitivity

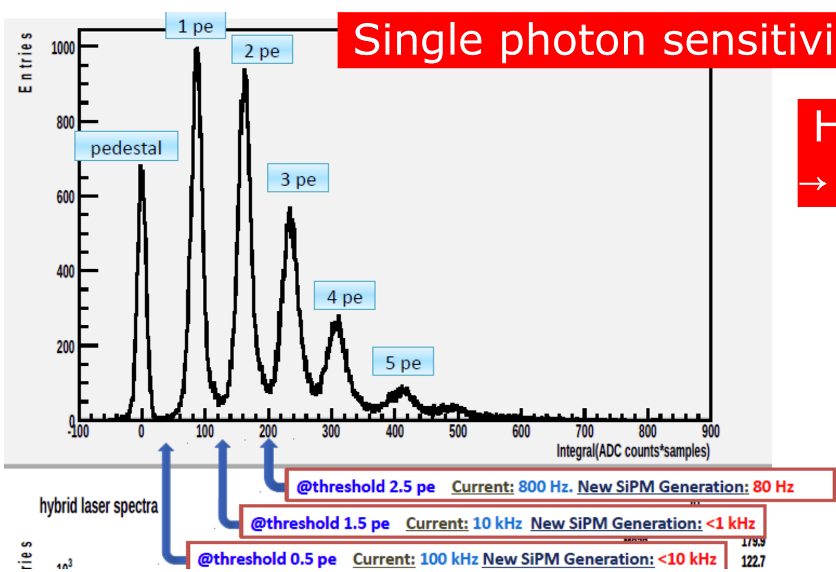

R.de Asmudis IPRD 2013

Homogeneous PDE~0.25 over 7mm^2 → surface enhancement x7

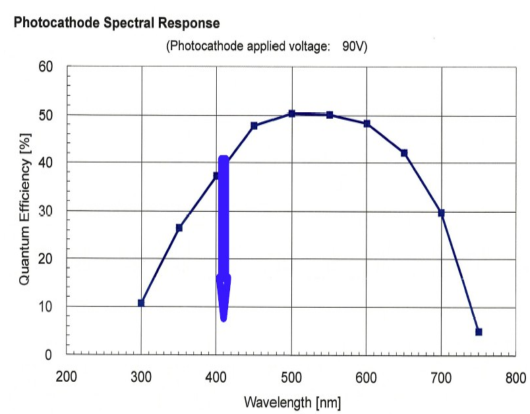

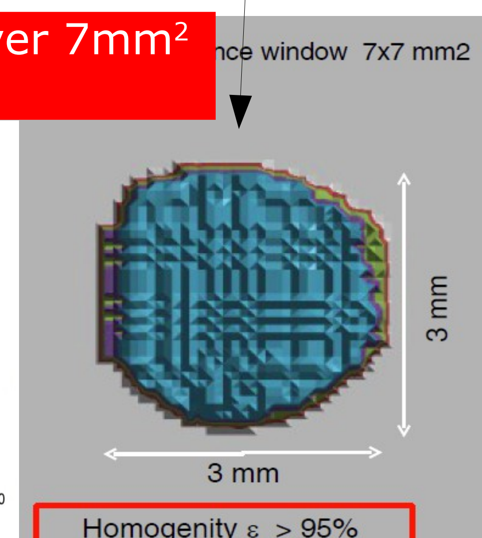

Large Area Photo-Detectors → hybrids

personal comments

Advantages of SiPM vs APD in hybrids

1) high gain in SiPM → no need for bombardment gain, just enough energy for photoelectrons to reach the active region → threshold ~ O(2-3kV)

2) gain stability
   - independent of HV stability
   - SiPM gain more stable than APD

3) less critical HV insulation

Note: e- detection efficiency is mainly limited by Fill Factor of SiPM
→ can keep over-voltage lower than usual for SiPM
→ VSiPMT might work at quite low noise O(10kHz), not MHZ !
(might need a bit of bombardment gain → compromise ?)

Note: VSiPM timing resolution expected to be better than same area Vacuum PMTs (limited mainly by fluctuations in photo-electron time of flight, and in NEA emission time lag)

Challenges common to all hybrids

1) use of photo-cathode → PDE, timing, ...cost
2) need high vacuum, cathode activation, protection against alkali
3) troubles with electronics in vacuum

Examples of
Cherenkov detectors based on SiPM

→ FACT: cherenkov telescope based on SiPM

→ Proximity focusing RICH with SiPM (Krizan et al)

→ Proximity focusing RICH with d-SIPM (FARICH)

FACT: First G-APD Cherenkov Telescope

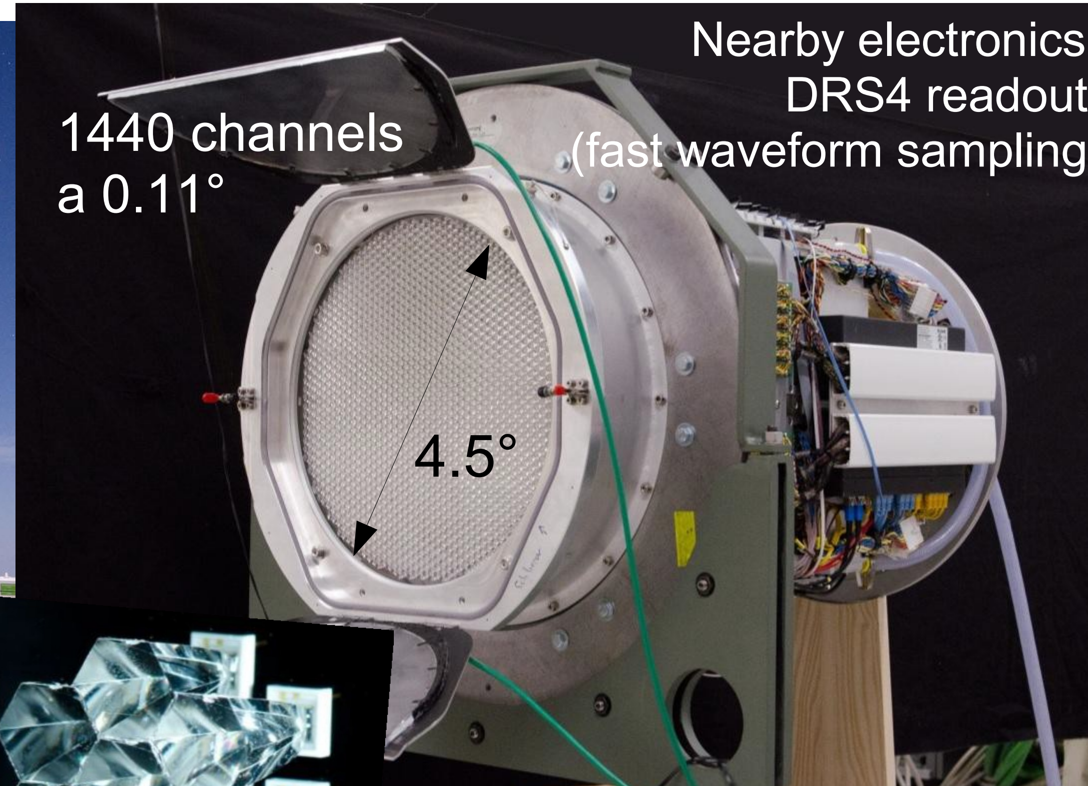

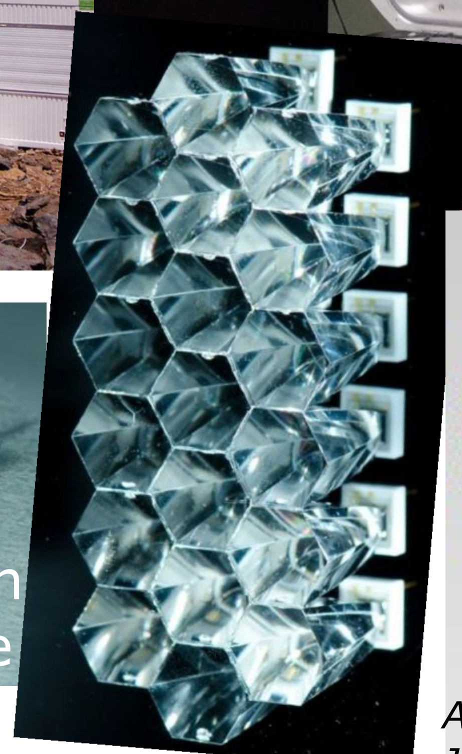

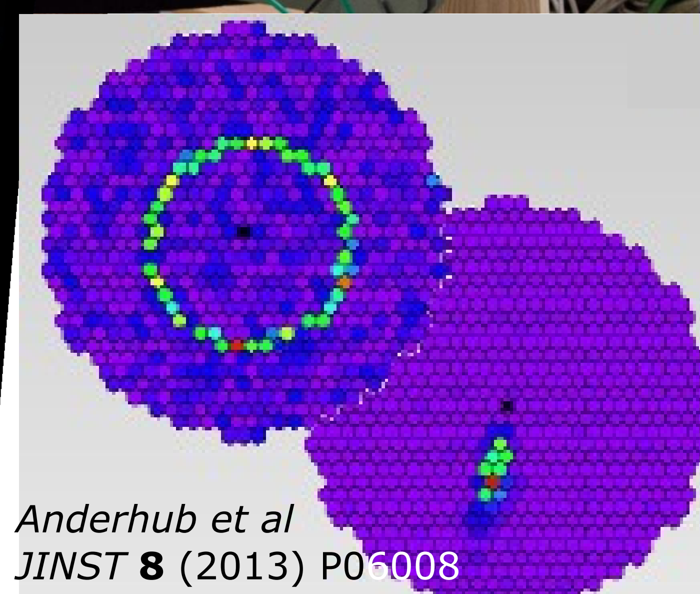

T.Krähenbühl at PhotoDet 2012

Anderhub et al
JINST **8** (2013) P06008

FACT: First G-APD Cherenkov Telescope

→ A.Biland at this Conference

Impressive demonstration of
1) single photon detection even in presence of background at high rate
→ thanks to fast sampling electronics

2) long term stability of detector response, thanks to
→ long term stability of SiPM behaviour (dependences on parameters)
→ feedback correction of Vbias → keep constant over-voltage against
  1) $V_{breakdown}$ changing with Temperature
  2) V drop across series resistors in HV bias circuit, changing with photon flux (full moon/new moon → very different "baseline" current levels drawn from bias supply)

stability check 1)

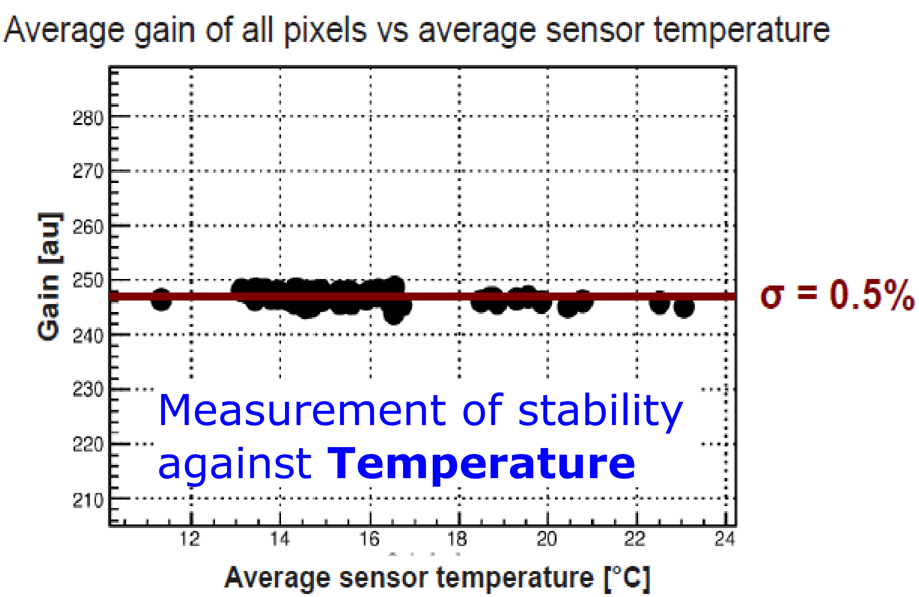

stability check 2)

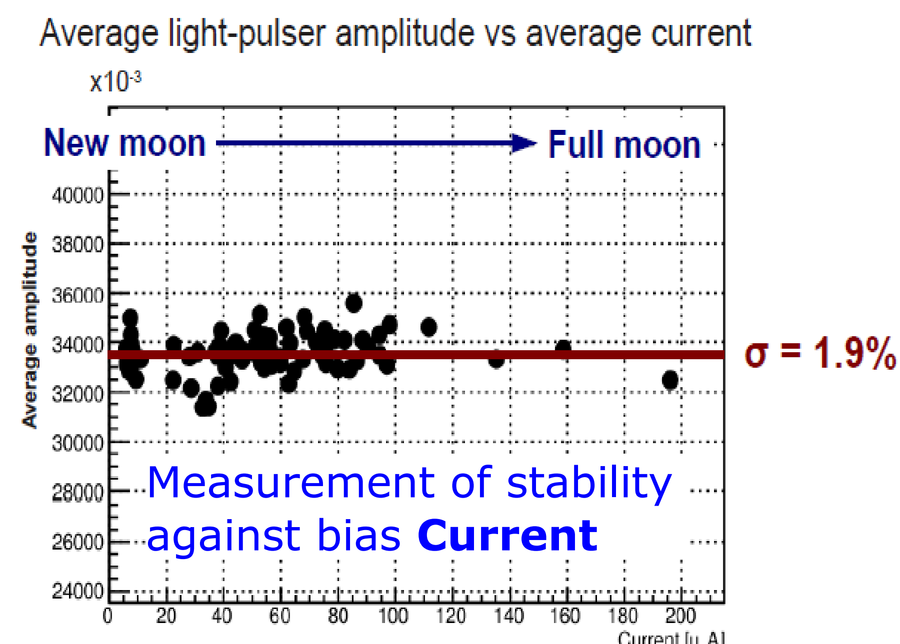

T.Bretz at IEEE NSS 2013

Proximity focusing RICH with SiPM readout

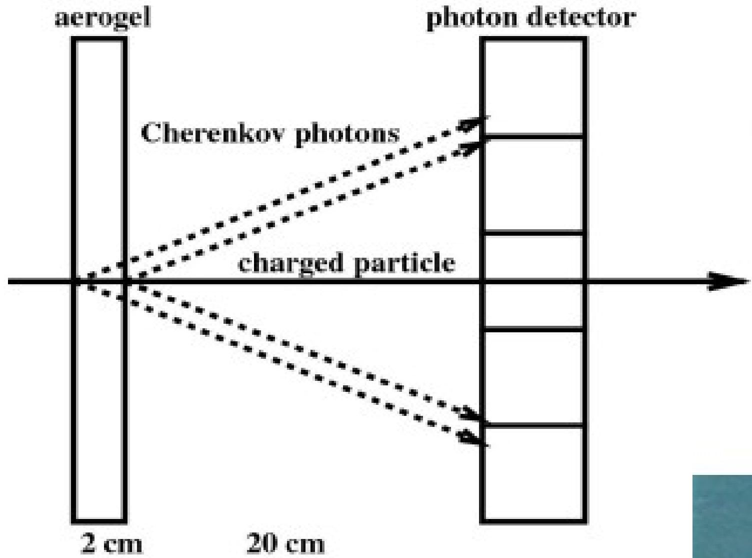

Baseline photo-detector for BelleII Endcap PID system is H-APD. Tests with SiPMs as option

P.Krizan, S.Korpar et al

Photon detector with SiPMs and light guides

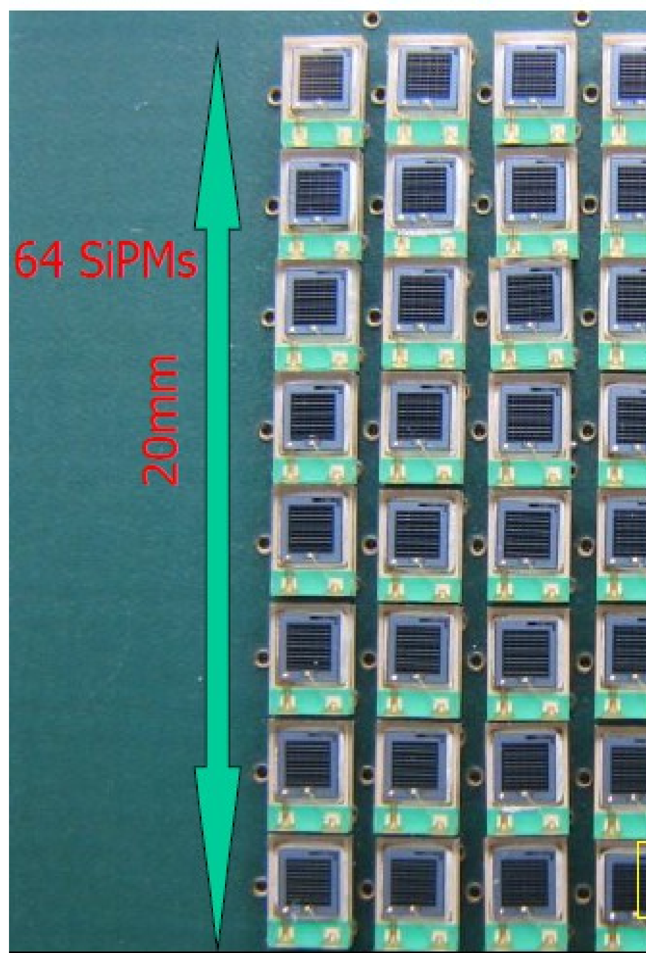

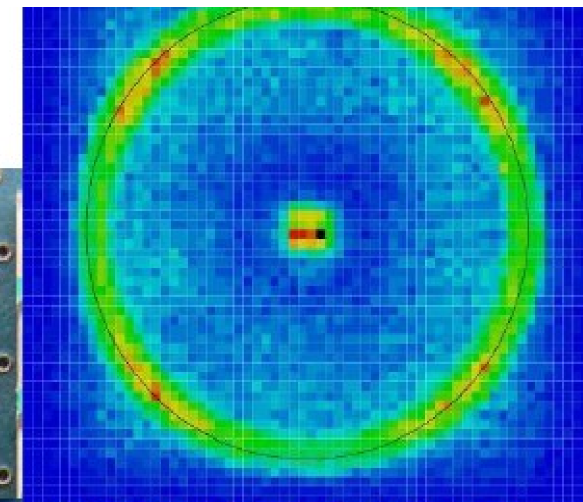

Korpar et al., NIM A613 (2010) 195

Improve S/N by using:

- narrow (<10ns) time coincidence
- light collectors and (adjusting the pad size to the ring thickness)

Proximity focusing RICH with SiPM readout

Array of SiPMs: Hamamatsu MPPC S11834-3388DF
- A novel type of a multi-pixel Photon Counter (MPPC)
- 8x8 SiPM array, with 5x5 mm2 SiPM channels
- Active area 3x3 mm2
- Cell size: 50 μm
- Rather low dark count rate (~100 kHz/mm2)
- Operating voltage: (70 ± 1) V

Most recent tests (2013) courtesy of P.Krizan et al

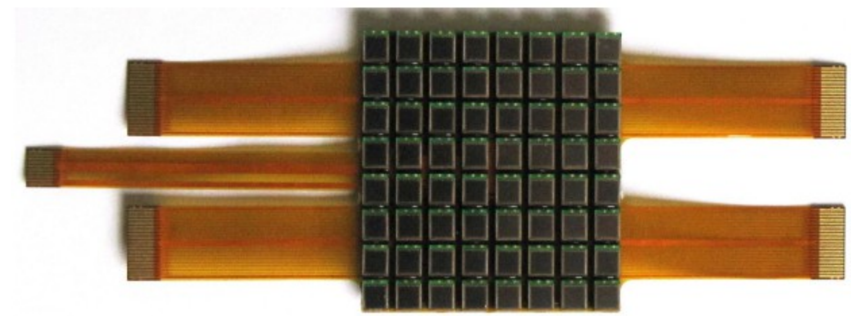

Optimization of light guides geometry
(truncated pyramids) → max acceptance

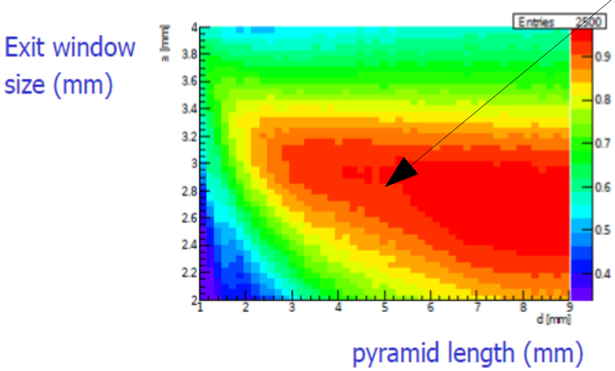

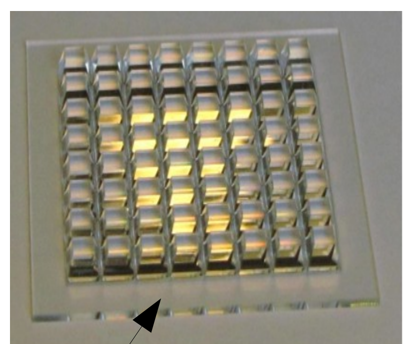

Quartz light concentrator
- Material: quartz (n = 1.48)
- Pyramids glued (n = 1.52) on a 1mm thick quartz plane plate
- Dimensions a=3mm d=3mm → ~91% acceptance (simulation)

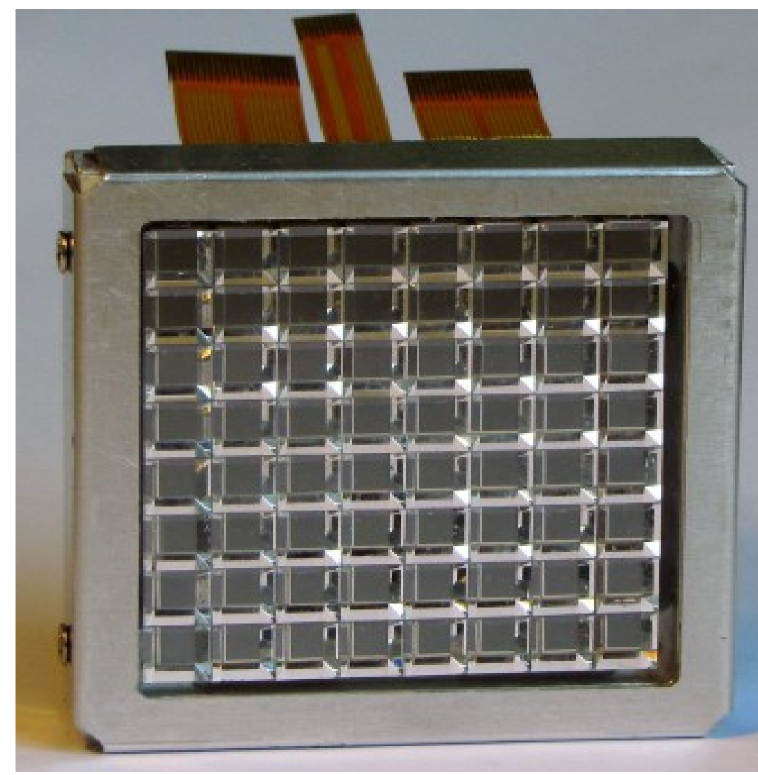

Detector Module

Measured gain: ~3.5 x 10^5 @ 72.8 V

Proximity focusing RICH with SiPM readout

Test Beam at DESY - 5 GeV/c electrons

Most recent tests (2013)
courtesy of P.Krizan et al

→ *see poster by S.Korpar et al at this conference*

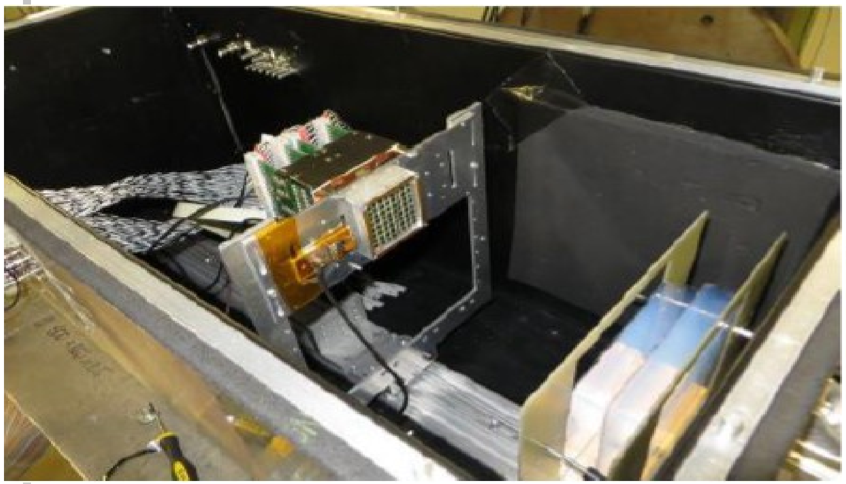

Setup
-One module of SiPMs
-Aerogel radiator
-2 MWPCs for tracking

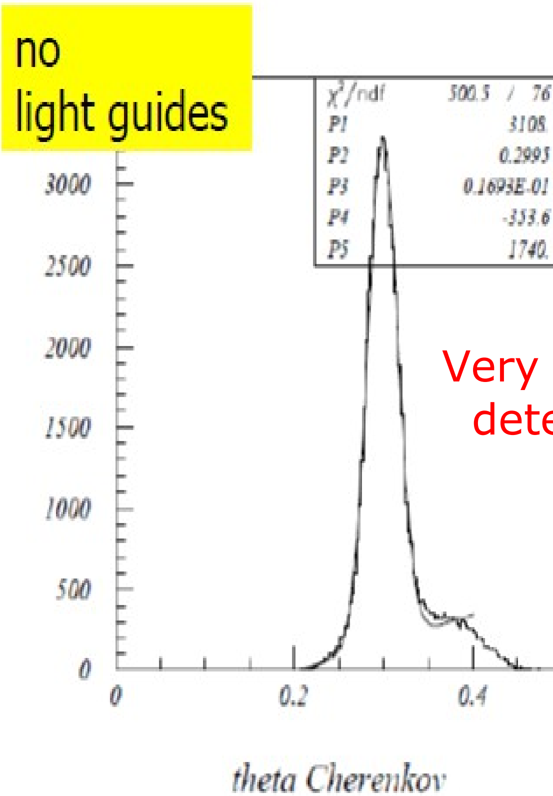

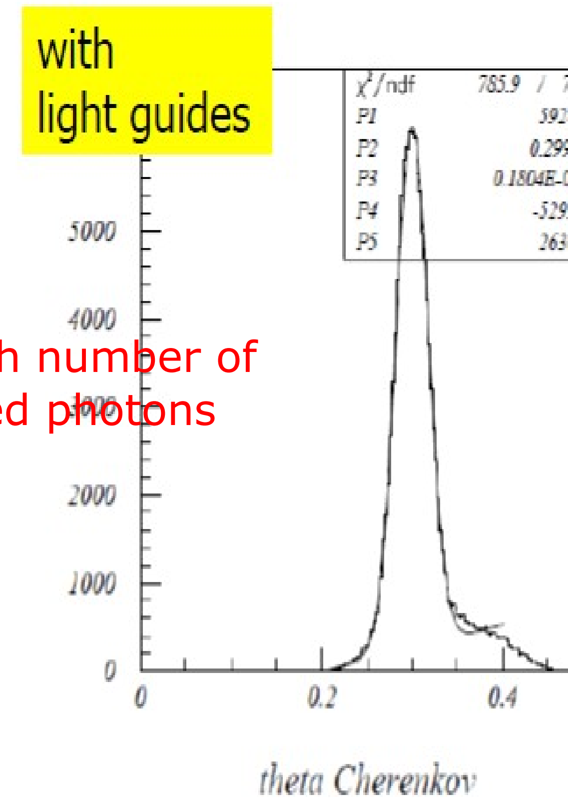

Very high number of detected photons

Results (preliminary)
- Covered area of the ring: ~1/9.5
- Run w/o light concentrator:
  2.0 hit/track, ~19 hits/ring
- Run w/ l.c.:
  3.8 hit/track ~36 hits/ring
- Area ratio ~2.8
- Hit ratio ~1.9

Conclusions
- many photons seen
- dark rate not so relevant
- no showstop !

Further plans
- New electronics: EASIROC ASIC and FPGA-TDC
- Eliminate rim and assemble modules to measure the whole Cherenkov ring

FARICH: Focusing Aerogel RICH with d-SiPM

→ *E.A.Kravchenko at this Conference*

Focusing Aerogel RICH for particle ID

→ Super Charm-Tau Factory (Novosibirsk): μ/π up to 1.7 GeV/c - 21m² detector area (SiPMs)
→ ALICE HMPID: π/K up to 10 GeV/c, K/p up to 15 GeV/c - 3m² area (SiPMs)
→ FWD Spectrometer PANDA: π/K/p up to 10 GeV/c - 3m² area (MaPMTs or SiPMs)

FARICH prototype

Square matrix 20x20 cm²

- Sensors: DPC3200-22-44
- 3x3 modules = 6x6 tiles = 24x24 dies = 48x48 pixels in total
- 576 time channels (576 dies)
- 2304 amplitude (position) channels (2304 pixels)
- 4 levels of FPGA readout: tiles, modules, bus boards, test board

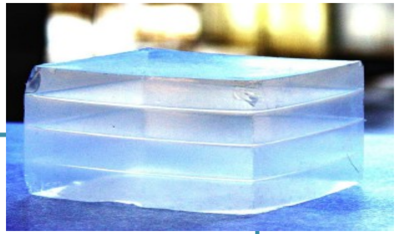

4-layer aerogel

- n_{max} = 1.046
- Thickness 37.5 mm
- Calculated focal distance 200 mm
- Hermetic container with plexiglass window to avoid moisture condensation on aerogel

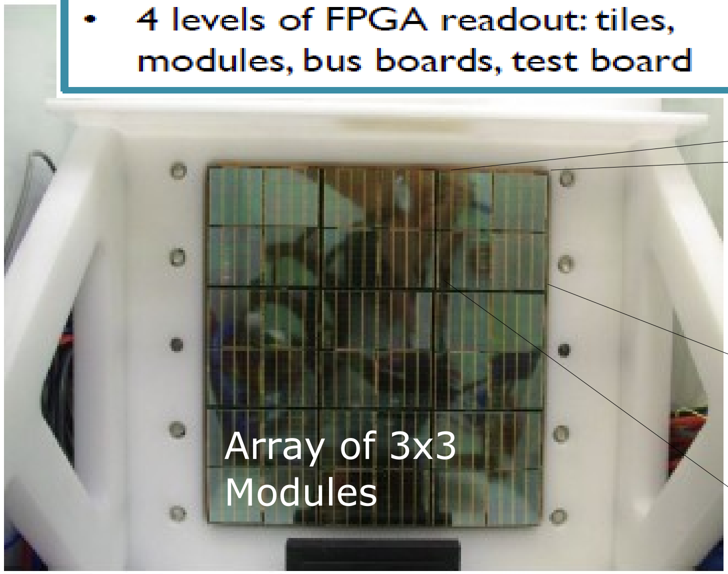

Module = Array of 8 x 8 dSiPMs

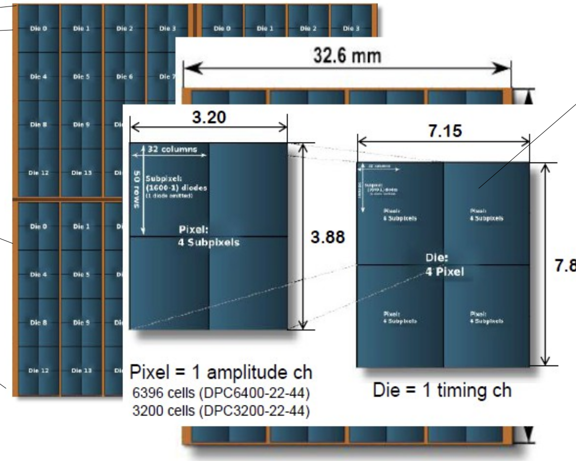

Pixels in module packing density ~70%

Digital Photon Counter (DPC)

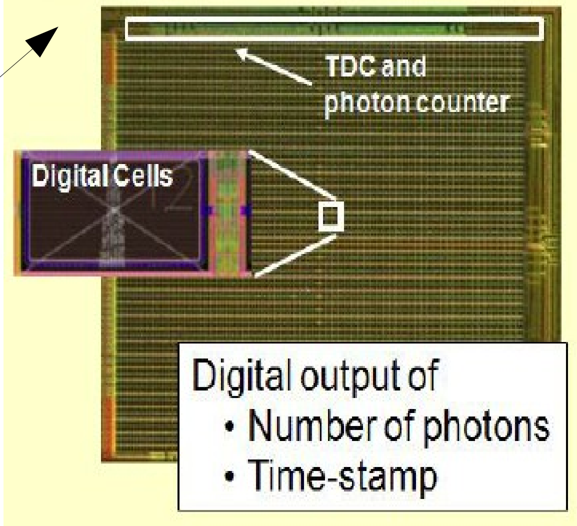

Digital output of
- Number of photons
- Time-stamp

S.Kononov Vienna Conference on Instrumentation 2013

FARICH test beam at CERN T10

Test conditions

- Positive polarity
  $e^+, \mu^+, \pi^+, K^+, p$
- Momentum: 1 - 6 GeV/c
- Trigger: a pair of sc. counters 1.5x1.5 cm² in coincidence separated by ~3 m
- No external tracking, particle ID, precise timing of trigger
- Hardware hit selection in a programmable time window to fit in data bandwidth

Pixel hit map

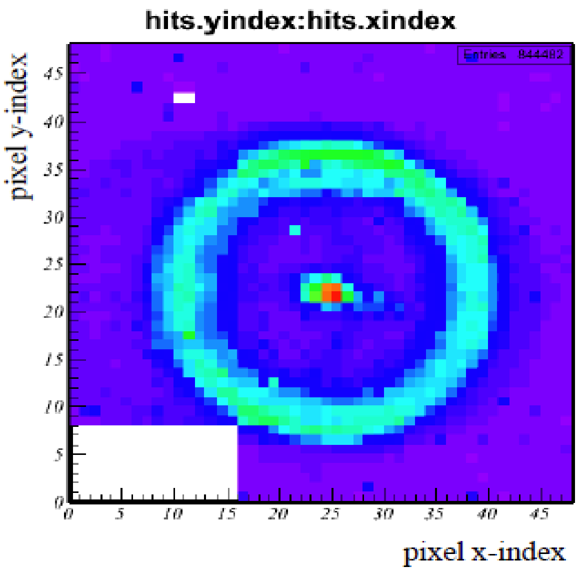

Event by Event ring fit

Hit selection and ring fit:

- Reject central hits
- Select hits in 4 ns time window
- More than 3 selected hits per event
- 4 parameters fitted: X_{center}, Y_{center}, R, t_0

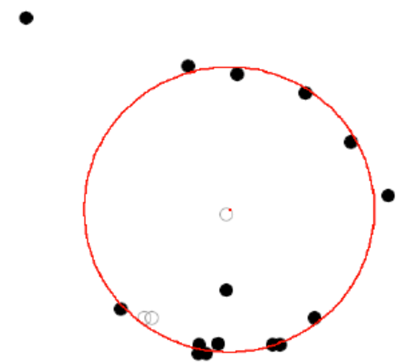

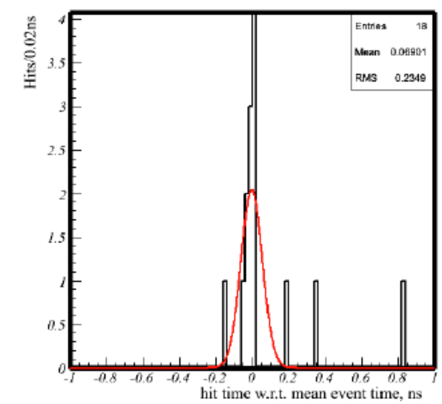

Timing resolution for Cherenkov hits

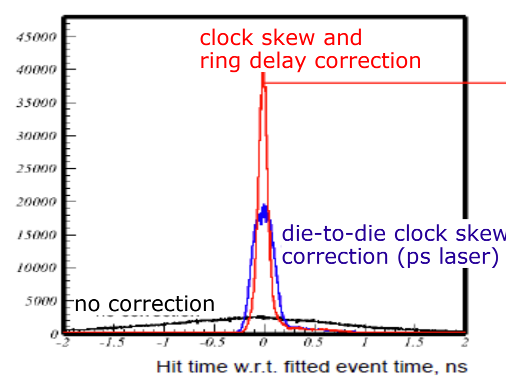

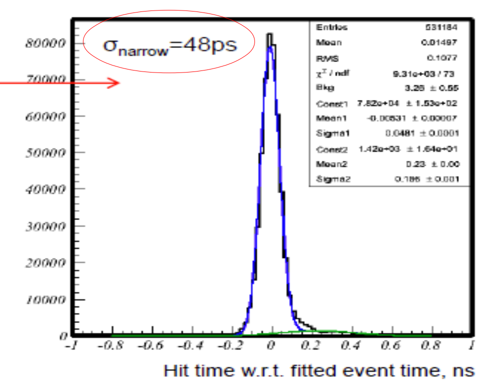

Fit two gaussians plus constant. 90% of area is contained in the narrow gaussian.

FARICH: Particle separation

$$S = 2\frac{R_\pi - R_K}{(\sigma_\pi + \sigma_K)}$$

S.Kononov Vienna Conference on Instrumentation 2013

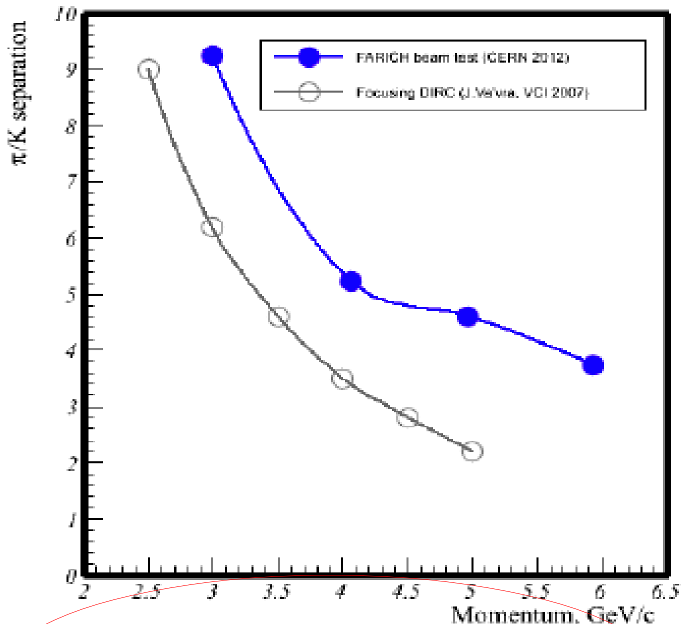

π /K: 3.8σ @ 6GeV/c
μ/π: 4.5σ @ 1 GeV/c

Remarkable results !!!

Rather idealized simulation for P=6 GeV/c gives
N_{pe} (π) = 24
π/K separation = 9 σ

Experimental results are far from simulated values, but there are reasons:

- Seems to be lower PDE than measured by PDPC previously (needs to be checked)
- Resolution deterioration due to pixel crosstalk
- No tracking (simulation relies on it)
- Probably: focusing aerogel tested gives wider ring than expected

PDE improvement expected for next generation dSiPM

Cross-Talk between dSiPM pairs (same die)

Crosstalk distribution of pixel pairs

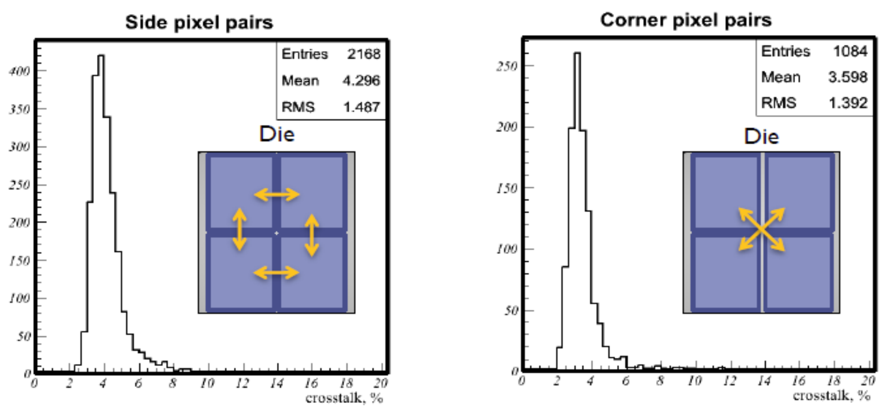

~4% crosstalk probability between pixels of one die → ring radius resolution deterioration

Note (G.C.) : after-pulsing and cross-talk between diodes are kept at very low level by active quenching/reset

What about **radiation Hardness** ? (electronics exposed to radiation together with sensors)

Conclusions: Analog vs Digital SiPM

Digital SiPM good features

- can turn off noisier micro-cells
- reduced after-pulsing (less charge)
- triggering at known photon level
- sophisticated triggering and
  time pickoff architecture
- inherently digital readout

Analog SiPM

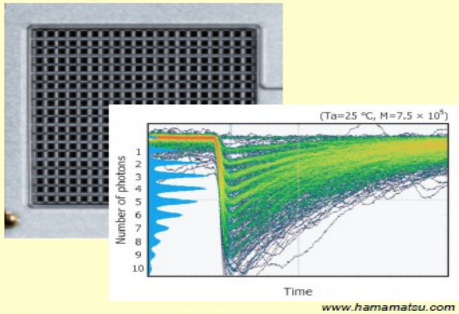

- Cells connected to common readout
- Analog sum of charge pulses
- Analog output signal

Digital SiPM

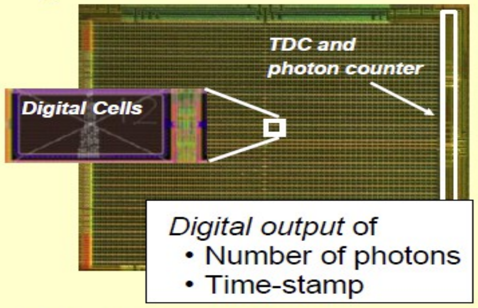

- Each diode is a digital switch
- Digital sum of detected photons
- Digital data output

In addition to Philips D-SiPM see other dSiPM by
→ Charbon et al at IEEE NSS 2013
→ Stoppa et al at IEEE NSS 2013

Digital SiPM most critical features

- scaled CMOS process has typically worse noise characteristics
  → mitigated by hottest single cells
- Fill Factor limited by area of silicon die used for digital circuits
  … unless exploiting 3D technology → *see Tetrault, Fontaine et al at IEEE NSS 2013*
- lower PDE due also to lower QE → can be further optimized
- Additional radiation damages to integrated electronics → tests to be done

Conclusions and outlook

Avalanche photo-diode:
- Internal multiplication: S/N improved → still >5 p.e. detectable
- Gain limited by the excess noise due to **avalanche multiplication noise**
- Practical use for single photon only in Hybrid photo-detectors (H-APD)

GM-APD based PM: technology of **SiPM** is mature
→ many flavours of SiPM → w/ external ("analog") or integrated electronics ("digital")
→ candidates for more and more experimental setups including Cherenkov detectors
→ price decreasing (competition) but far from production cost of O(10$/cm^2) (analog SiPM)

- **Dark noise (DC)** still the most limiting factor → **limited active area**
  → **large area hybrid detectors** demonstrated feasible (VSiPM or H-GMAPD)

- **Correlated excess charge (AP,CT)** under control → lower gain (small cells) desirable
  … → **tiny cells (low gain)** for reducing noises (DC,AP,CT)
  and mitigating radiation damage impact on performances too
  → **active quenching** is mitigates those issues → Digital-SiPM (MOS-SiPM might be the "analog" alternative)

- **Low T:** SiPM perform ideally in the range 100K < T < 200K
  → best candidates for applications (superior to PMT also for radio-purity)

Development of GM-APD:up to now development focused on multi-photon and blue light applications → plenty of room for new devices in different directions:
- ultra-fast timing specific SiPM → relatively easy, but still missing
- position sensitive → relatively easy but still missing
- DUV/VUV sensitive devices → can be done with Si, just started
- IR/NIR sensitive devices → possibly based on different semiconductors
- charge particle detection → just started

Thanks for your attention

Additional material →

Digital SiPM

- Operating frequency: 200MHz
- 2 x TDC (bin width 23ps, 9bit)
- Configurable trigger network
- Validation logic to reduce sensor dead time due to dark counts
- JTAG for configuration and scan test
- Electrical trigger input for test and TDC calibration

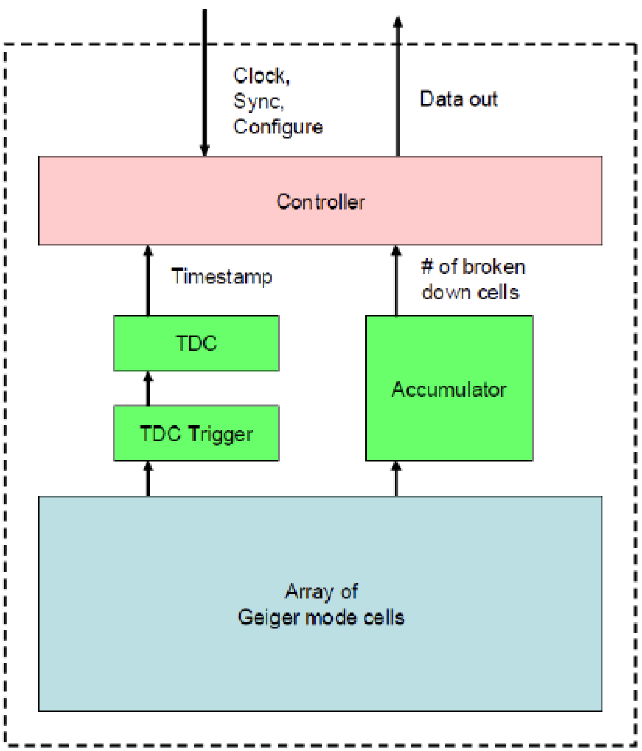

Sensor Architecture

Digital SiPM – State Machine

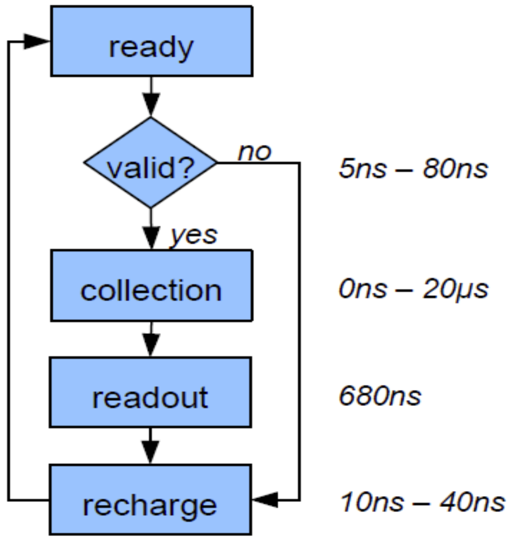

- *200MHz (5ns) system clock*
- *Variable light collection time up to 20µs*
- *20ns min. dark count recovery*
- *dark counts => sensor dead-time*
- *data output parallel to the acquisition of the next event (no dead time)*
- *Trigger at 1, ≥2, ≥3 and ≥4 photons*
- *Validate at ≥4 … ≥64 photons (possible to bypass event validation completely)*

Digital SiPM – Trigger Logic

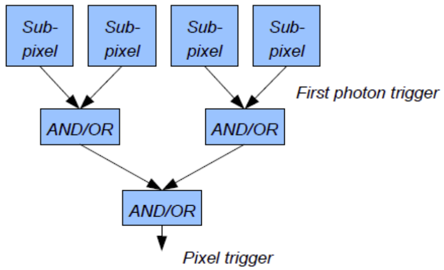

- *Each sub-pixel triggers at first photon*
- *Sub-pixel trigger can be OR-ed or AND-ed to generate probabilistic trigger thresholds*
- *Higher trigger threshold decreases system dead-time at high dark count rates at the cost of time resolution*

T.Frach Heraeus Seminar 2013

Digital SiPM 8x8 Array (“Module” 64 time channels 256 position channels)

DPC3200-22-44
DPC6400-22-44

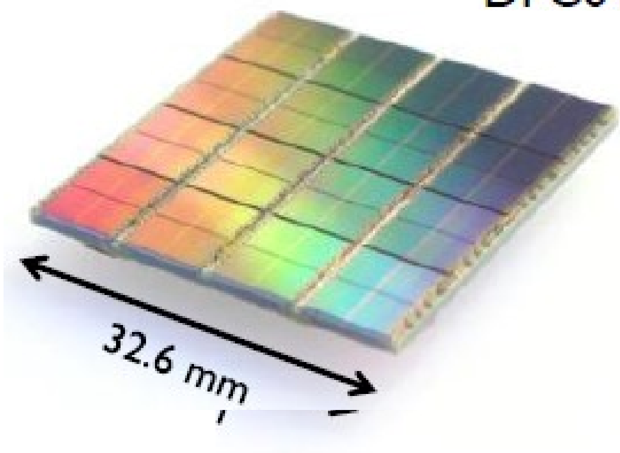

FPGA
- Clock distribution
- Data collection/concentration
- TDC linearization
- Saturation correction
- Skew correction

Flash
- FPGA firmware
- Configuration
- Inhibit memory maps

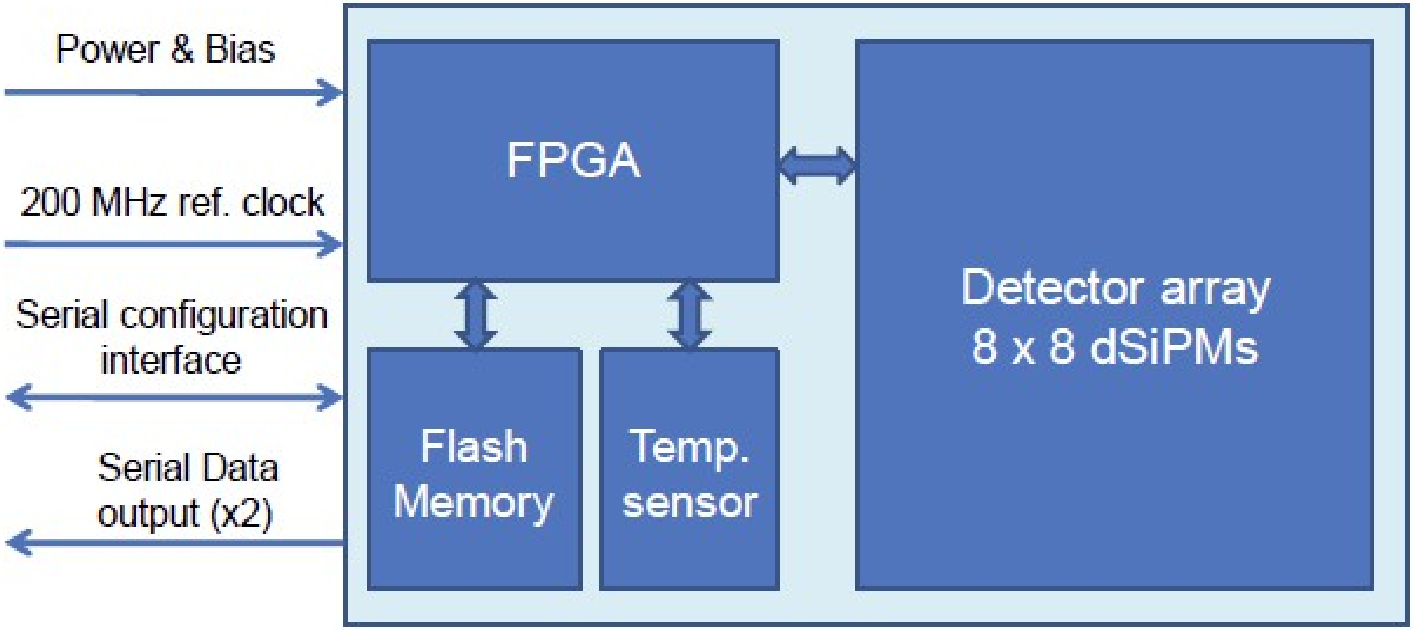

Radiation damage

Radiation damage: two types

- Bulk damage due to Non Ionizing Energy Loss (NIEL) ← neutrons, protons
- Surface damage due to Ionizing Energy Loss (IEL) ← γ rays

(accumulation of charge in the oxide (SiO2) and the Si/SiO2 interface)

Assumption: damage scales linearly with the amount of Non Ionizing Energy Loss (NIEL hypothesis)

G.Lindstrom et al. NIM A426(1999)1-15

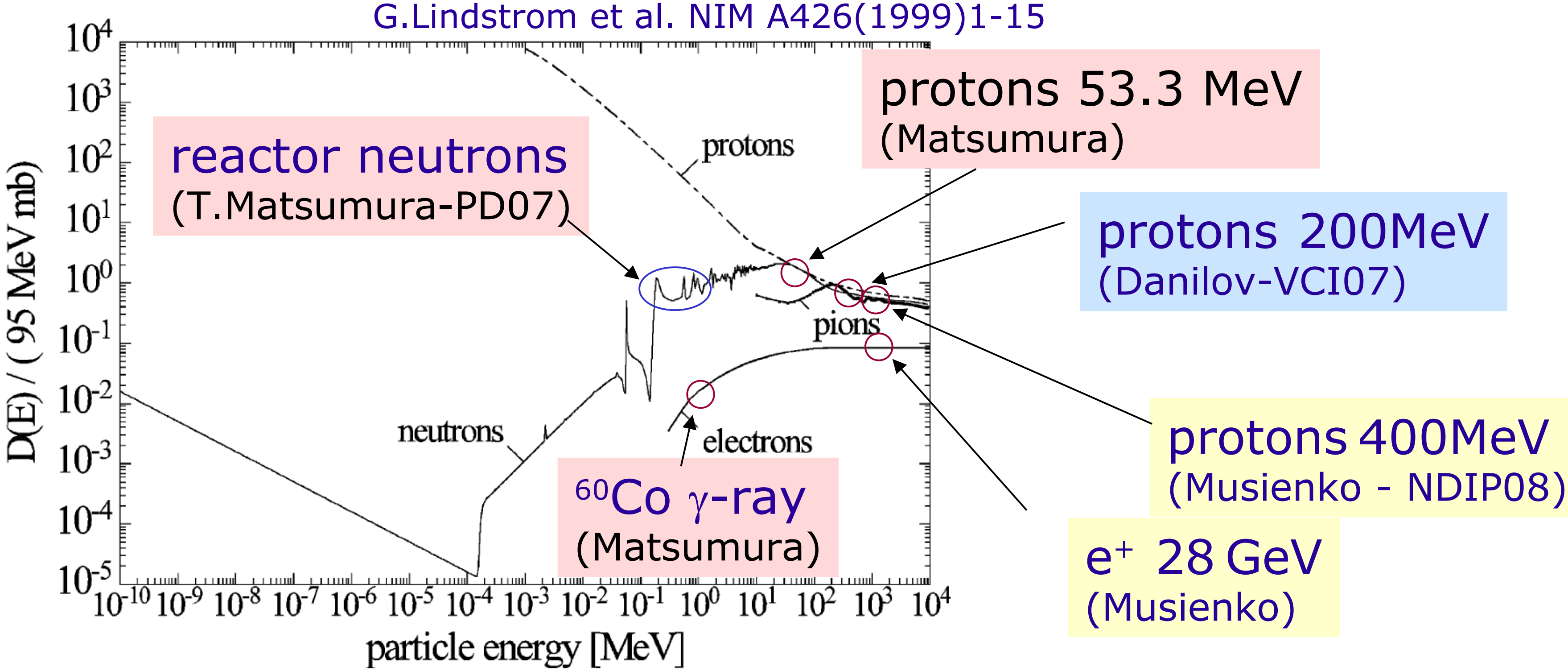

Examples of radiation tolerances for HEP and space physics

ATLAS inner detector ... 3×10^{14} hadrons/cm^2/10 year

~ 10^4 hadrons/mm^2/s

General satellites ... ~ 10 Gy/year

Expectations:

protons / γ-ray ~ 100

protons / neutrons ~ 2~10

Radiation damage: effects on SiPM

1) Increase of dark count rate due to introduction of generation centers

Increase (ΔR_{DC}) of the dark rate:
$\Delta R_{DC} \sim P_{01}\ \alpha\ \Phi_{eq}\ Vol_{eff} / q_e$
where $\alpha \sim 3 \times 10^{-17}$ A/cm is a typical value of the radiation damage parameter for low E hadrons and $Vol_{eff} \sim Area_{SiPM} \times \varepsilon_{geom} \times W_{epi}$

NOTE:
The effect is the same as in normal junctions:
- independent of the substrate type
- dependent on particle type and energy (NIEL)
- proportional to fluence

2) Increase of after-pulse rate due to introduction of trapping centers

→ loss of single cell resolution → no photon counting capability

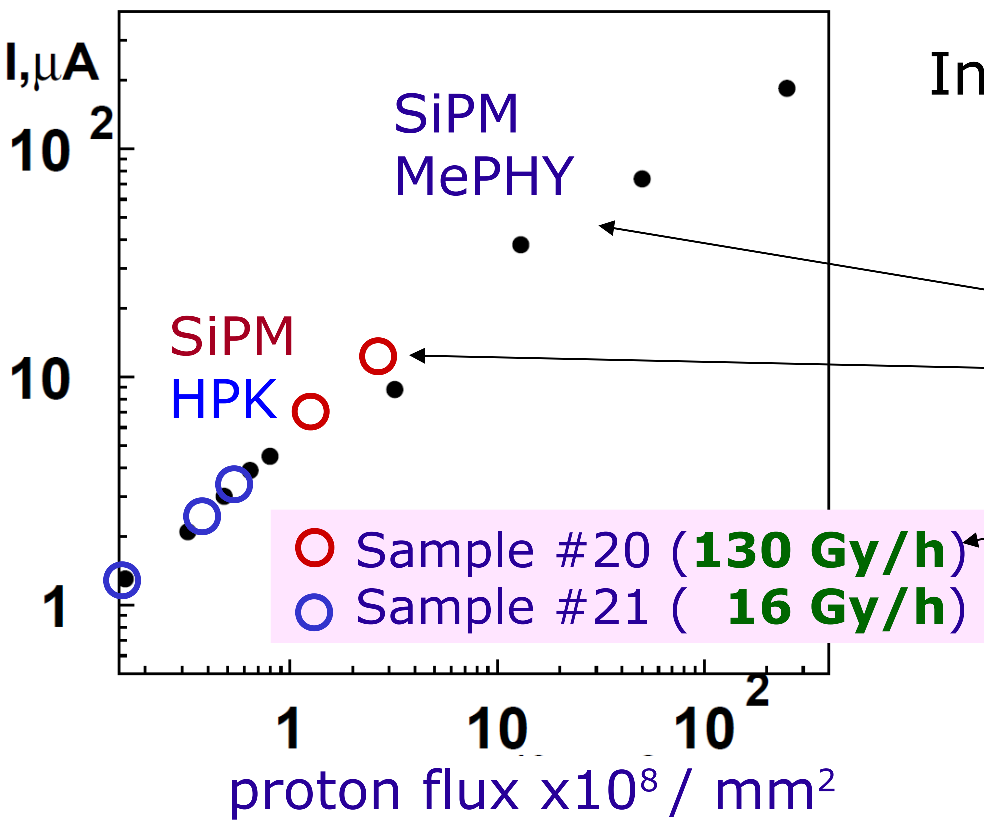

Indications from measurements:

1) no dependence on the device
similar effects found for SiPM from MePHY (Danilov) and HPK (Matsumura)
(normaliz. to active volume)

2) no dependence on dose-rate
HPK (Matsumura)

3) n similar damage than p

4) p x10¹-10² more damage than γ

Damage comparison

HPK devices
T.Matsumura – PD07

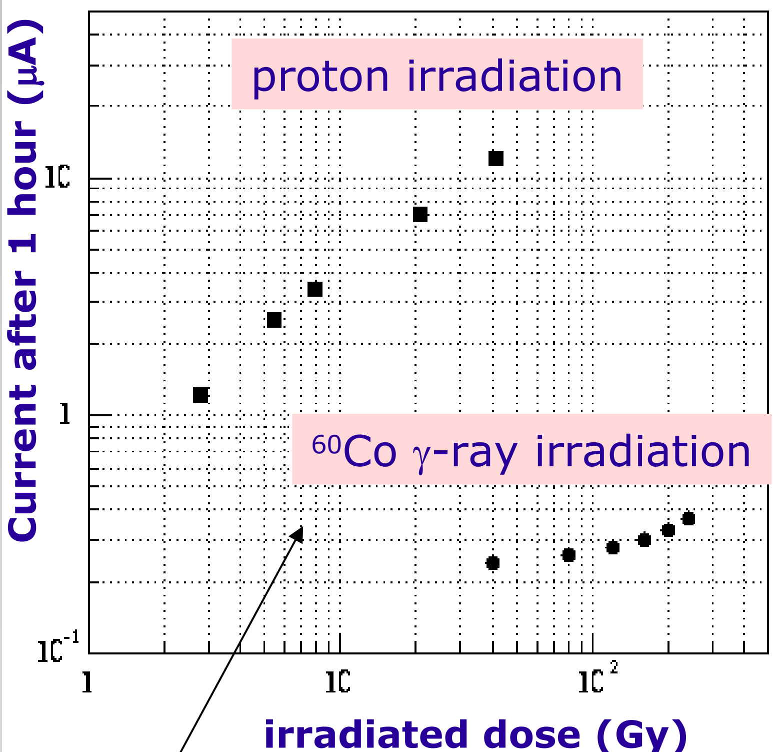

Damage effect ...
1~2 orders larger with protons than γ-ray irradiation

Damage effect ...
almost the same for protons and neutrons

2.3×10^5 p/mm²/s (130 Gy/h)
I_{leak} @ (V_{op}, 1.4×10^8 p/mm²) = 6.7 μA

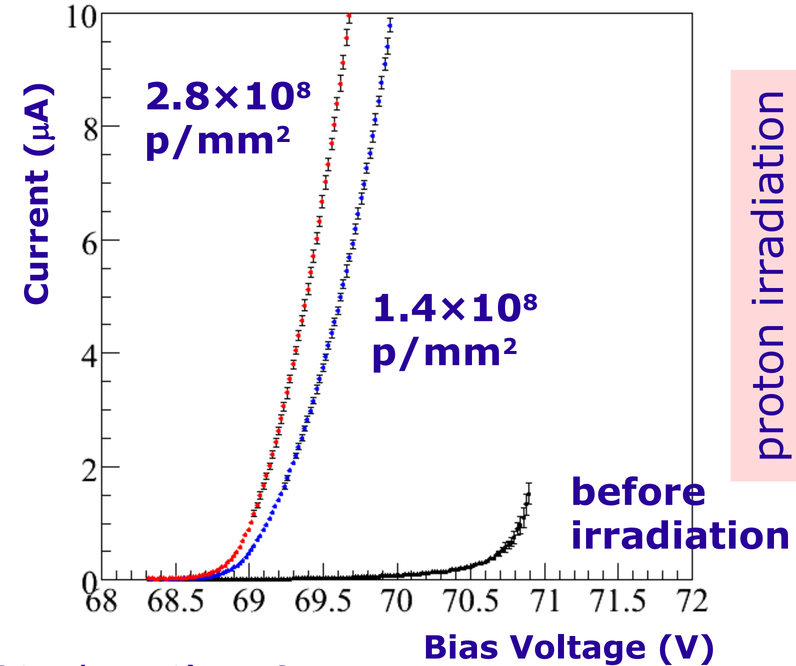

4.2×10^5 n/mm²/s
I_{leak} @ (V_{op}, 1.0×10^8 n/mm²) = 8.5 μA

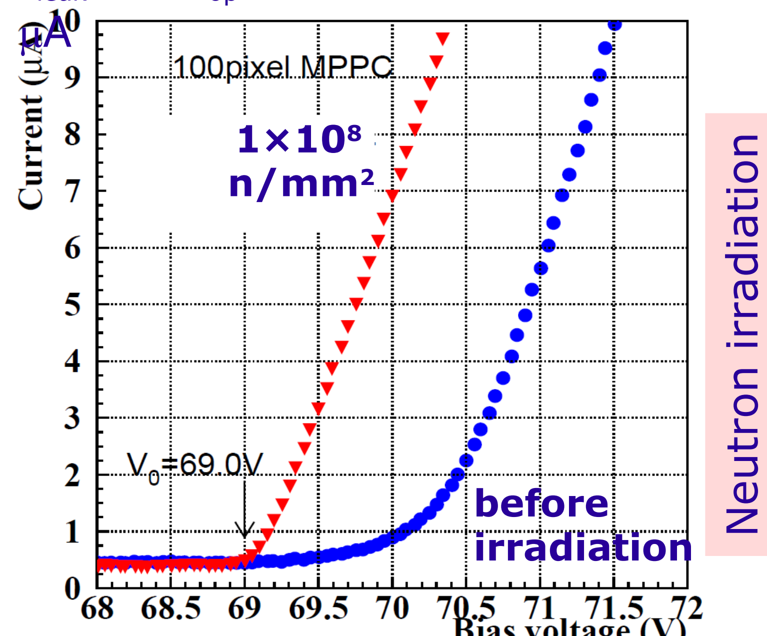

T.Matsumura – PD07

Radiation damage: neutrons (0.1 -1 MeV)

8.3×10^{4} n/mm^{2} 3.3×10^{5} n/mm^{2} 1.0×10^{8} n/mm^{2}

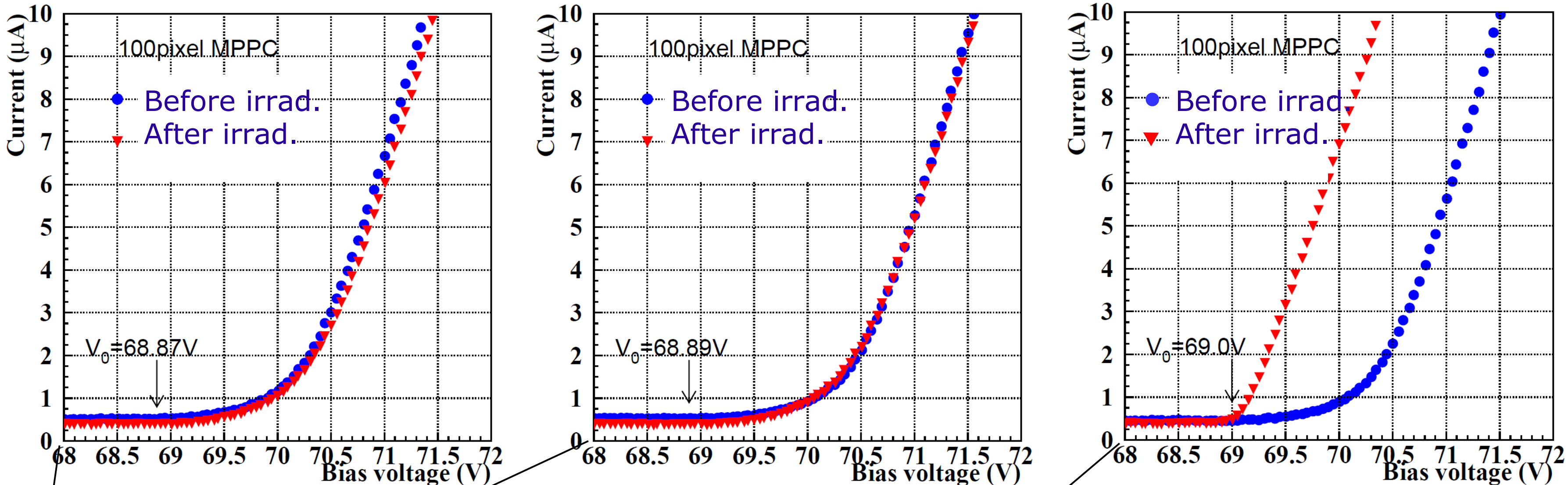

T.Matsumura – PD07

10^{5} n/mm^{2} 10^{6} n/mm^{2} 10^{7} n/mm^{2} 10^{8} n/mm^{2} 10^{9} n/mm^{2} 10^{10} n/mm^{2}

n dose

No significant change

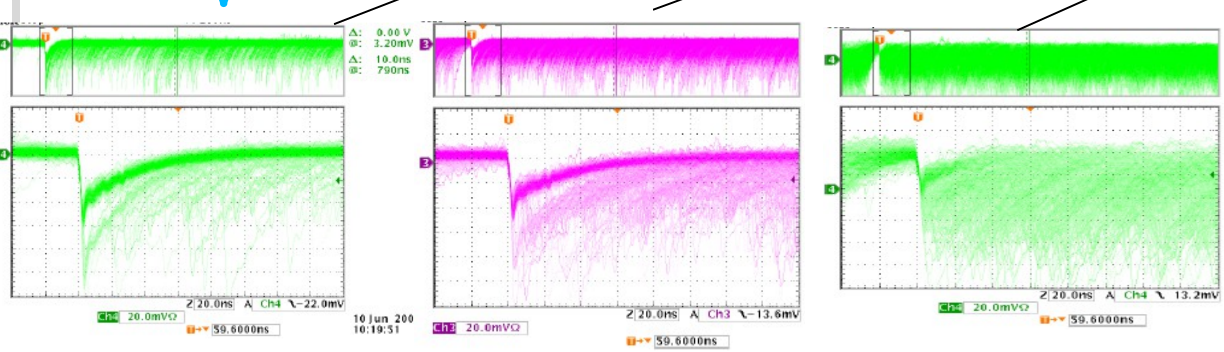

I-V drastically change.
Signal pulse is still there,
but continuous pulse height.
(No photon-counting capability)

No signal

Nakamura at NDIP08

Radiation damage: neutrons 1 MeV E_{eq}

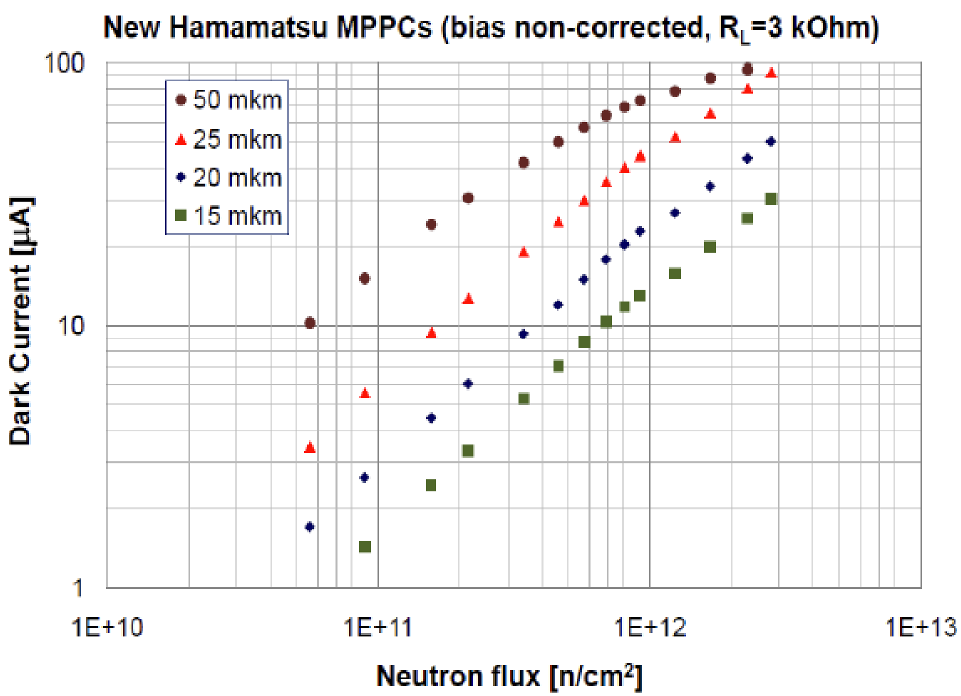

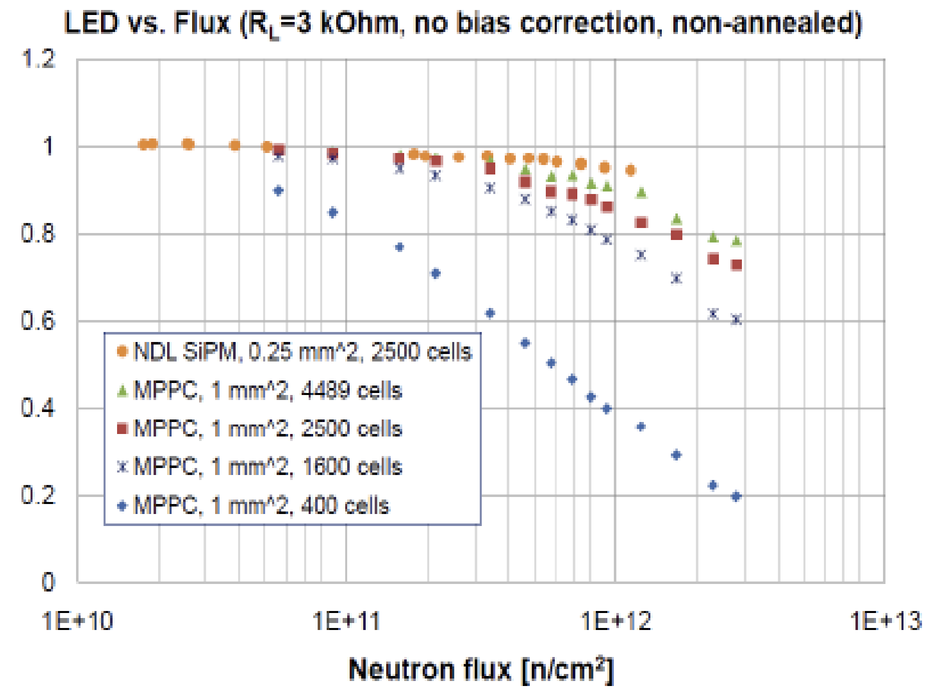

- No change of V_{bd} (within 50mV accuracy)
- No change of R_q (within 5% accuracy)
- I_{dark} and DCR significantly increase

SiPMs with high cell density and fast recovery time can operate up to $3*10^{10}$ n/mm^2 ($\delta G < 25\%$)

Y.Musienko at SiPM workshop CERN 2011

Radiation damage effects are mitigated by using devices with:
→ **small cells** → smaller charge flow (smaller gain → charge)
→ thin epi-layer

FARICH: Stability → radiation and thermal cycles

Note: radiation dose was not monitored during the experiment

Radiation damage: Dark count rate changing

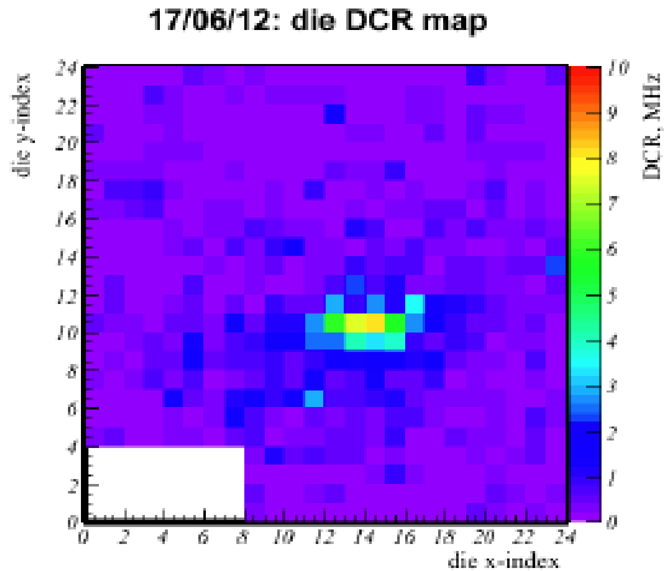

5th day of beam

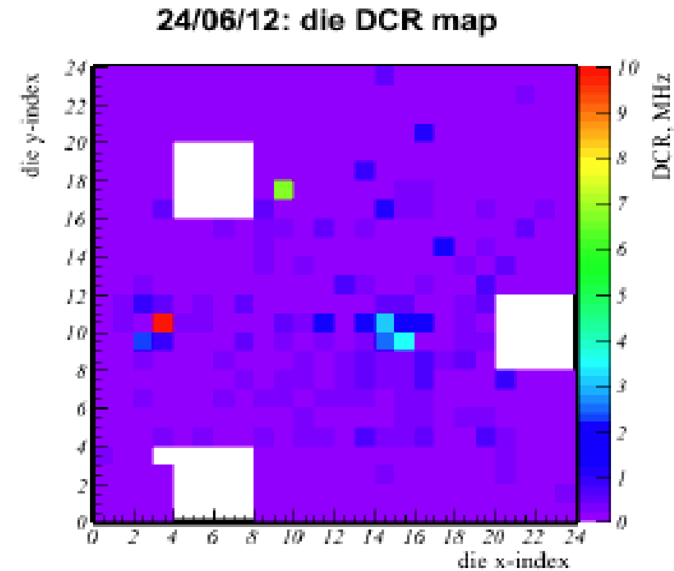

10th day of beam with 2 days break at +30°C

Partial recovery is observed after annealing for 2 days at 30°C

Breakage: only 4 of 36 tiles failed after 2 weeks and several thermal cycles. DPC modules and tiles was not designed to work routinely at low temperature with frequent thermal cycles. It was just a first test.

S.Kononov Vienna Conference on Instrumentation 2013

Electronics

Front-end electronics: general comments

- **Strong push for high speed front-end > GHz**

– Essential for timing measurements
– Several configurations to get GBW > 10 GHz
– Optimum use of SiGe bipolar transiistors

- **Voltage sensitive front-end**

– Easiest : 50Ω termination, many commercial amplifiers
– Beware of power dissipation
– Easy multi-gain (time and charge)

- **Current sensitive front-end**

– Potentially lower noise, lower input impedance
– Largest GBW product

- **In all cases, importance of reducing stray inductance**

see C.de la Taille – PhotoDet 2012

Front-end electronics: different approaches

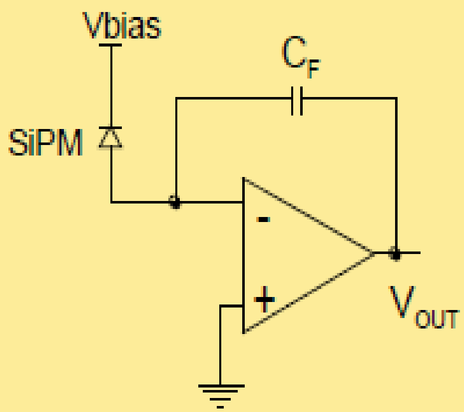

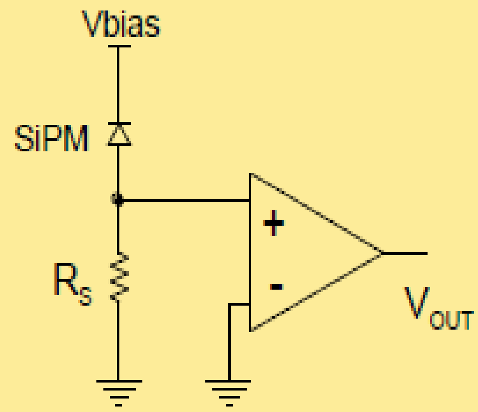

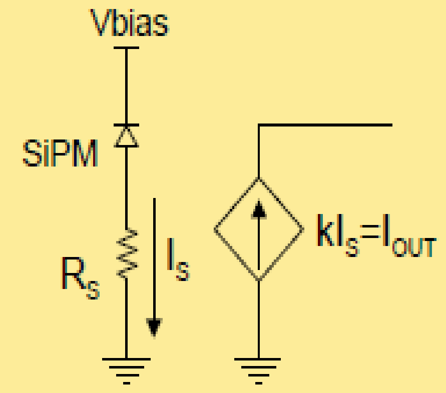

Charge sensitive amplifier

The charge Q delivered by the detector is collected on C_F

If the maximum ΔV_{OUT} is 3V and Q is 50pC (about 300 SiPM microcells), C_F must be 16.7pF

⬇

Perspective limitations in dynamic range and die area with low voltage, deep submicron technologies

Voltage amplifier

A I-V conversion is realized by means of R_S

The value of R_S affects the signal waveform

V_{OUT} must be integrated to extract the charge information: thus a further V-I conversion is needed

Current buffer

R_S is the (small) input impedance of the current buffer

The output current can be easily replicated (by means of current mirrors) and further processed (e.g. integrated)

The circuit is inherently fast

The current mode of operation enhances the dynamic range, since it does not suffer from voltage limitations due to deep submicron implementation

see F.Corsi et al – Pixel 2008

ASICs for SiPM signal readout (QDC/TDC)

W.Kucewicz "Review of ASIC developments for SiPM signal readout" - talk at CERN 11-2-2011

Chip Name	Measured quantity	Application	Input configuration	Technology
FLC_SiPM	Pulse charge	ILC Analog HCAL	Current input	CMOS 0,8 μm
MAROC	Pulse charge, trigger	ATLAS luminometer	Current input	SiGe 0,35 μm
SPIROC	Pulse charge, trigger, time	ILC HCAL	Current input	SiGe 0,35 μm
NINO	Trigger, pulse width	ALICE TOF	Differential input	CMOS 0,25 μm
PETA	Pulse charge, trigger,time	PET	Differential input	CMOS 0,18 μm
BASIC	Pulse height, trigger	PET	Current input	CMOS 0,35 μm
SPIDER (VATA64-HDR16)	Pulse height, trigger, time	SPIDER RICH	Current input	
RAPSODI	Pulse height, trigger	SNOOPER	Current input	CMOS 0,35 μm

ASICs for SiPM signal readout (QDC/TDC)

W.Kucewicz - CERN 11-2-2011

Chip Name	# of channels	Digital output	Power supply	Area [sqr mm]	Dynamic range	Input resistance	Timing jitter	Year
FLC_SiPM	18	n	5V (0,2W)	10			-	2004
MAROC2	64	y	5 V	16	80 pC	50 Ω		2006
SPIROC	36	y	5 V	32				2007
NINO	8	n	(0,24W)	8	2000 pe	20 Ω	260 ps	2004
PETA	40	y	(1,2W)	25	8 bit		50 ps	2008
BASIC	32	y	3,3 V	7	70 pC	17 Ω	~120 ps	2009
SPIDER (VATA64-HDR16)	64	n		15	12 pC			2009
RAPSODI	2	y	3,3 V (0,2W)	9	100 pC	20 Ω	-	2008

- Only a few of the suitable for low light intensity

Note: Electronics → fast sampling

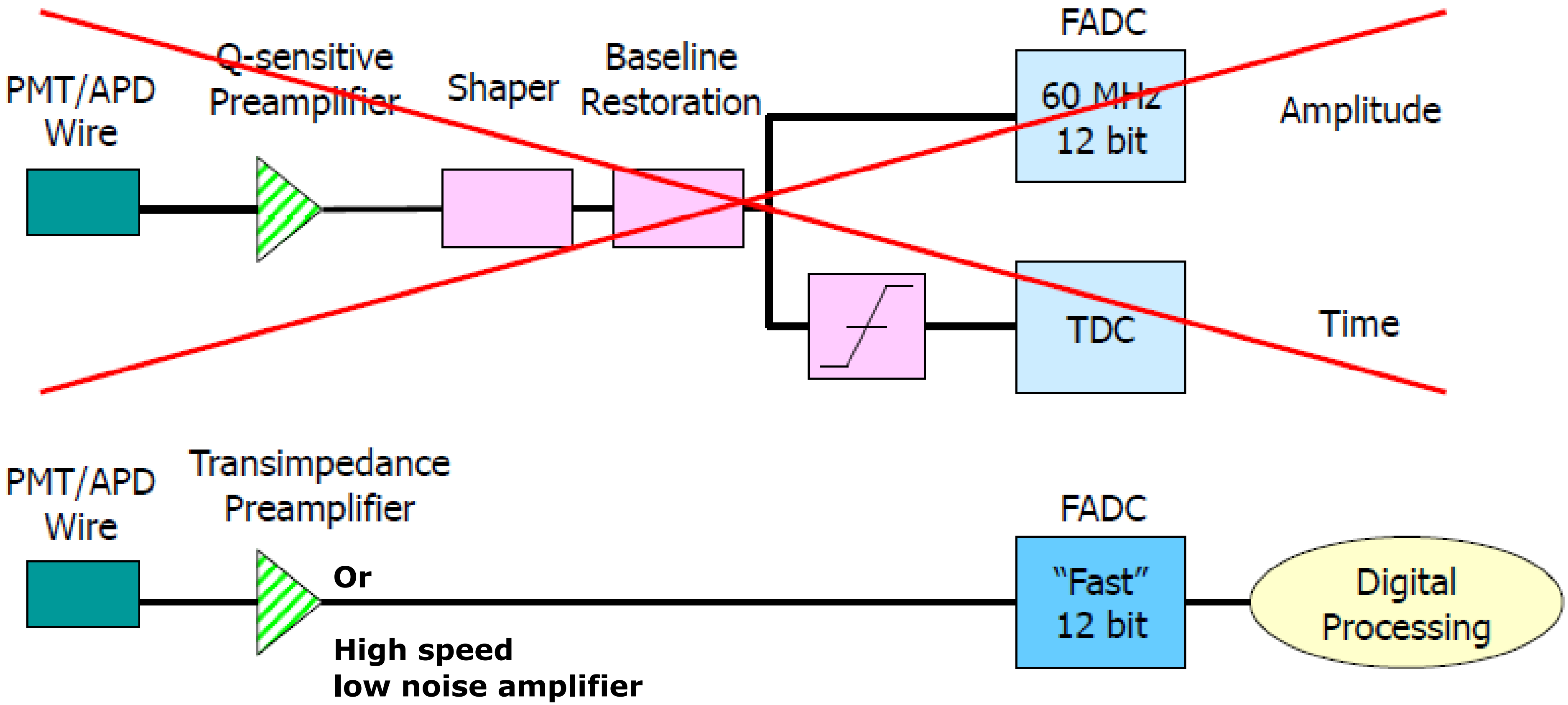

- Shaping stage can only remove information from the signal
- Shaping is unnecessary if FADC is "fast" enough
  = sampling speed 2x maximum frequency (Nyquist-Shannon)
- All operations (CFD, optimal filtering, integration) can be done digitally

Intro

Photo-detection in two steps

1. Photo-electric conversion with or without emission in vacuum

"external" photo-emission

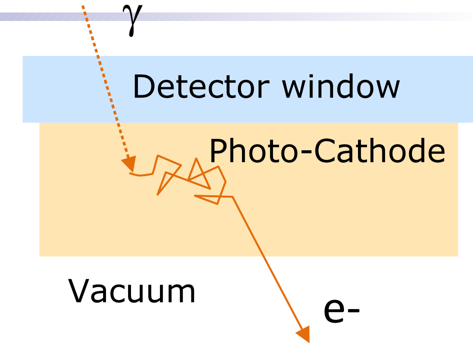

Emission in vacuum implies

→ low detection efficiency

→ low dark count rate

"internal" photo-emission

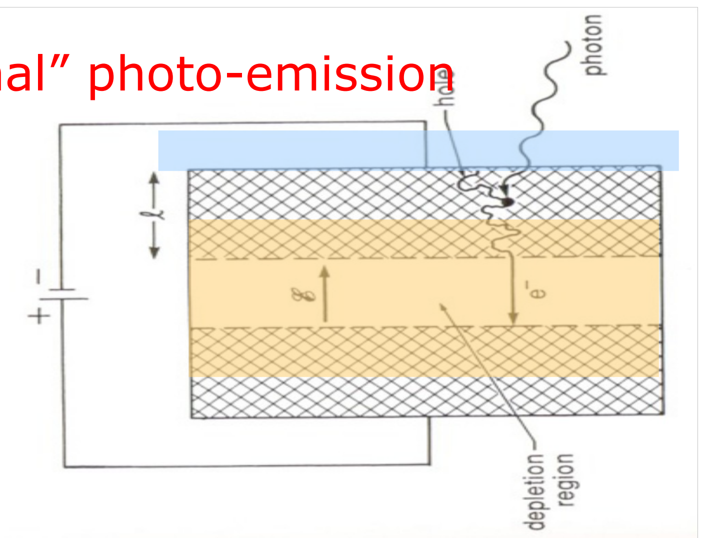

...source of differences between vacuum and solid state devices including multiplication mechanisms...

2. Internal charge multiplication implies

→ better Signal/Noise ratio

→ intrinsic fluctuations in amplitude and timing (depending on the multiplication mechanism)

SSPD with internal gain

Reverse biased junction: internal gain via impact ionization in high E field

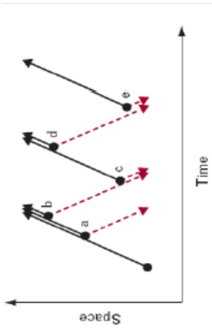

APD: avalanche photo-diode

- Bias **below** V_{bd} ($V_{APD} < V < V_{bd}$)
- Linear Mode/ **amplifier** device
- Multiplication < 10^3 (fluctuations)
- **Sensitivity ~ 5 ph.e** (T_{room})

  (1p.e. at low T slow electronics)

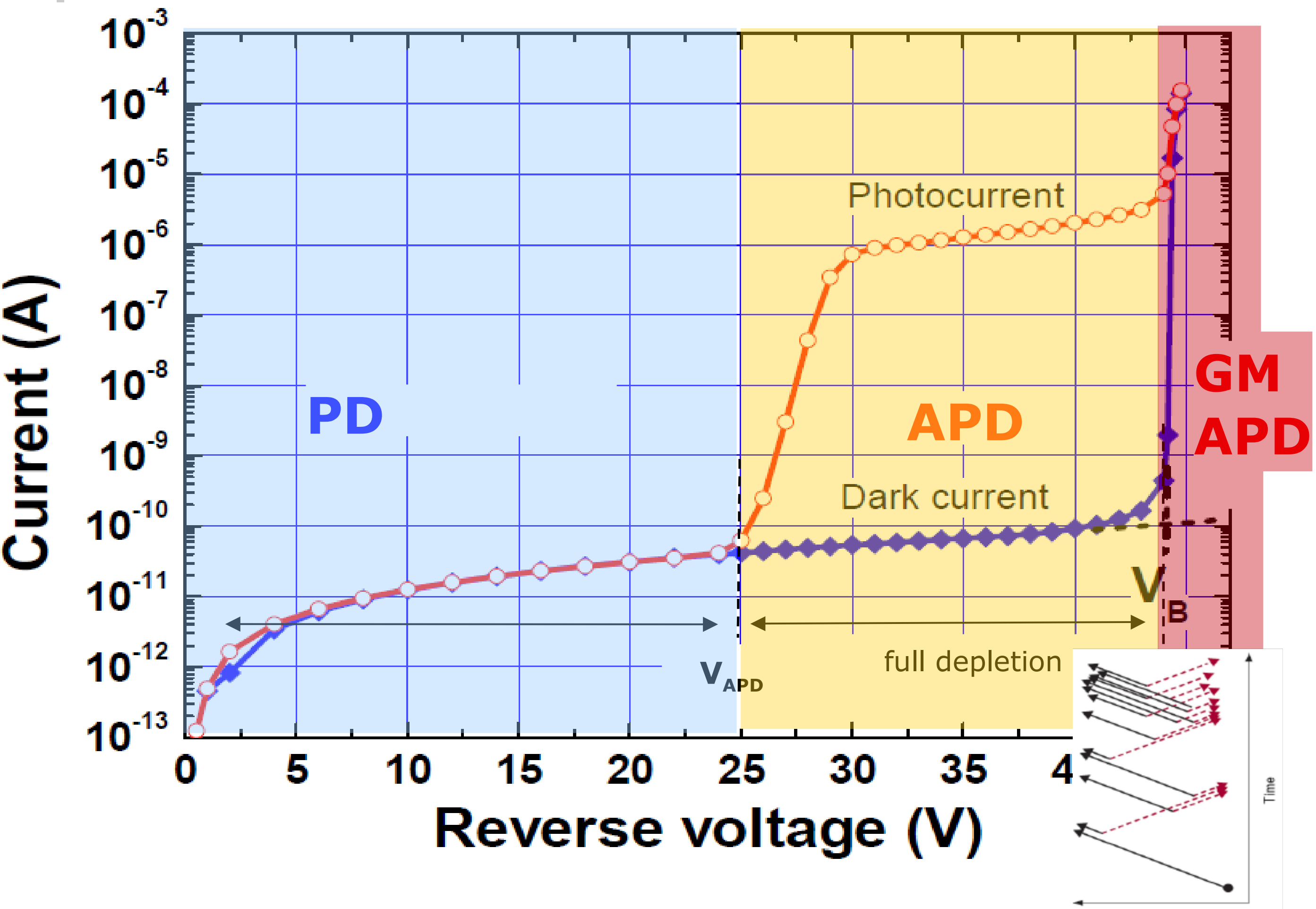

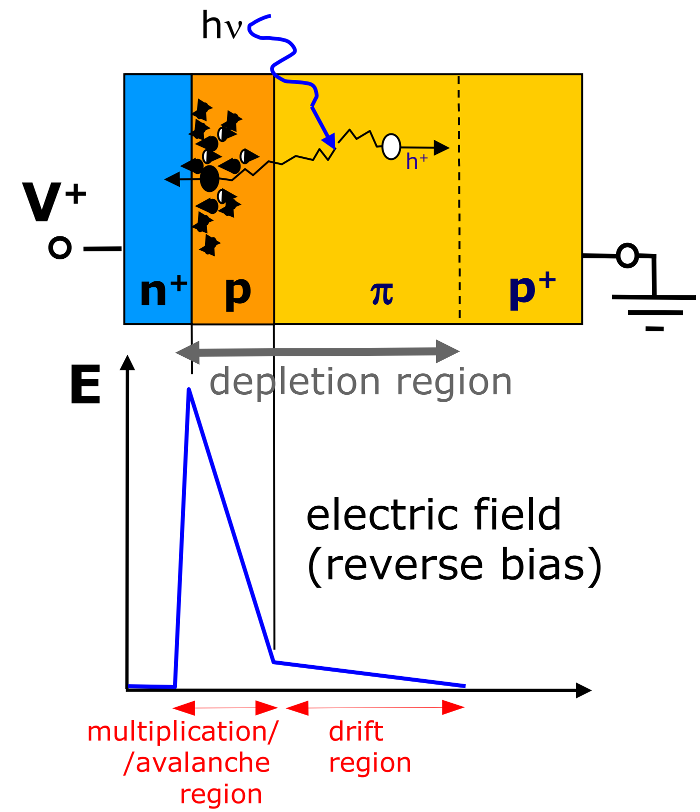

GM-APD: Geiger Mode

- Bias **above** V_{bd} (a few V)
- **binary** device
- Gain: ~10^6 (lim. by noises)
- **Single ph.e. resolution**
- Limited by dark count rate
- **Need Quenching/Reset**

SiPM vs APD for single photon

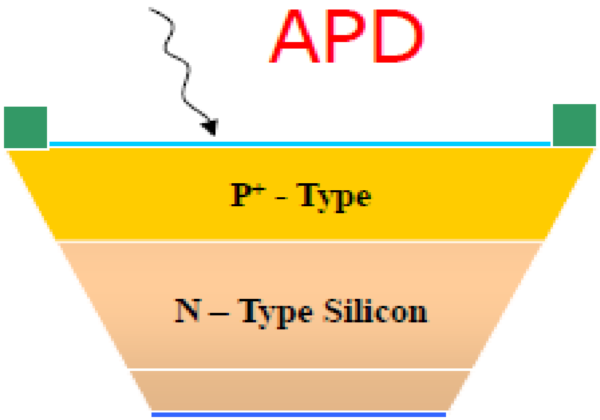

→ ENF increases with increasing gain
→ Temperature coefficient also increases with gain (… gain stability)

Devices with high multiplication noise are not good for single photon counting

Single photon counting is possible, but at **low temperature (T~77K)** and with slow electronics (and PDE~20%)

A. Dorokhov et al, JournalMod.Opt. v51 2004 p.1351

Reminder SiPM correlated noise:

1) no multiplication (excess) noise in SER
2) SER width due to intrinsic fluctuations in doping densities and non-uniformity of parameters among cells
3) Correlated noise is there, namely After-Pulsing and Cross-Talk "excess charge factor (ECF)" but it does not prevent clean single photon

Silicon technology

Two different approaches for SPAD or GM-APD arrays

Custom technology

- control/tune shape of E field
  → high PDE
  → optimized timing resolution
  → low Dark Count Rate
  → low After-pulsing

- possible both Planar and Reach Through
  → tune spectral sensitivity

- limited integrated electronics
  (no libraries for complex functionalities
  and for deep-submicron features)
  → simple integrated electronics
  (few large MOS)
  → it limits array dimensions and fill factor

Ancillary electronics (quenching/readout):
→ completely external → **SiPM**
→ hybrid → **SPAD arrays** … complex fabrication

CMOS HV technology

- no optimization of shape of E field
  + high curvature sub-micron tech.
  → special care for guard ring
  (limited range of GR possible
  only STI demonstrated ok)

- only Planar structures
  → UV/Blue sensitivity

- fully supported sub-micron technology
  with models and libraries →complex electr.
  → processing of large amount of data
  → high density → imaging
  → ultra-fast timing

Ultrafast and/or **imaging**
monolithic SPAD arrays

Silicon technology – few examples

Custom technology

SiPM “RGB” FBK – **external** electronics

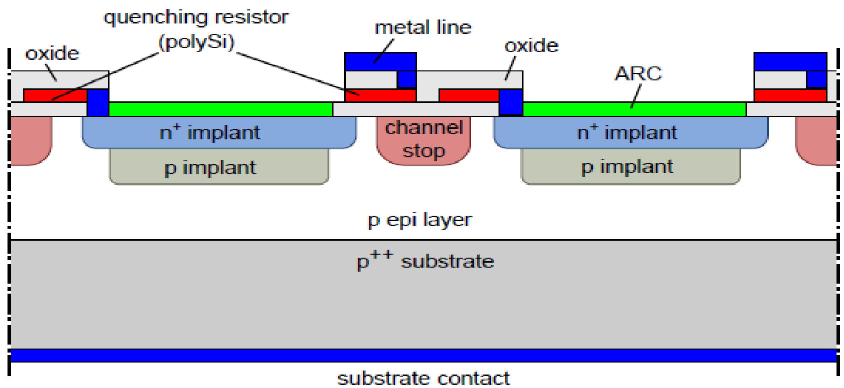

N.Serra et al JINST 8 (2013) P03019

CMOS HV technology

integrated electronics

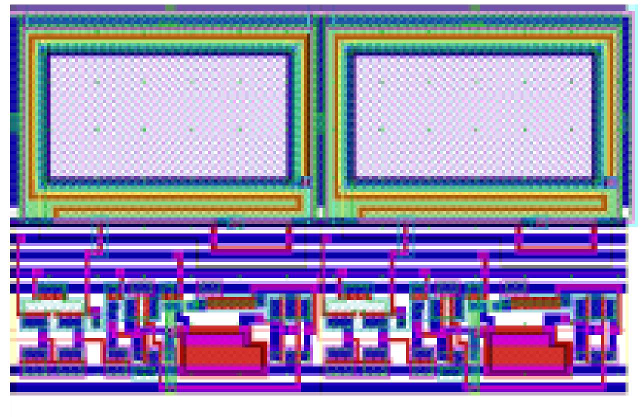

Stapels et al Procs. SPIE 7720 2009

Custom CMOS technology

SPAD array - **hybrid** electronics

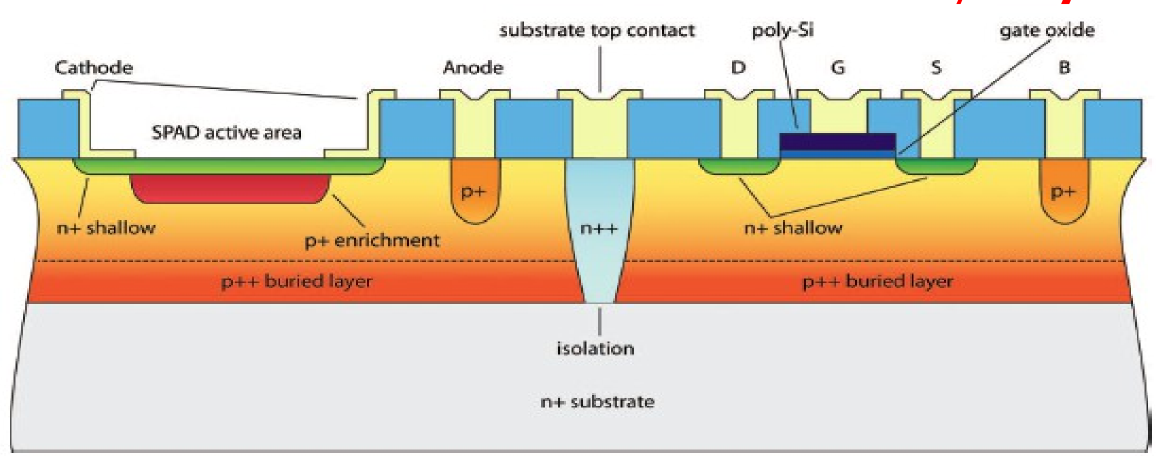

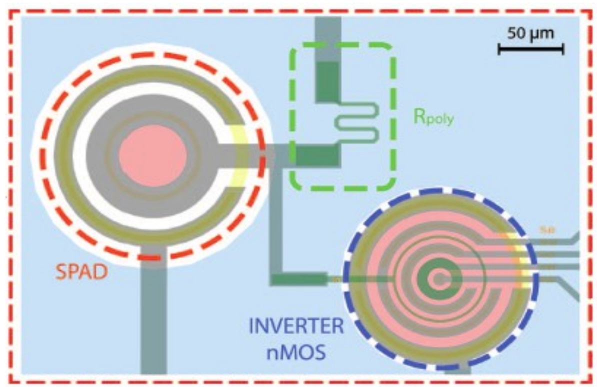

Cammi et al Rev Sci Instr 83 (2012) 033104

The Guard Ring structure

- high E field structure, not uniform
- neutral region (timing tails)
- limited fill factor

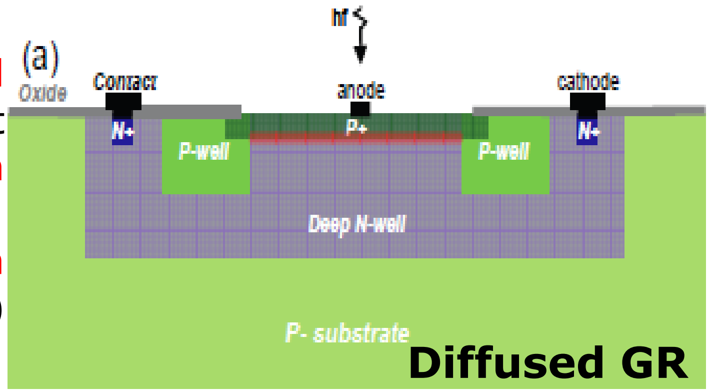

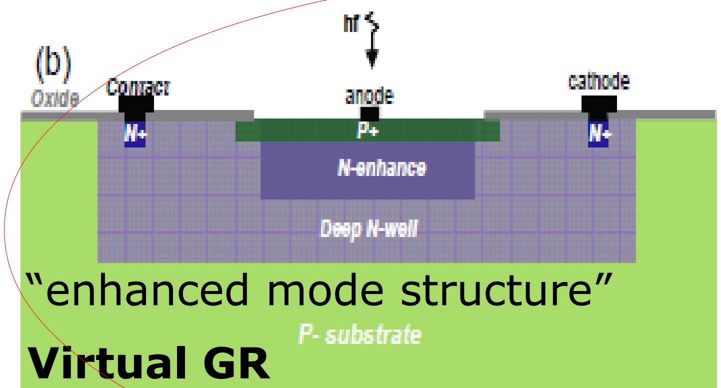

- well tuned high E field structure
- no additional neutral regions
- fill factor less limited

- alternative to Diffused GR
- difficult to implement

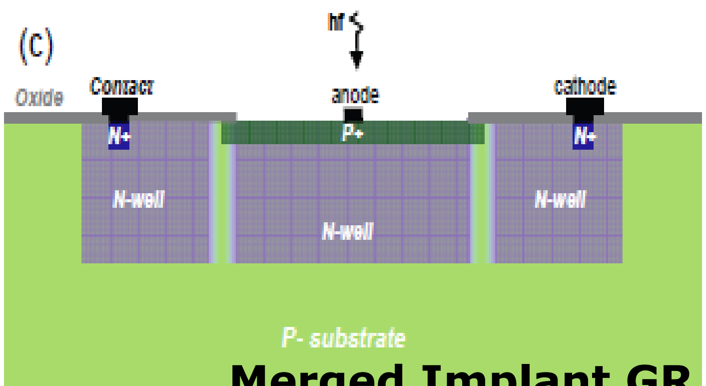

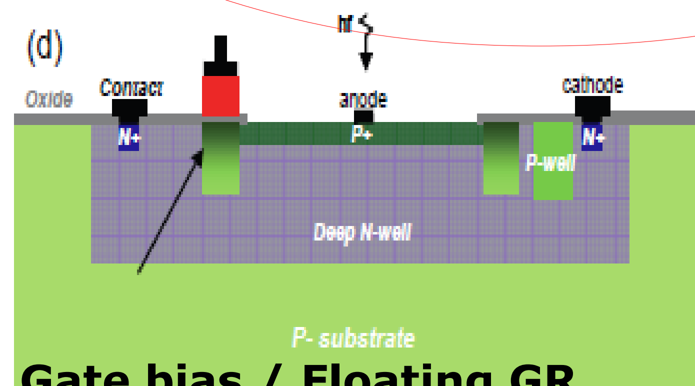

- less commonly exploited
- careful modeling required

- developed by S.Cova and coll. (fully custom)
- state of the art SPAD timing and PDE (red enhanced)

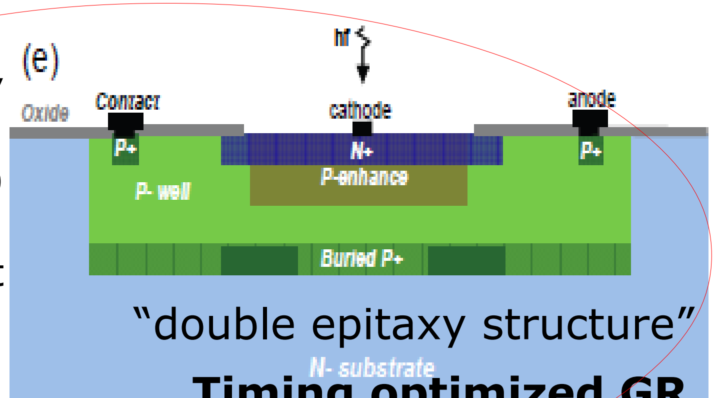

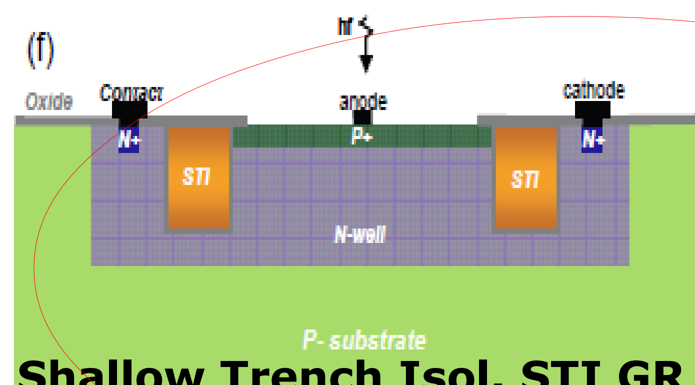

- physically blocks and confines the high E field in active region
- might cause high DCR due to
  - tunneling
  - etching induced defects/traps

from "Avalanches in Photodiodes" G.F.Dalla Betta Ed., InTech Pub. (2011)

Passive Quenching: tread-off τ_{quench} vs $\tau_{recovery}$

If R_Q is high enough the internal current is so low that statistical fluctuations may quench the avalanche

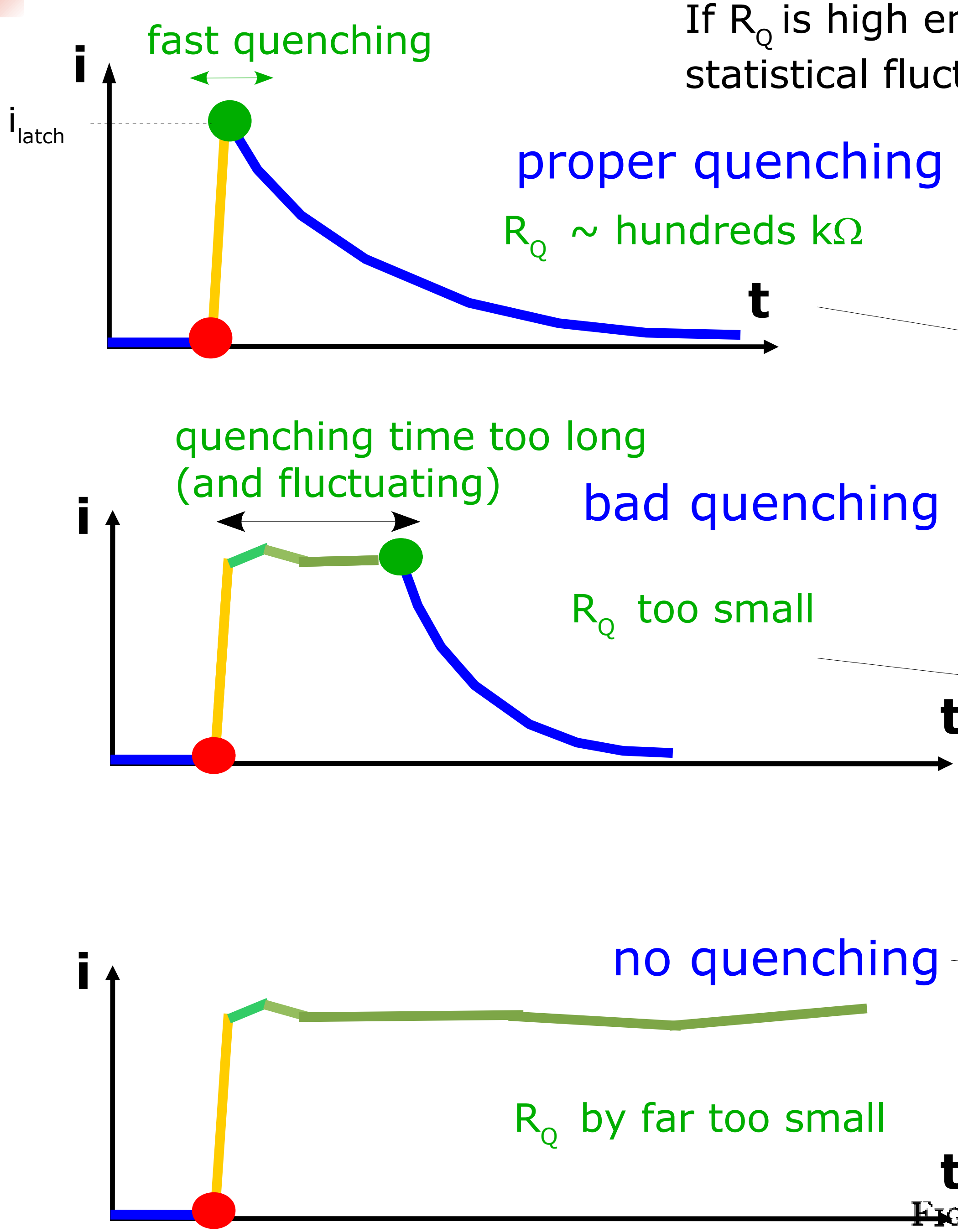

Haitz JAP 35 (1964)

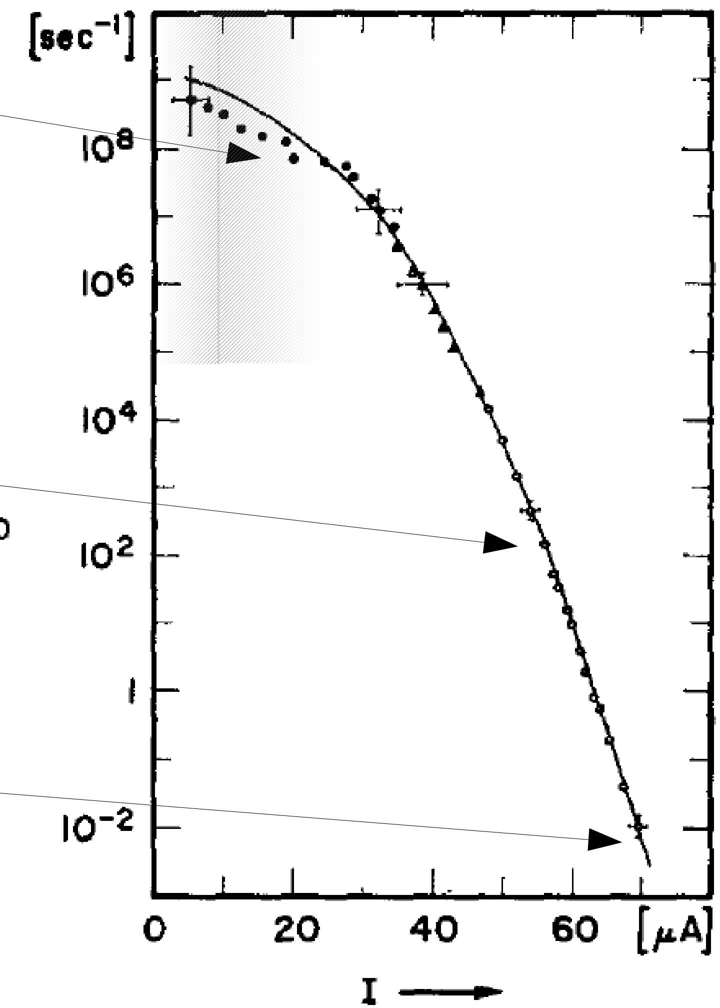

FIG. 2. Turnoff probability per second as function of pulse cu

Passive Quenching (Resistive)

1) common solution: poly-silicon

2) alternative: metal thin film
→ higher fill factor
→ milder T dependence

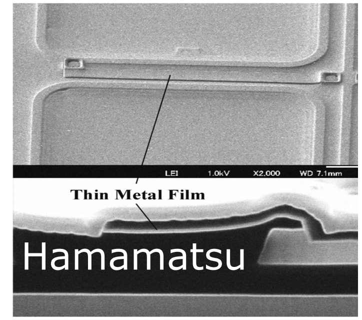

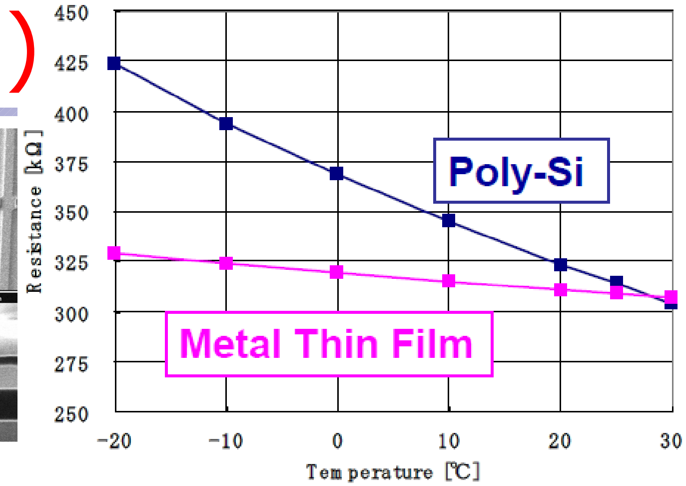

Nagano IEEE NSS-MIC 2011

3) alternative principle: bulk integrated resistor
→ flat optical window → simpler ARC
→ fully active entrance window
→ high fill factor (constraints only from guard ring and X-talk)
→ diffusion barrier against minorities
→ less X-talk
→ positive T coeff. (R~ $T^{+2.4}$)
→ production process simplified → cost

pros

contra

← Rq matching constraints
cells' pitch/wafer thickness

← vertical R is JFET
→ non-linear I-V
→ long recovery

Ninkovic et al NIM A610 (2009) 142
and NIM A628 (2011) 407
Richter et al US patent № 2011/0095388

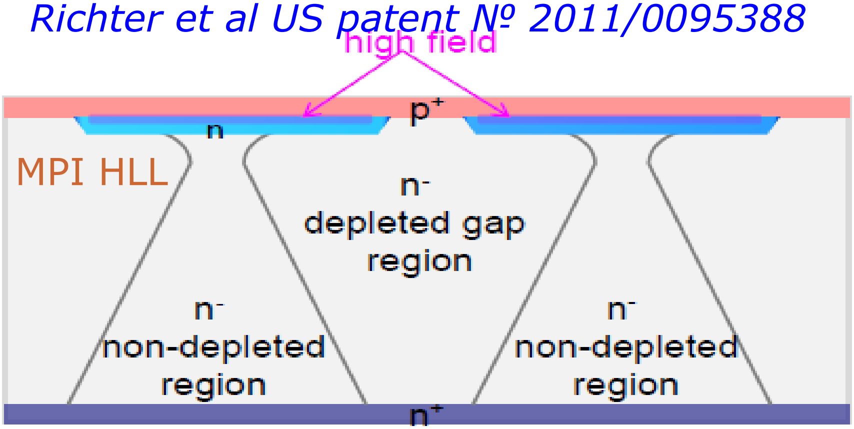

principle proved

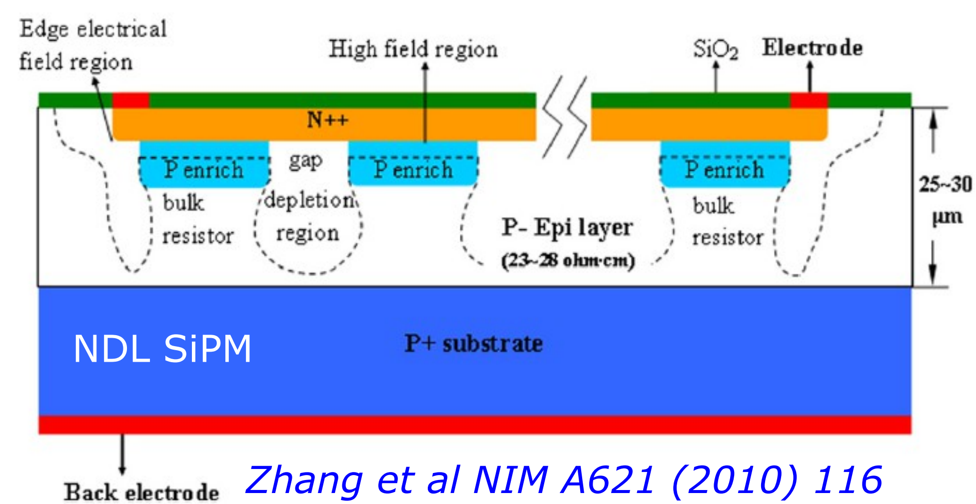

Zhang et al NIM A621 (2010) 116

V_{bd} vs T → T coefficient (ΔV stability)

Breakdown Voltage

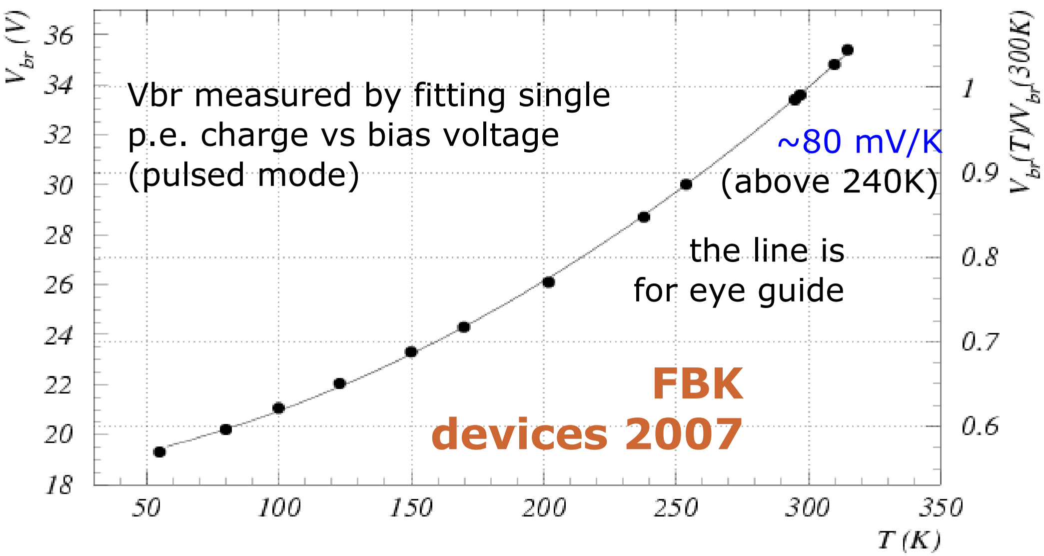

G.C. et al NIM A628 (2011) 389

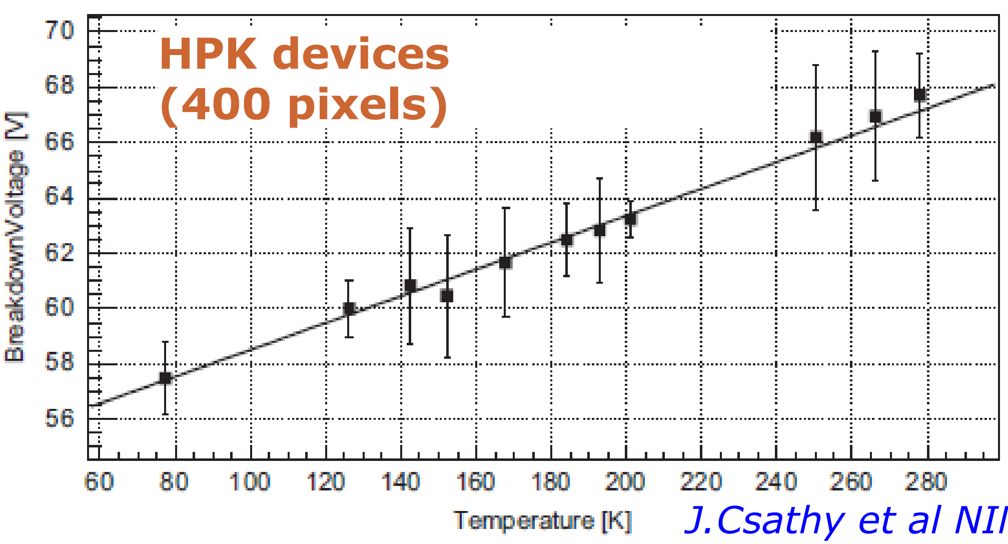

J.Csathy et al NIM A 654 (2011) 225

Fig. 6. Breakdown voltage as a function of temperature of the MPPC with 400 pixels.

Temperature coefficient

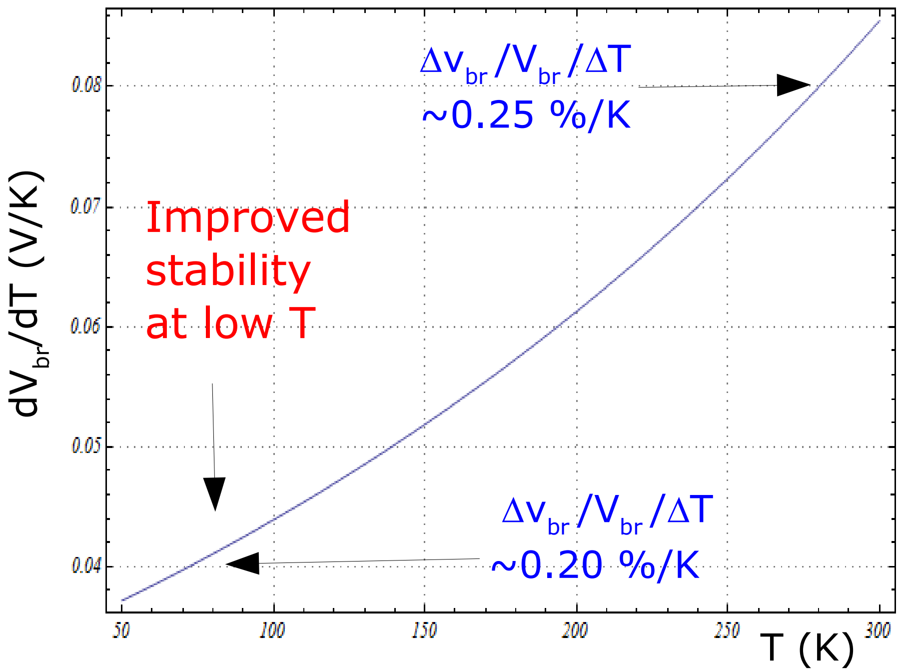

Note: How to improve stability & over-voltage range ?

Engineering high electric field & depletion/drift layer profiles

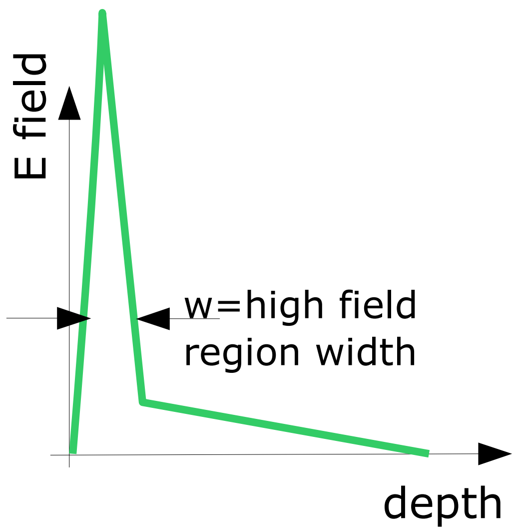

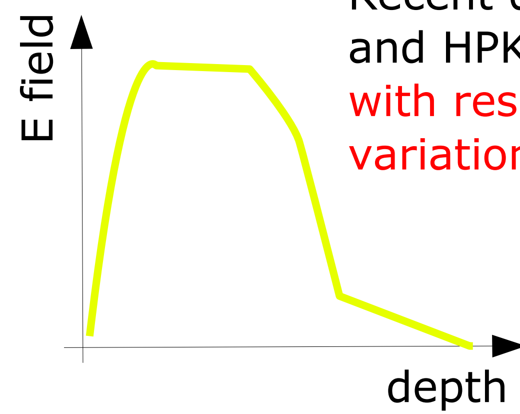

Recent devices (eg FBK and HPK) are more stable with respect to T and ΔV variations

Improved V_{bd} temperature coefficient → stability & ΔV range

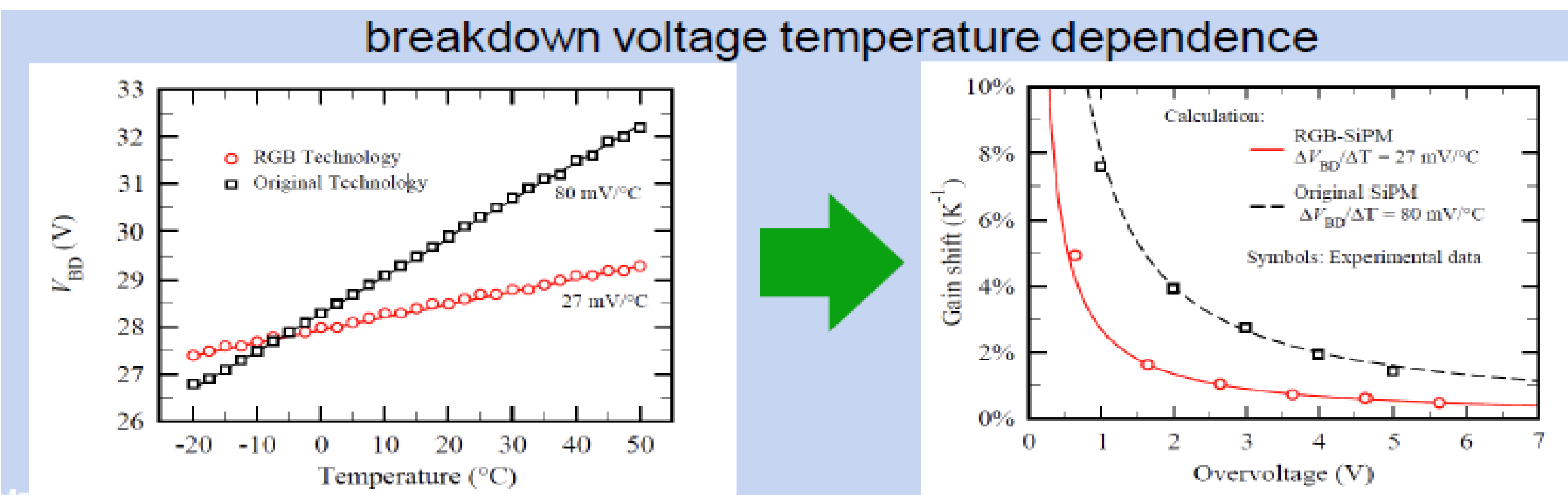

Recent progresses in FBK-Advansid devices

N.Serra: "Characterization of new FBK SiPM technology for visible light detection", JINST 2013 JINST 8 P03019

Dynamic range and non-linearity

analog SiPM output =
sum of binary cell's output

• Due to **finite number of cells** → signal **saturation**

• Correction possible BUT
→ **degraded resolution**

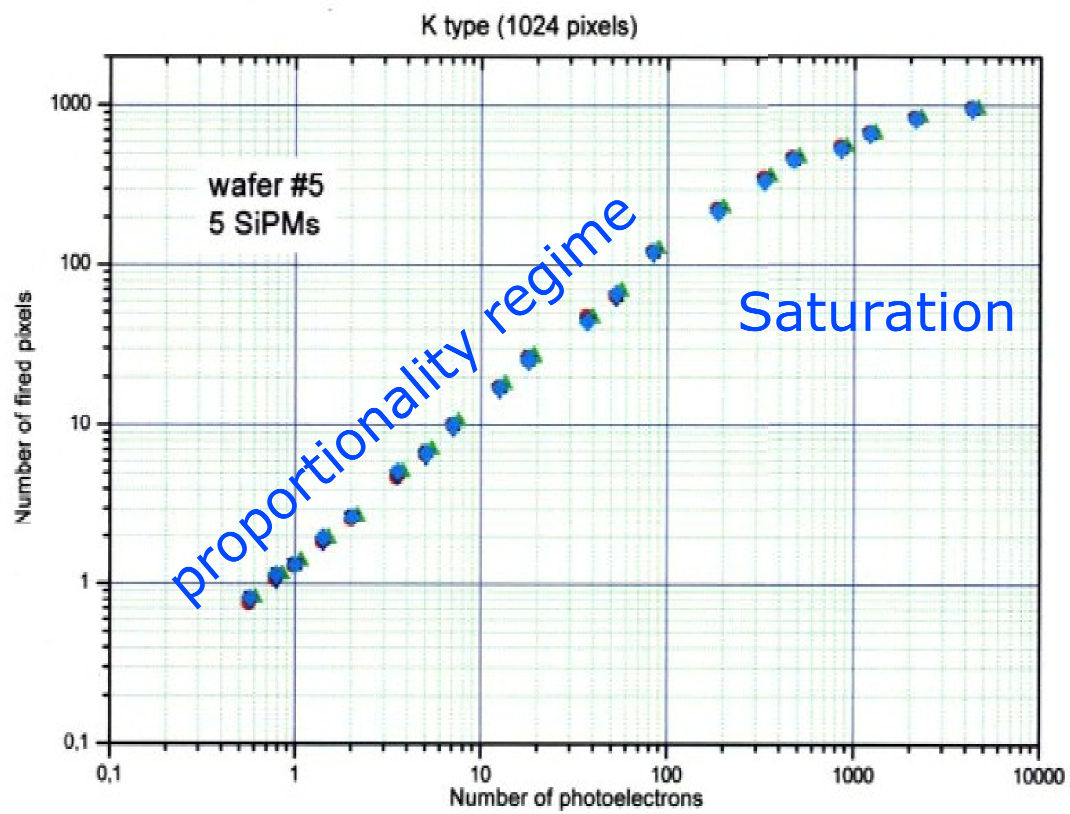

$$A \approx N_{firedcells} = N_{total} \cdot (1 - e^{-\frac{N_{photon} \cdot PDE}{N_{total}}})$$

eg: 20% deviation from linearity
if 50% of cells respond

➡ Best working conditions: $N_{\text{photo-electrons}} < N_{\text{SiPM cells}}$

Additional complications:
1) need correction to $N_{\text{fired-cells}}$ due to cross-talk and after-pulse
2) effective dynamic range depends on recovery time and time scale of signal burst

Amplitude fluctuations

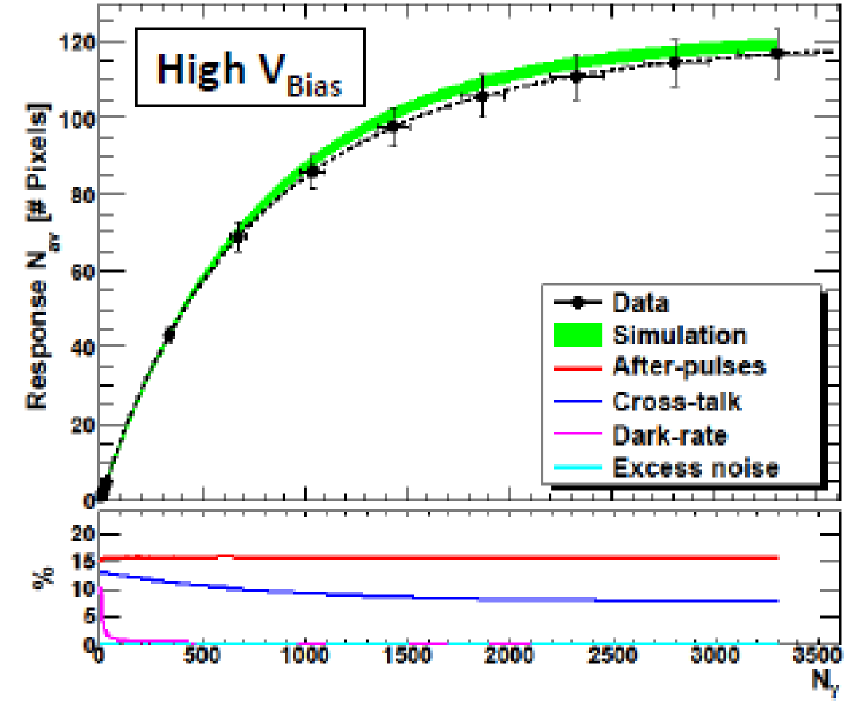

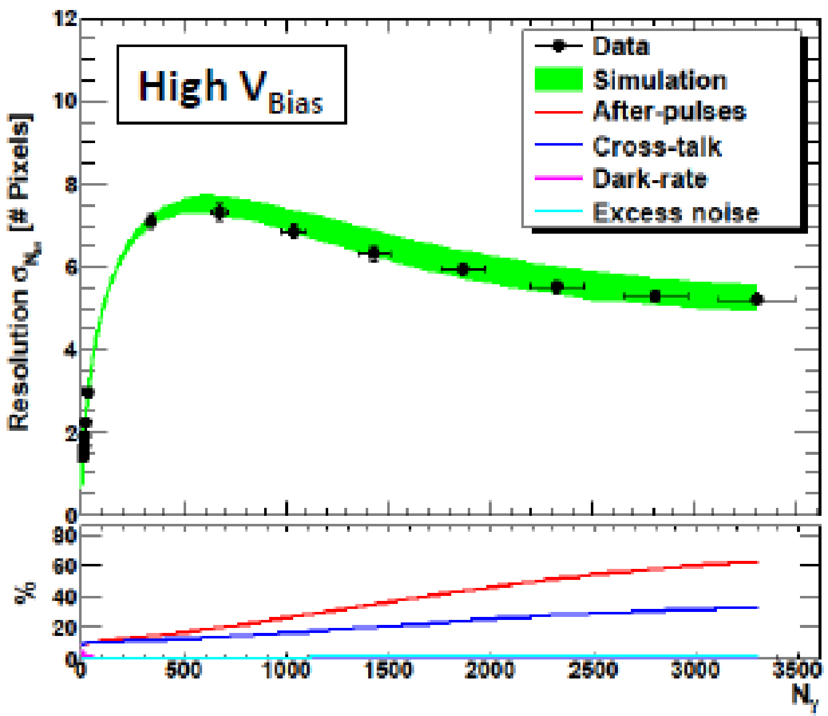

finite number of pixels: constraint
→ limit in resolving the number of photons

Eckert et al, Procs. of PhotoDet 2012

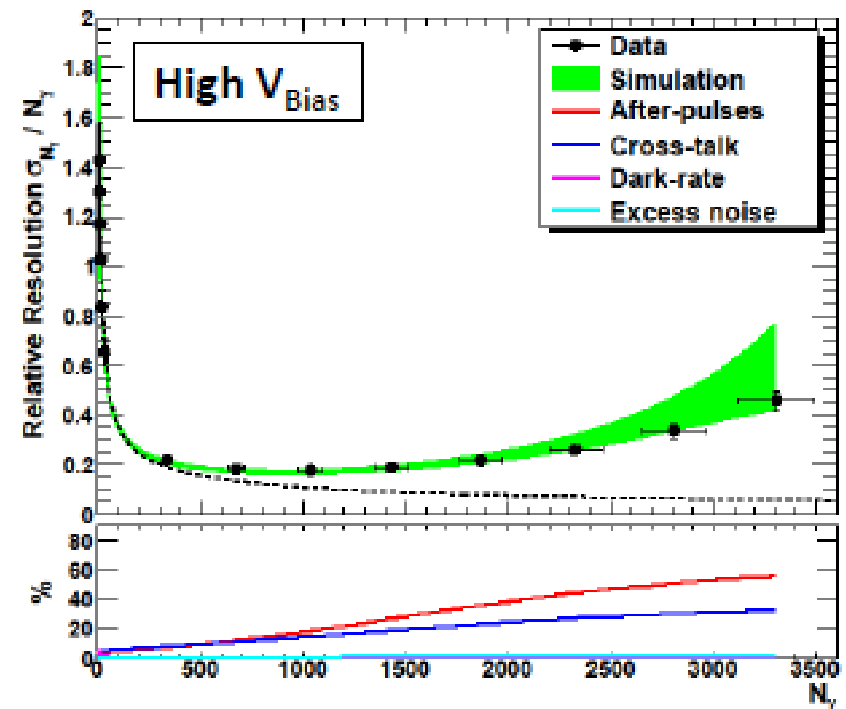

$$\frac{\Delta N_\gamma}{N_\gamma} \approx \frac{\overset{\text{DR}}{a}}{N_\gamma} \oplus \frac{\overset{\text{PDE, CT, AP}}{b}}{\sqrt{N_\gamma}}$$

see also Musienko et al JINST 2 2007 P0600

Disentangling noise components

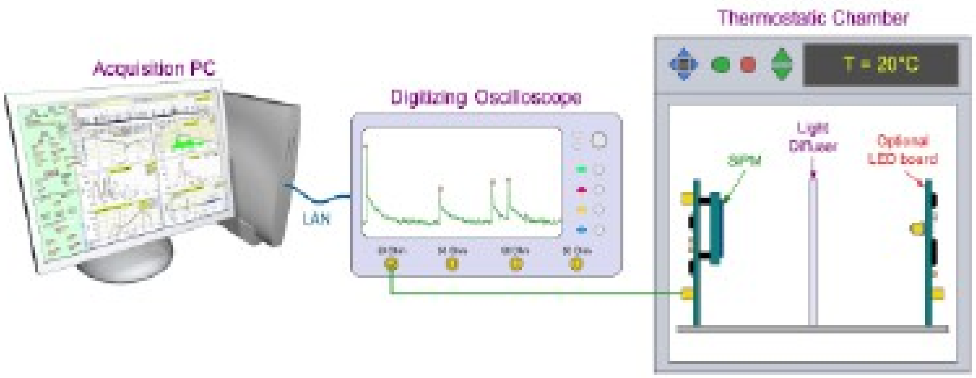

We acquire ms-long waveforms

Signal filtered to reduce pulse length

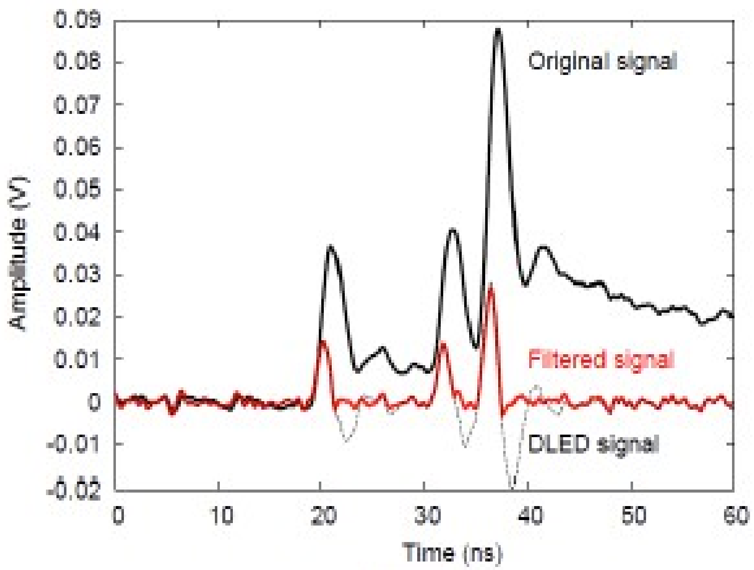

→ time delay array
→ amplitude array

Disentangling noise components

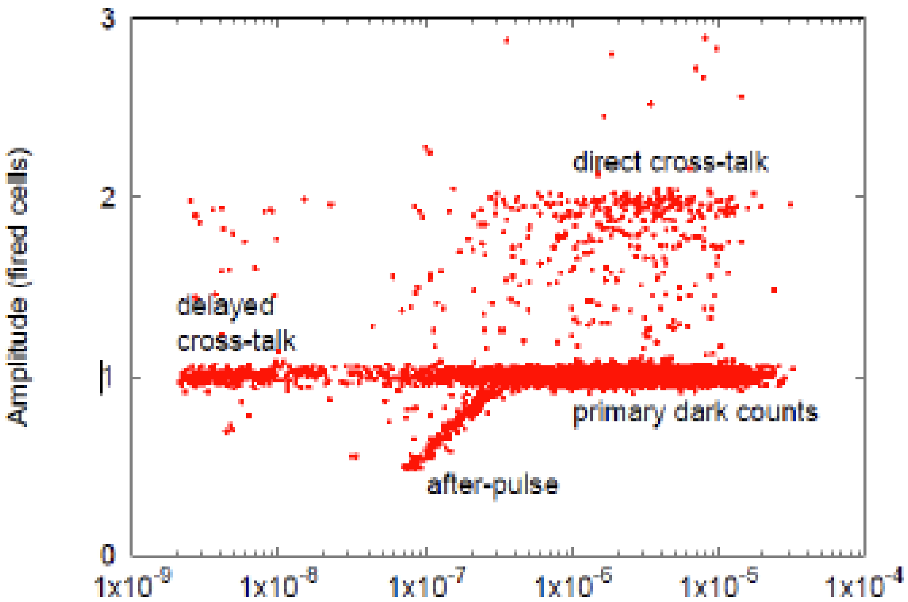

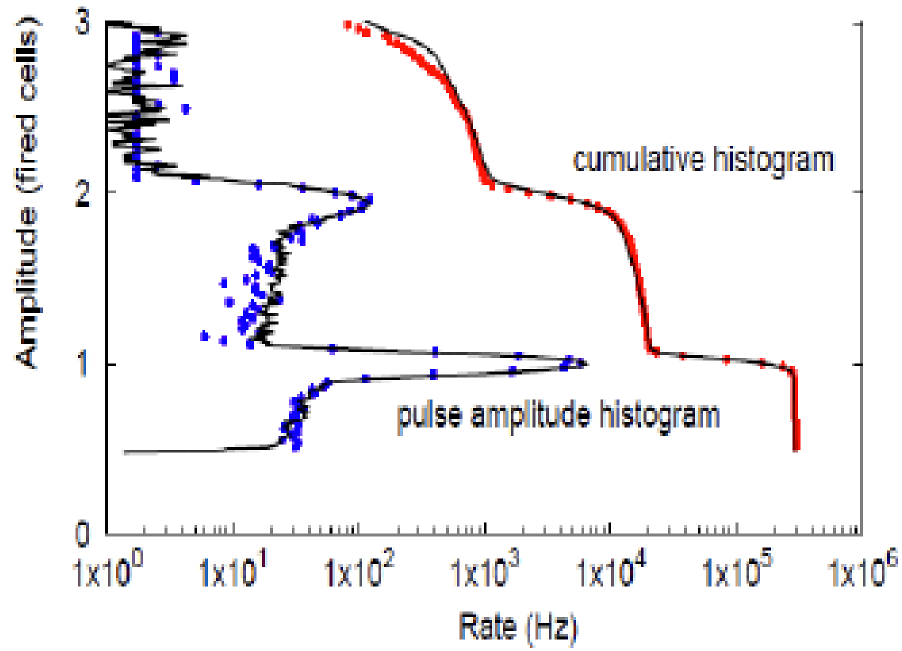

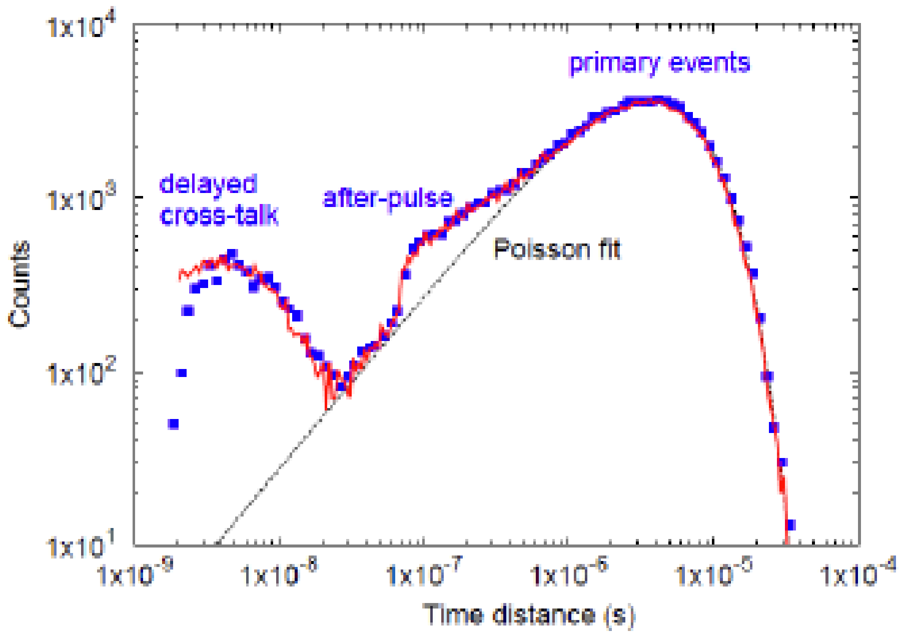

→ primary dark rate (DCR)
→ direct cross-talk
→ delayed correlated components

QE → PDE shape vs λ

W.Knidt PhD Thesis 1999

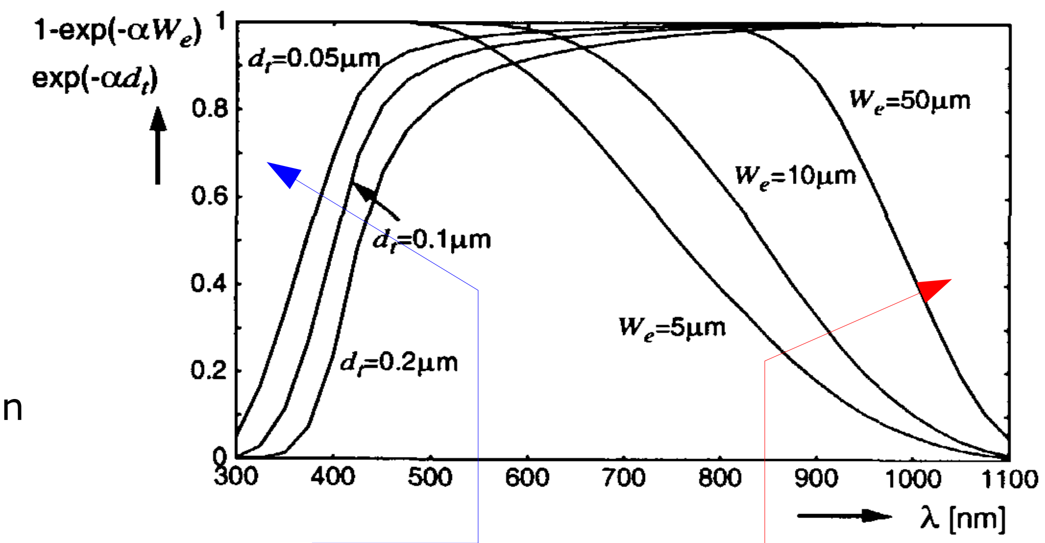

short wavelength limits
- ARC Transmittance
- Superficial Recombination

Most critical issue for **Deep UV SiPM**
note: reduced superficial recombination in n-on-p wrt p-on-n

Decreasing thickness of top layer

Increasing thickness sensitive layer

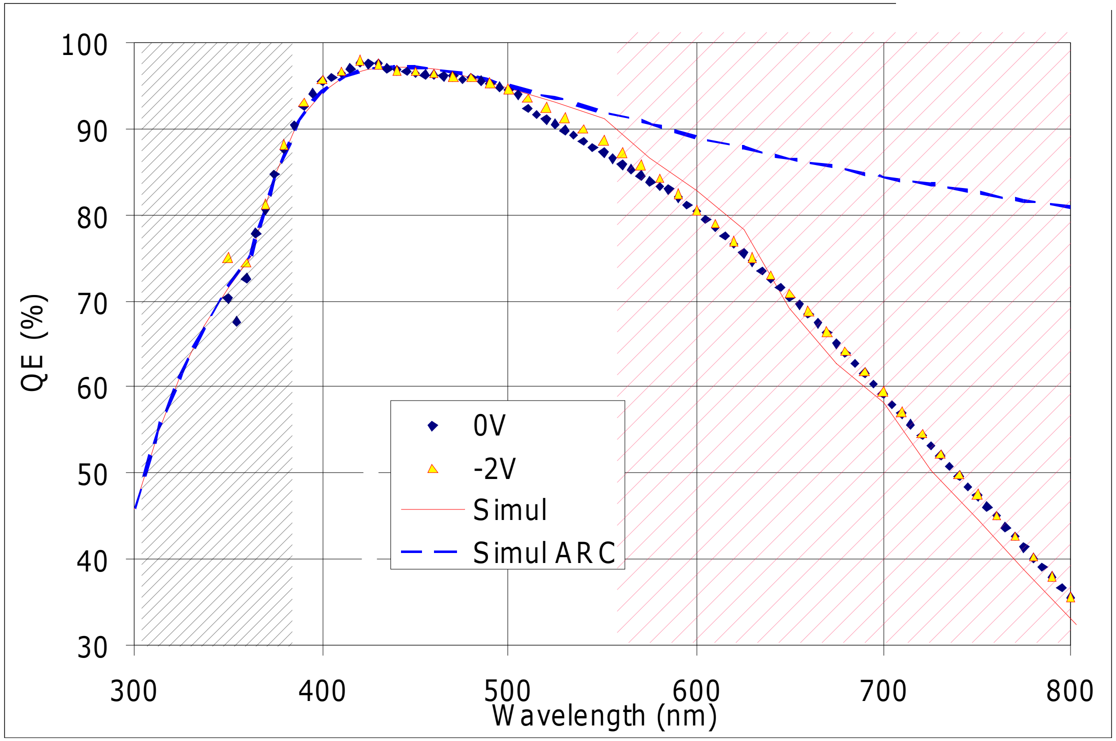

long wavelength limits
- depth of π layer thickness or depleted region

FBK single diode (2006)

photo-voltaic regime (V_{bias}~ 0 V)

Recent measurement: Angular response

Lecoq et al – IEEE NSS 2013

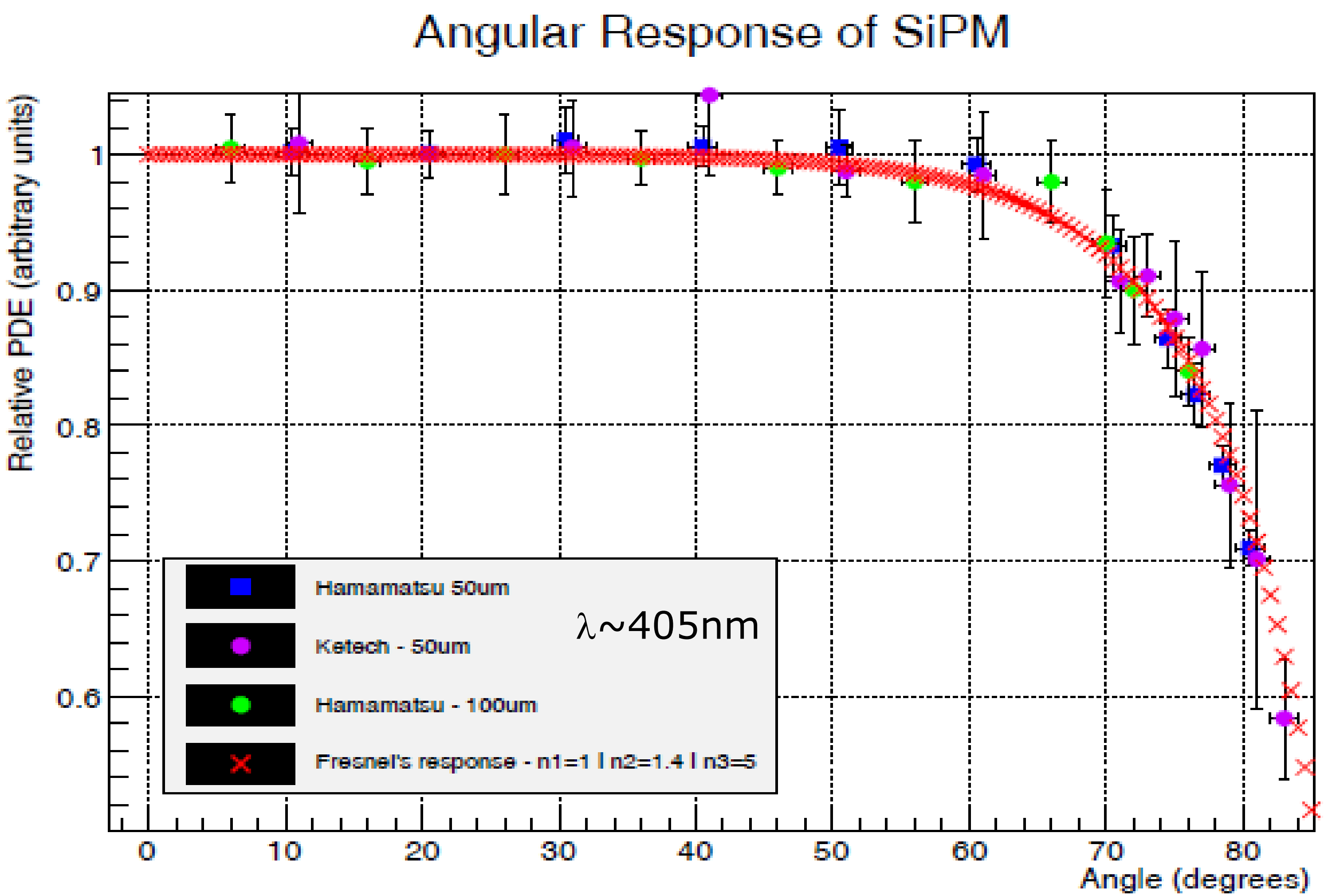

Variation of response with incident angle:
- understood with Fresnel reflections on entrance optical windows
  → if multilayer optical stack and polarization effects are accounted for
- interference effects not negligible when layers width ~ wavelength
- no effects seen in correlation with over-voltage and cell size

Improving PDE by E field engineering

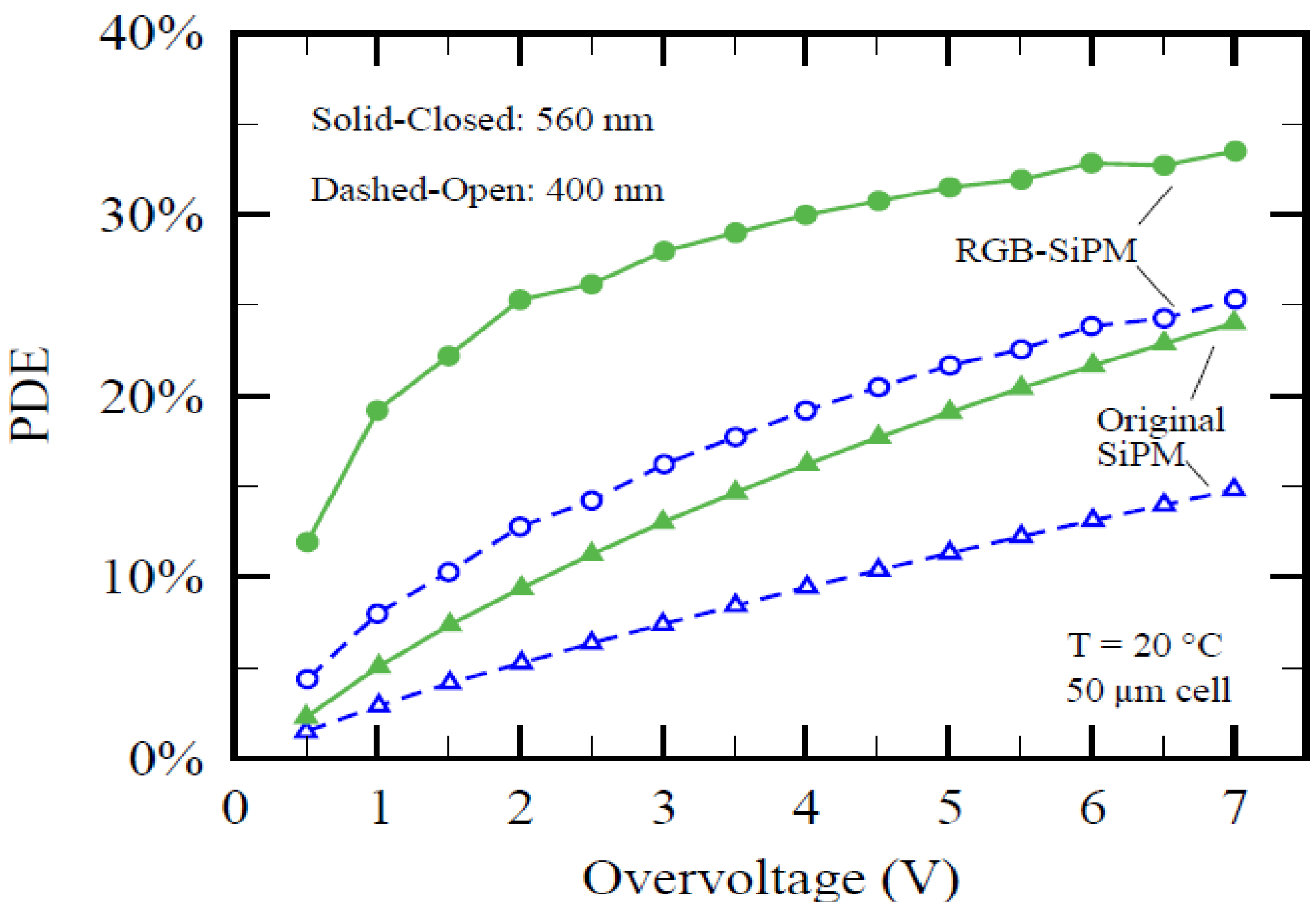

Latest "RGB" FBK devices vs older devices

N.Serra et al
JINST 8 (2013) P03019

Table 1. Main properties of the fabricated RGB-SiPMs.

FBK n-on-p RGB-SiPMs.			
SiPM size (mm^2)	1×1, 3×3, 4×4	Gain (1)	$4 \cdot 10^6$
Cell pitch (μm)	25-50-70-100	R quenching (at 20°C)	500 kΩ
Fill-factor (%)	21-45-58-72	Cell capacitance (1)	170 fF
V_{BD} (at 20°C)	28.5 V	Rise time (1)(2)	5.6 ns
Dark count rate (1)	480 kHz	Recovery time (1)(2)	350 ns

(1) 1×1 mm^2 SiPM, 50 μm cell at 20°C, OV=4 V; (2) Single-cell pulse, see figure 2.

Trend: Higher PDE & lower DCR...

D.Renker JINST 5 2010 P01001

A most significant plot: DCR vs PDE

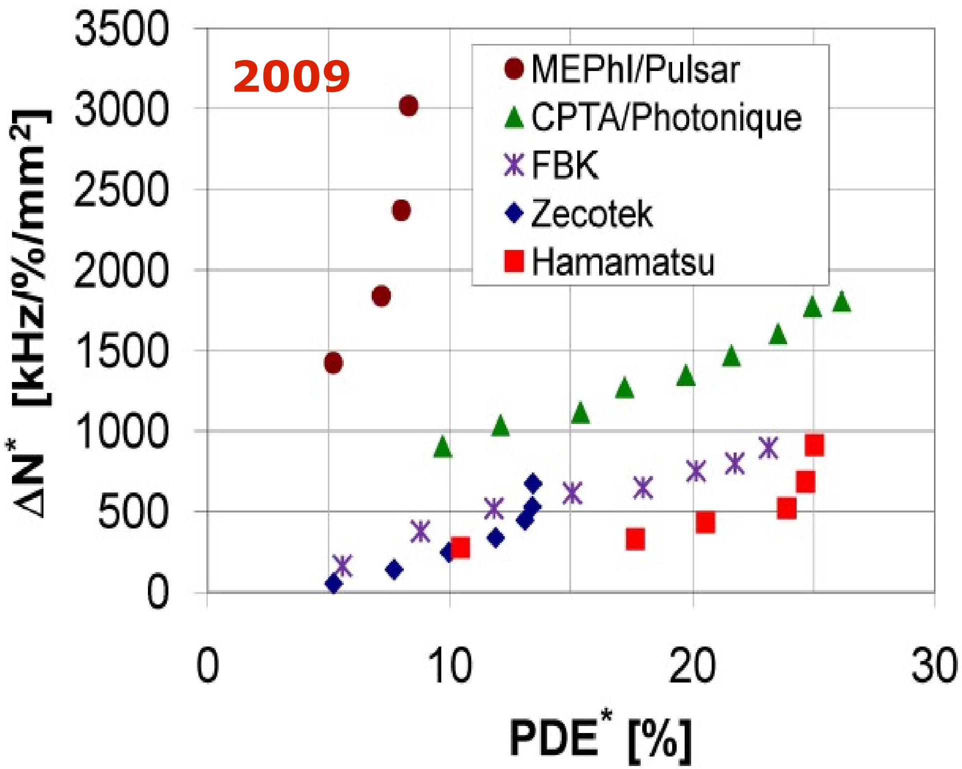

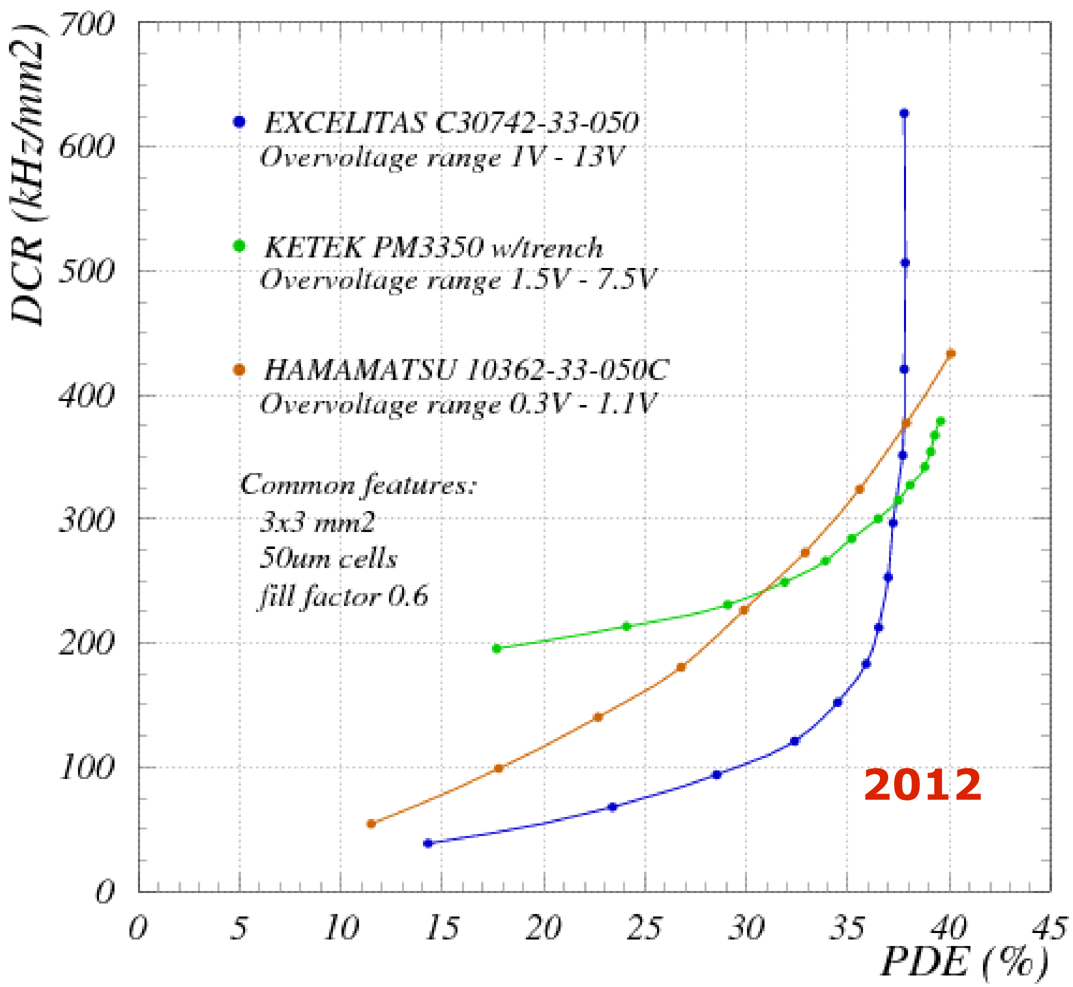

G.C. from published data

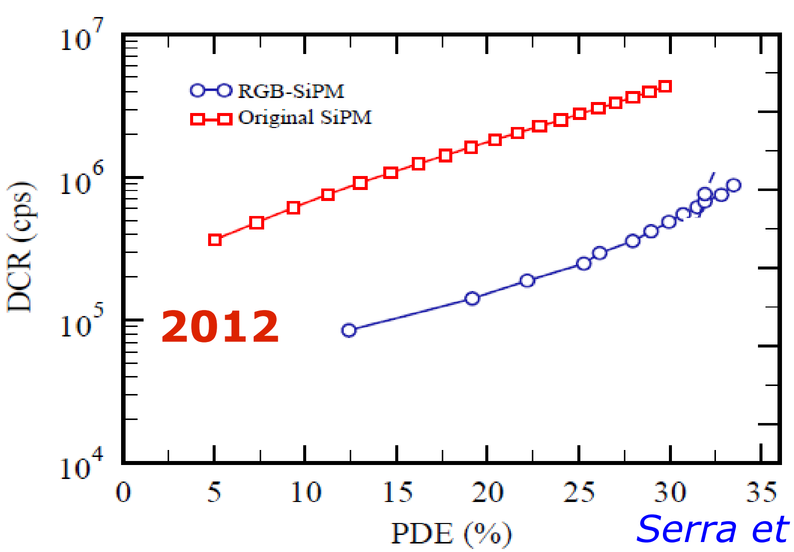

Serra et al (FBK) JINST 8 2013 P03019

PDE vs Temperature (ΔV constant)

G.C. et al NIM A628 (2011) 389

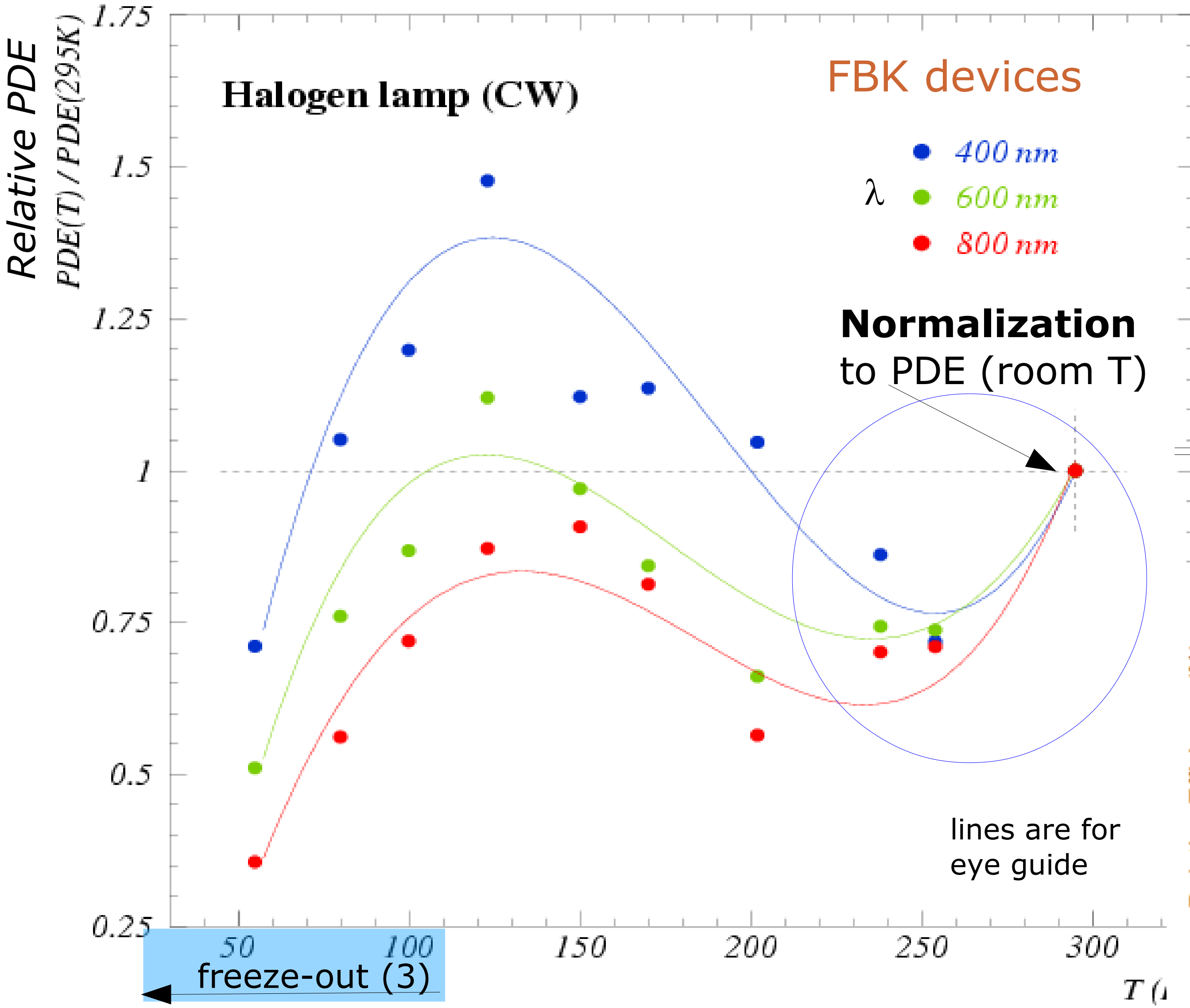

When T decreases:

1) silicon E_{gap} increasing
→ larger attenuation length
→ lower QE (for larger λ)

2) mobility increasing
→ larger impact ionization
→ larger trigg. avalanche P_{01}

3) carriers freeze-out
onset below 120K
→ loss of carriers

RMD APD at 400nm < λ < 700nm
Johnson et al, IEEE NSS 2009

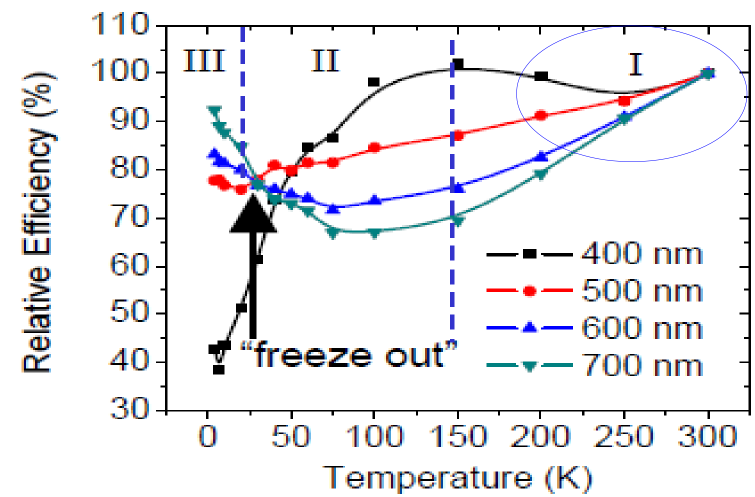

Additional effects in APD
(depletion region depends on T, ...)

Further measurements needed !!!

Metal Quenching Resistor (Hamamatsu)

Sato et al IEEE NSS 2013

Improves
→ temperature stability of Rq
→ uniformity of Rq
→ Fill Factor (high trasmittance → deposited directly on active surface)
→ control amount of parasitic Cq (parallel to Rq) → timing performances

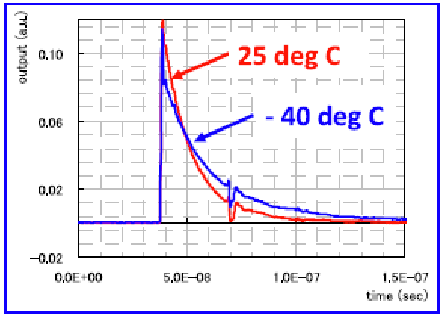

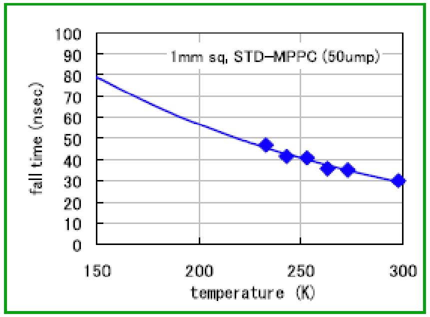

The quenching resistor value increases as environmental temperature decreases. The larger resistor makes the pulse amplitude lower and the tail longer.

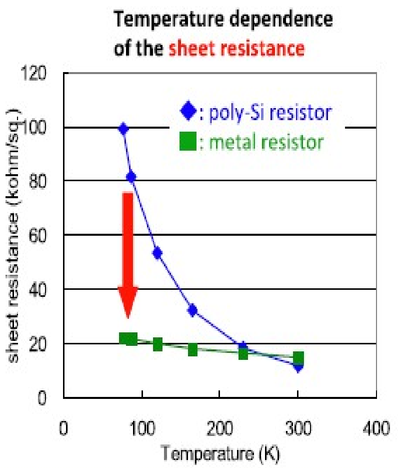

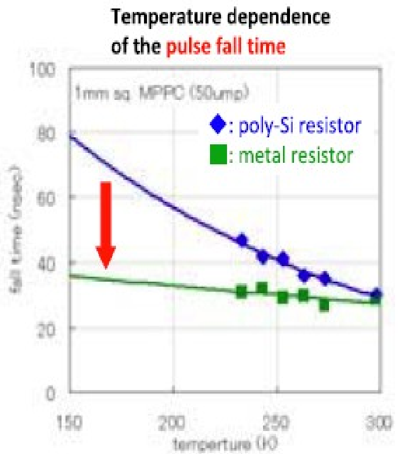

Metal quenching resistor achieved 1/5 temperature dependence

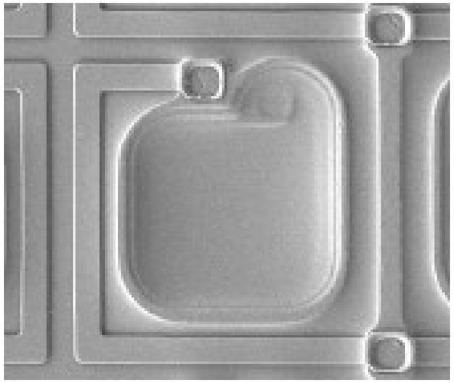

polysilicon

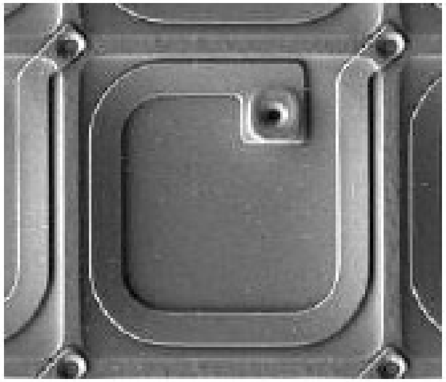

metal

Timing

Timing jitter: prompt and delayed components

1) Prompt component: gaussian with time scale O(100ps)

Statistical fluctuations in the avalanche:

- **Longitudinal** build-up (minor contribution)
- **Transversal** propagation (main contribution)

  - via multiplication assisted diffusion (dominating in few μm thin devices) *A.Lacaita et al. APL and El.Lett. 1990*

  - via photon assisted propagation (dominating in thick devices – O(100μm)) *PP.Webb, R.J. McIntyre RCA Eng. 1982* *A.Lacaita et al. APL 1992*

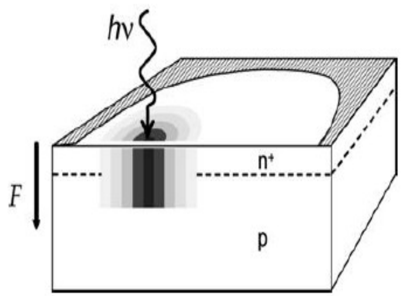

Multiplication assisted diffusion

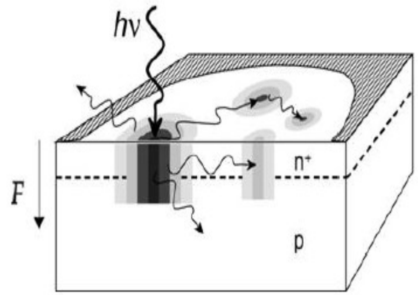

Photon assisted propagation

Fluctuations due to

a) impact ionization statistics

b) variance of longitudinal position of photo-generation: finite drift time even at saturated velocity note: saturated ve ~ 3 vh (n-on-p are faster in general)

→ Jitter at minimum → **O(10ps)**
(very low threshold → not easy)

Fluctuations in shock-wave due to

c) variance of the transverse diffusion speed v_{diff}

d) variance of transverse position of photo-generation: slope of current rising front depends on transverse position

→ Jitter → **O(100ps)**
(usually threshold set high)

Timing jitter: prompt and delayed components

2) delayed component: non-gaussian tails with time scale O(ns)

Carriers photo-generated in the neutral regions above/beneath the junction and reaching the electric field region by diffusion

G.Ripamonti, S.Cova Sol.State Electronics (1985)

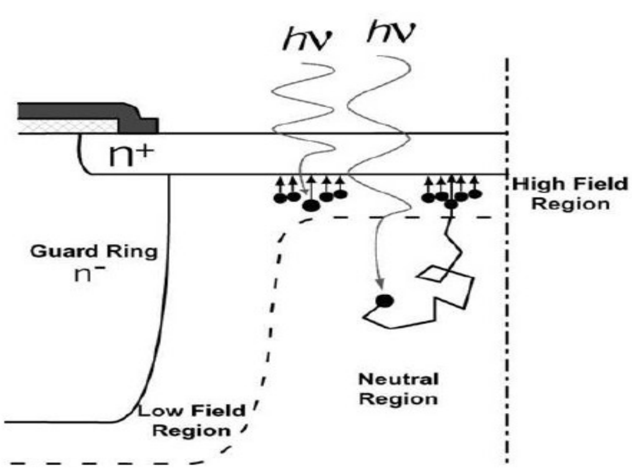

S.Cova et al. NIST Workshop on SPD (2003)

tail lifetime: $\tau \sim L^2 / \pi^2 D$ ~ up to some ns
L = effective neutral layer thickness
D = diffusion coefficient

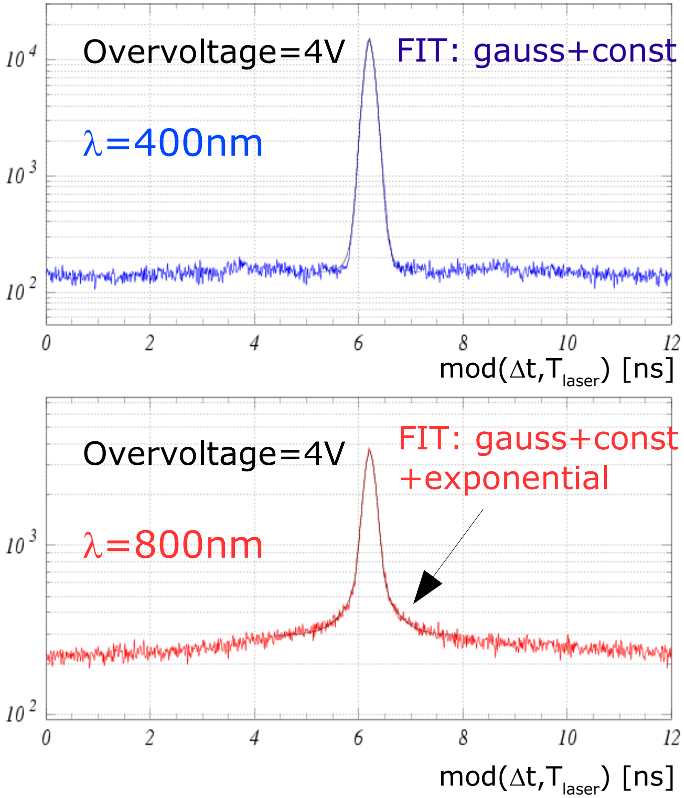

G.C. et al NIMA 581 (2007) 461

→ **Neutral regions** underneath the junction : timing tails for long wavelengths
→ **Neutral regions** in APD entrance: timing tails for short wavelengths

PDE vs timing trade off / optimization

C.H.Tan et al IEEE J.Quantum Electronics 13 (4) (2007) 906

k=ratio of hole (β) to electron (α) ionization coefficient (increasing with E field)

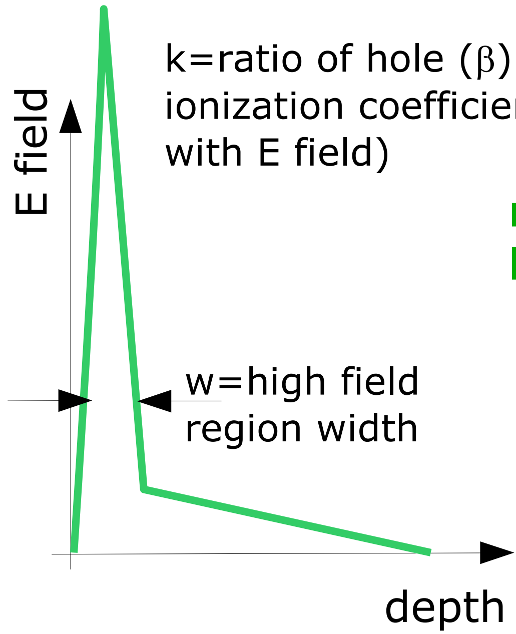

narrow avalanche region, high E:
- **small w**
- **high k = β / α**

better for **TIMING**

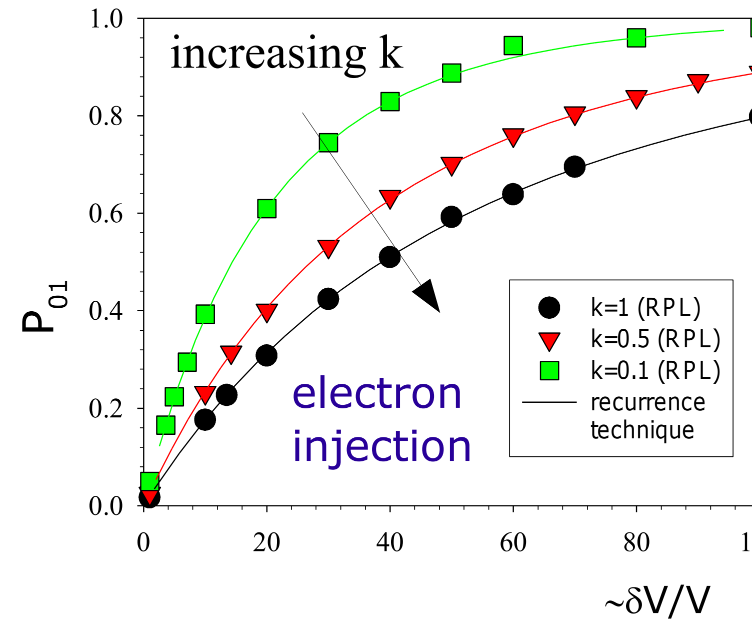

better for **PDE**

wide avalanche region, low E:
- **wide w**
- **small k = β / α**

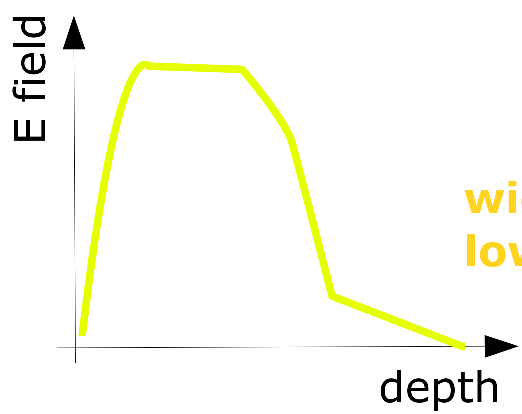

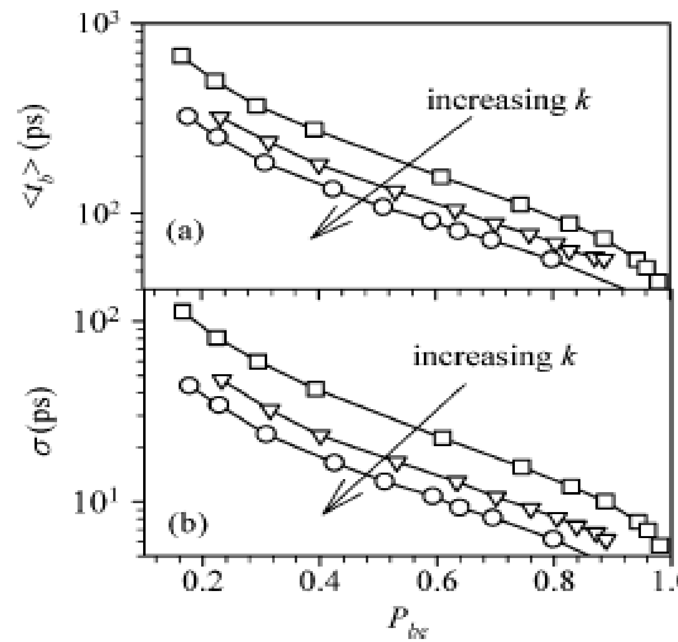

Optimizing signal shape for timing

Single cell model → $(R_d||C_d)+(R_q||C_q)$

SiPM + load → $(||Z_{cell})||C_{grid} + Z_{load}$

Signal = slow pulse ($\tau_{d\ (rise)}, \tau_{slow\ (fall)}$) +
+ fast pulse ($\tau_{d\ (rise)}, \tau_{fast\ (fall)}$)

- $\tau_{d\ (rise)} \sim R_d(C_q+C_d)$ [intrinsic]
- $\tau_{fast\ (fall)} = R_{load}\ C_{tot}$ (fast; parasitic spike)
- $\tau_{slow\ (fall)} = R_q\ (C_q+C_d)$ (slow; cell recovery)

F.Corsi, et al. NIM A572 (2007) 416
S.Seifert et al. IEEE TNS 56 (2009) 3726

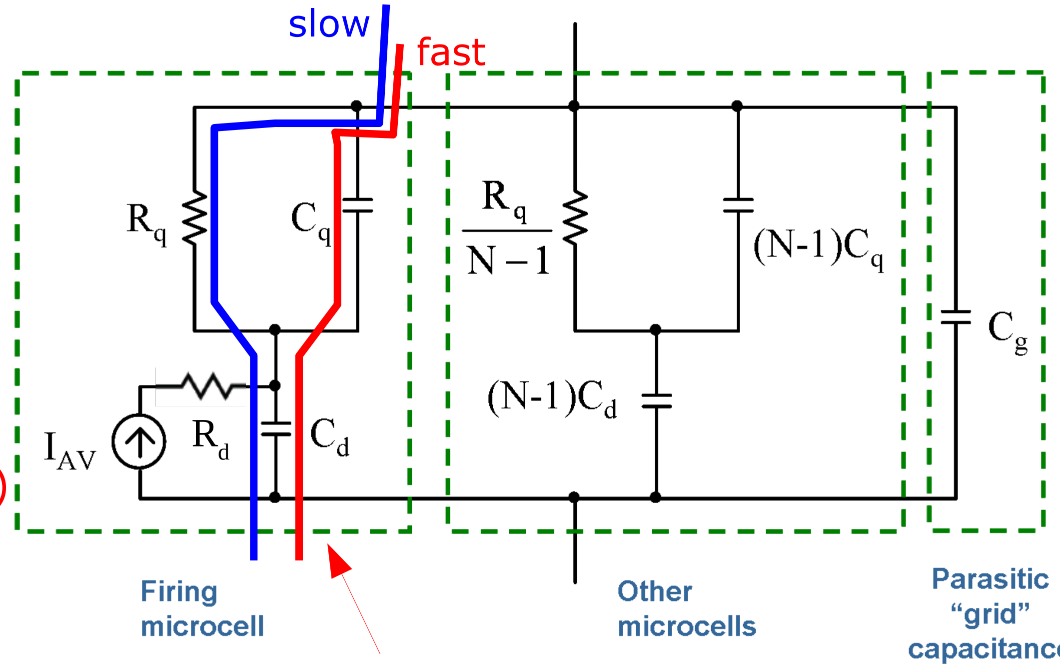

Cq → fast current supply path in the beginning of avalanche

Pulse shape

- Rise: Exponential
- Fall: Sum of 2 exponentials: transient + recovery

Sp.Charge Rd x Cd,q filtered by parasitic inductance, stray C, ... (Low Pass) → $O(R_{load}\ C_{tot})$

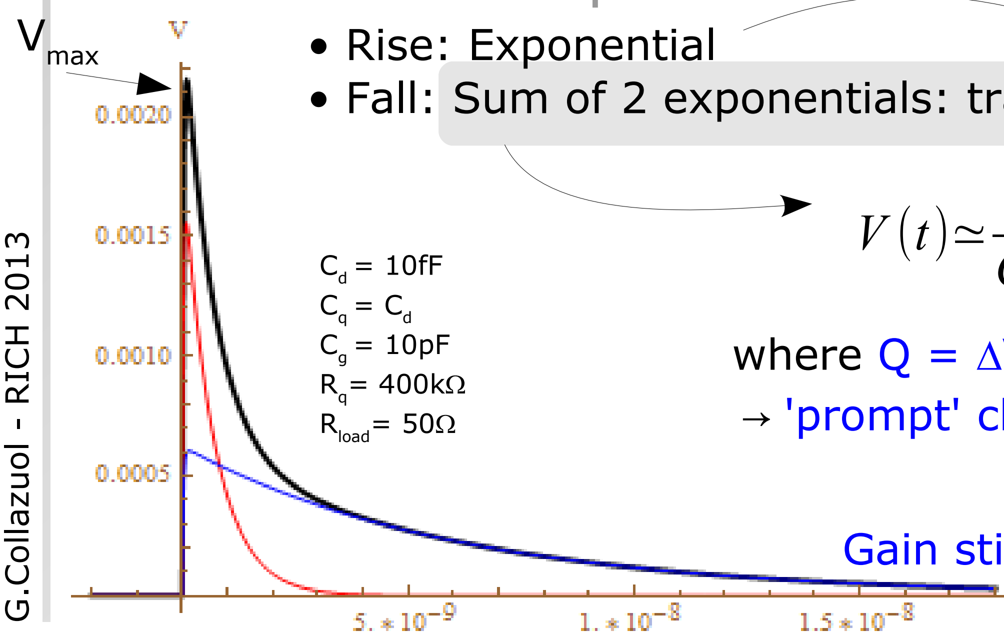

$$V(t) \simeq \frac{Q}{C_q+C_d}\left(\frac{C_q}{C_{tot}}e^{\frac{-t}{\tau_{FAST}}} + \frac{R_{load}}{R_q}\frac{C_d}{C_q+C_d}e^{\frac{-t}{\tau_{SLOW}}}\right) \text{ for } R_{load} << Rq$$

where $Q = \Delta V\ (C_q+C_d)$ is the total charge released by the cell
→ 'prompt' charge on C_{tot} is $Q_{fast} = Q\ C_q/(C_q+C_d)$

Gain still well defined: $G = \int dt \frac{V(t)}{q_e R_{load}} = Q/q_e = \frac{\Delta V (C_d+C_q)}{q_e}$

G.Collazuol - RICH 2013

Pulse shape parameters

$$V(t) \simeq \frac{Q}{C_q+C_d}\left(\frac{C_q}{C_{tot}}\, e^{\frac{-t}{\tau_{fast}}} + \frac{R_{load}}{R_q}\frac{C_d}{C_q+C_d}\, e^{\frac{-t}{\tau_{slow}}}\right) = \frac{Q\,R_{load}}{C_q+C_d}\left(\frac{C_q}{\tau_{fast}}\, e^{\frac{-t}{\tau_{fast}}} + \frac{C_d}{\tau_{slow}}\, e^{\frac{-t}{\tau_{slow}}}\right)$$

Note: valid for low impedance load $R_{load} << Rq$

- $\tau_{fast} = R_{load}\ C_{tot}$
- $\tau_{slow} = R_q\,(C_q+C_d)$

→ gain $G = \int dt \frac{V(t)}{q_e R_{load}} = Q/q_e = \boxed{\frac{\Delta V(C_d+C_q)}{q_e}}$ independent of R_q

→ charge ratio $\boxed{\frac{Q_{slow}}{Q_{fast}} \sim \frac{C_d}{C_q}}$

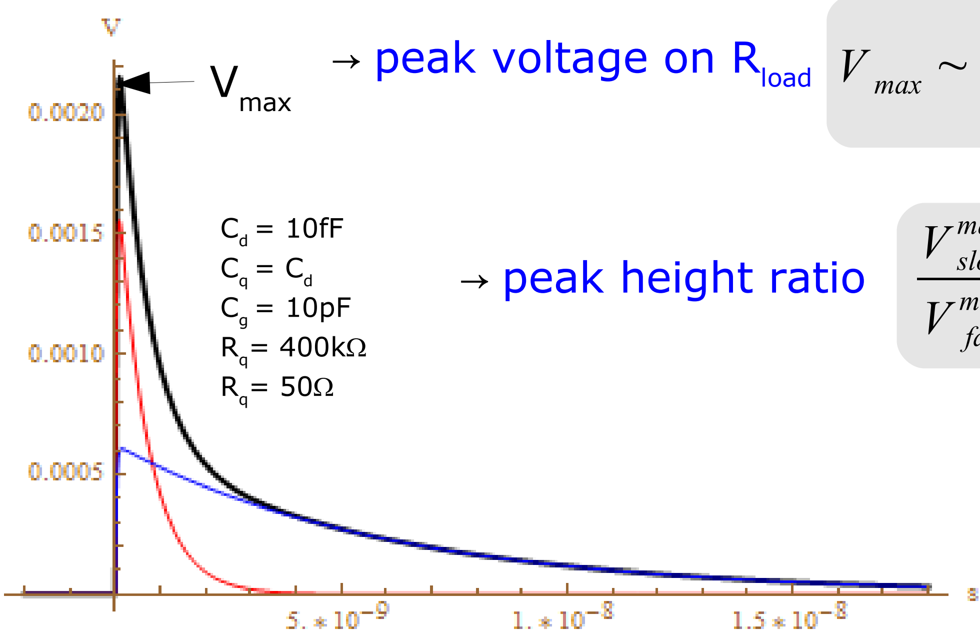

→ peak voltage on R_{load} $\boxed{V_{max} \sim R_{load}\left(\frac{Q_{fast}}{\tau_{fast}} + \frac{Q_{slow}}{\tau_{slow}}\right)}$ dependent on R_q (increasing with $1/R_q$)

→ peak height ratio $\boxed{\frac{V^{max}_{slow}}{V^{max}_{fast}} \sim \frac{C_d\,C_{tot}\,R_{load}}{C_q^2\,R_q}}$ increasing with C_d and $1/R_q$

Increasing C_q/C_d or/and R_q/R_{load}
→ spike enhancement → better timing
→ slow recovery tail suppressed
→ reduced baseline fluctuations

Spares

Vacuum based PD

PMT: 80 years old... still the most used sensor for low-level light detection

Features
- sensitivity from DUV to NIR
- **high gain**
- **low noise**
  - → single photon sensitivity
  - → large area at ~low cost
  - → low capacitance
- imaging capabilities (large pixels)
- high frequency response
  - → fast response
- stability

Issues
- intrinsic **limit QE < 40%**
- broad SER
- high voltage, bulky, fragile
- influenced by B, E fields
- damaged by high-level light
- ageing (eg. He)
- radiopurity

Developement

→ photocathodes: new materials and geometries → high QE

→ ultra-fast, large area, imaging MCP based PMTs

→ hybrids (eg photo-cathode + SiPM) → narrow SER

Large Area Pico-second MCP Photo-detectors

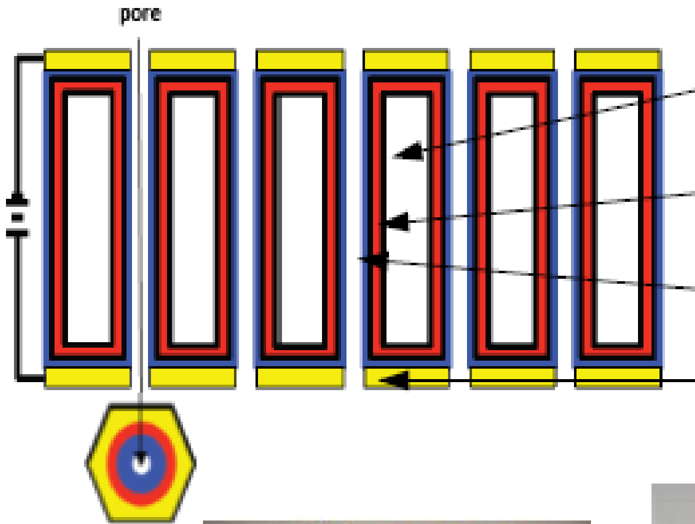

Porous glass

Resistive coating ~100nm (ALD)

Emissive coating ~ 20nm (ALD)

Conductive coating
(thermal evaporation or sputtering

Incom glass substrate

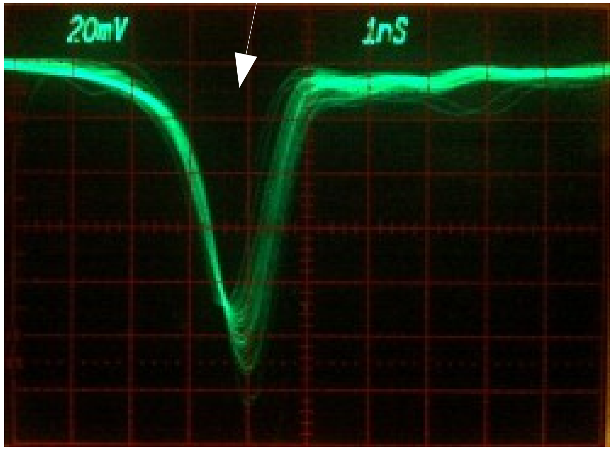

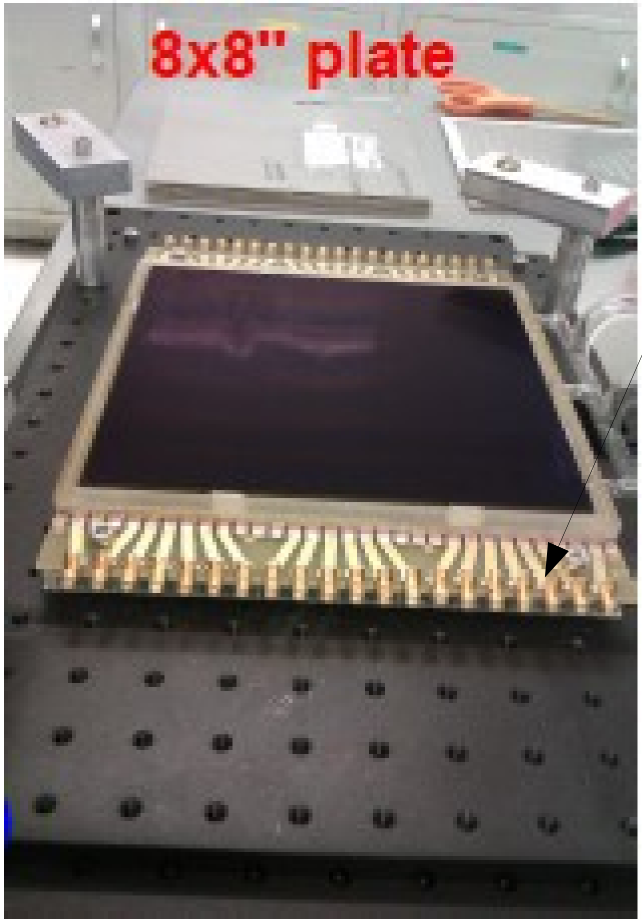

RF strip-line anodes

- 50 Ω impedance
- 1.6-0.4GHz bandwidth

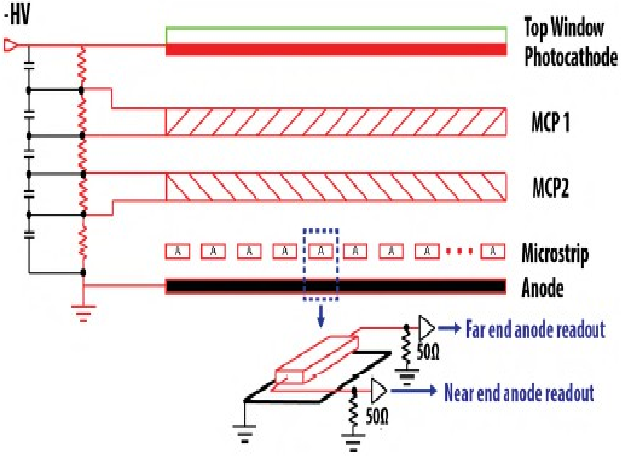

LAPPD

http://psec.uchicago.edu/

Large Area Photo-Detectors → HPD

"Bombardment" gain

1) Photo-emission from photo-cathode
2) Photo-electron acceleration to **ΔV ~ 10-20kV**
3) charge multiplication in Si by ionization
→ **reduced fluctuations** due to Fano factor (F~0.12 in Si)

$$G = \frac{\Delta V - V_{thr.}}{W_{Si}}$$

$$\sigma_G = \sqrt{F \cdot G}$$

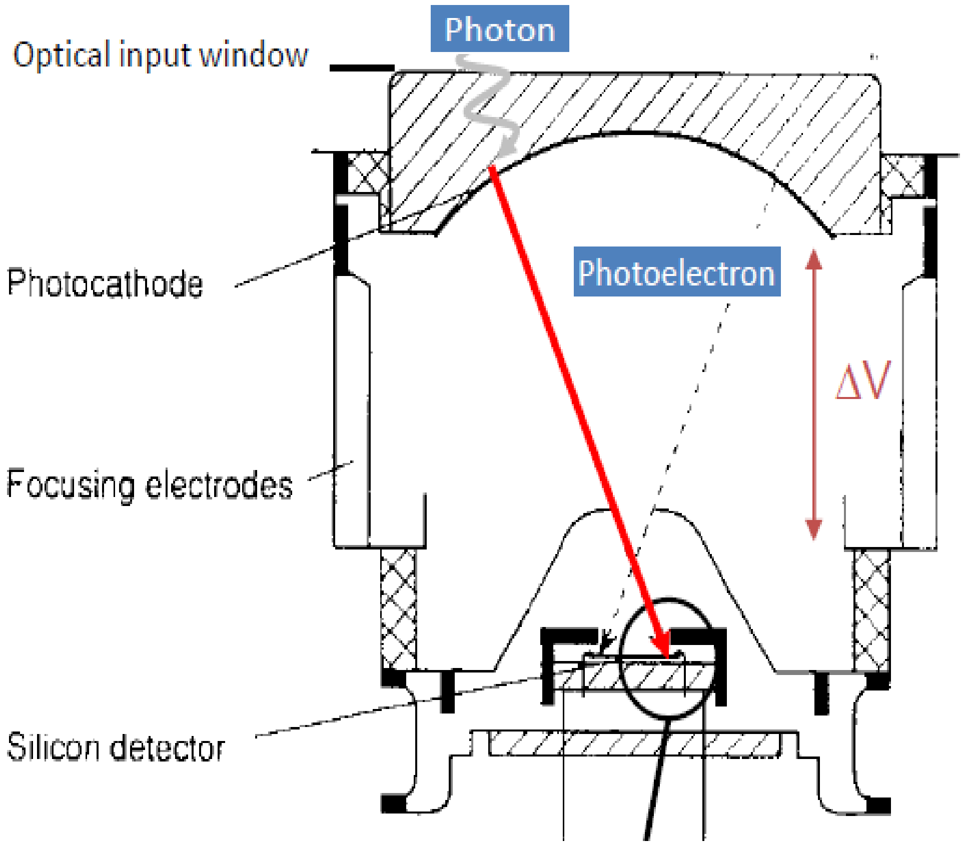

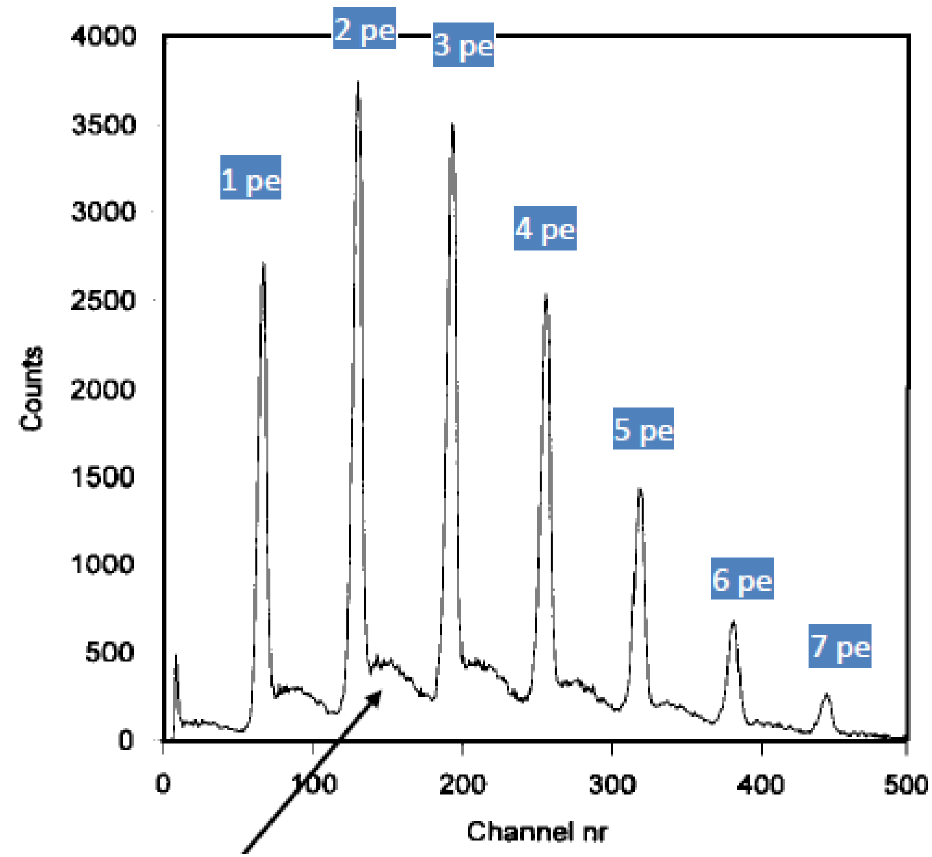

EDIT 2011 School at CERN - photodetectors

background from electron back-scattering at Si surface

see talk by S.Eisenhardt at this conference

Light guides

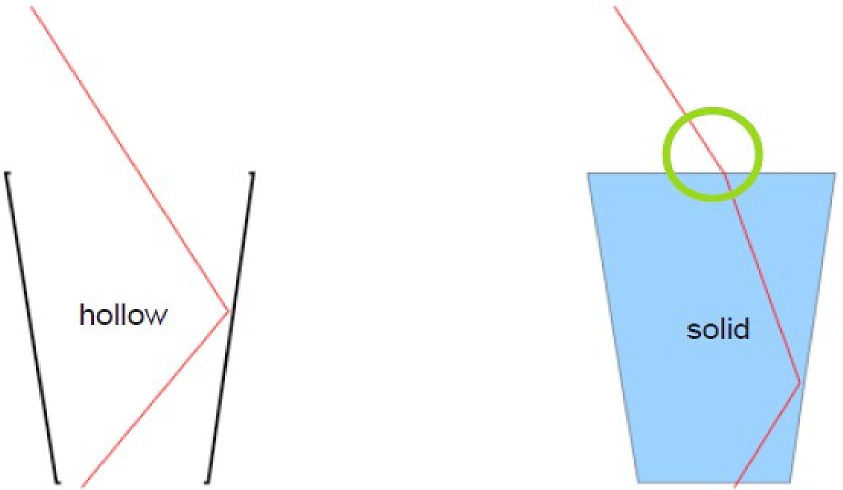

→ **higher concentration than hollow cones due to change of refractive index,** O(12-17)

Solid vs Hollow

Optical coupling

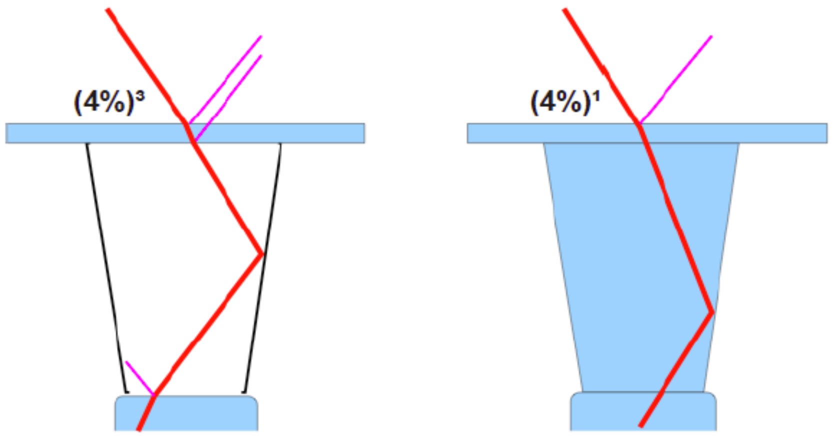

→ **two Fresnel reflections less, ~8% gain**

→ needs *good* optical coupling, i.e. good glueing